Escola de Camins
Escola Tècnica Superior d'Enginyeria de Camins, Canals i Ports
UPC BARCELONATECH

Dynamic identification of structures

TREBALL FINAL DE MÀSTER

Treball realitzat per:
Irene Josa i Culleré

Dirigit per:
José Turmo Coderque
José Antonio Lozano Galant
Gonzalo Ramos Schneider

Màster en:
Enginyeria de Camins, Canals i Ports

Barcelona, setembre del 2017

Departament d'Enginyeria Civil i Ambiental

E.T.S. DE INGENIERIOS DE CAMINOS, CANALES Y PUERTOS DE BARCELONA

Dynamic identification of structures

Master's final thesis

Directed by

José Turmo Coderque

José Antonio Lozano Galant

Gonzalo Ramos Schneider

Written by

Irene Josa i Culleré

September 2017, Barcelona

Abstract

The need for cheap and simple methods for structural inspection has grown tremendously over past decades. This is due to the fact that complex modern engineering structures, for example, stadiums, dams, skyscrapers, tunnels, etc. have to maintain their integrity and functionality. Failure of these structures leads to tragic consequences as well as heavy material losses. Also, when damage occurs during the building structures' service-life, the mechanical characteristics of the structure change and it is important to be able to assess these variations in the structural properties.

Structural System Identification (SSI) is an interdisciplinary domain which's prerogative is to evaluate the integrity and the state of structures using non-destructive techniques.

This thesis deals with the problem of determining the actual characteristics of a structure such as Young's modulus, area, inertia and/or products of them using dynamic measurements.

A SSI method that uses the Observability technique has already been developed using static measurements. It is based on the information provided by the monitoring of static nondestructive tests. The subset of characteristics of the structure can be uniquely defined only when an adequate subset of deflections and reactions are provided.

As a difference with the static formulation, the dynamic one uses masses, modal frequencies and modal deflections to obtain the mechanical parameters. In this thesis, first of all the Direct SSI is presented as a means of obtaining the actual modal frequencies and deflections. Then, the formulation of the Inverse SSI is proposed and its results validated by applying the method to a structure. Finally, a parametric analysis of a more complex structure is presented to illustrate the performance of the method.

The results obtained show, for the very first time, how observability techniques might be efficiently used for the identification of structural systems using dynamic data. These lead to significant conclusions regarding the functioning of an SSI method based on dynamic measurements and the importance of knowing the actual characteristics of a structure.

Keywords: Structural System Identification, Observability method, structural dynamics.

Resumen

La necesidad de métodos baratos y simples para inspecciones estructurales ha crecido enormemente en las últimas décadas. Ello es debido al hecho que las actuales estructuras ingenieriles complejas como por ejemplo, estadios, presas, rascacielos, túneles, etc. tienen que mantener su integridad y funcionalidad. El fallo de estas estructuras conduce tanto a consecuencias trágicas como a pérdidas materiales. Además, cuando durante la fase de servicio las estructuras sufren algún tipo de daño, las características mecánicas de la estructura cambian y es importante poder evaluar estar variaciones de las propiedades estructurales.

La Identificación de Sistemas Estructurales (ISE) es un área interdisciplinar la prerrogativa del cual es evaluar la integridad y el estado de estructuras usando técnicas no destructivas.

Esta tesis trata el problema de determinar las características reales de una estructura tales como el módulo de Young, el área, la inercia y/o los productos de los mismos usando medidas dinámicas.

Un método de ISE que se basa en la técnica de observabilidad ha sido ya desarrollada usando medidas estáticas. Se basa en la información proporcionada por el monitoreo de tests estáticos no destructivos. El subconjunto de características de la estructura puede ser definido singularmente sólo cuando se proporciona un subconjunto adecuado de desplazamientos y reacciones.

A diferencia de la formulación estática, la formulación dinámica usa masas, frecuencias modales y desplazamientos modales con tal de obtener los parámetros mecánicos. En esta tesis, en primer lugar el ISE Directo se presenta como una forma de obtener las frecuencias y desplazamientos modales reales. Entonces, la formulación del IES inverso es propuesto y sus resultados validados aplicando el método a una estructura. Finalmente, un análisis paramétrico de una estructura más compleja es llevado a cabo con tal de ilustrar el funcionamiento del método.

Los resultados muestran cómo, por primera vez, las técnicas de observabilidad pueden ser eficientemente usadas para la identificación de sistemas estructurales usando medidas dinámicas. Esto lleva a conclusiones significativas relacionadas con el funcionamiento del método de ISE basado en medidas dinámicas y la importancia de conocer las características reales de una estructura.

Palabras clave: Identificación de Sistemas Estructurales, Método de la observabilidad, dinámica estructural.

Acknowledgements

The author thanks its support to the *Ministerio de Economía y Competitividad* and to the FEDER funds (BIA2013-47290-R).

First and foremost, I would like to express my sincere gratitude to Professor José Turmo, who has been one of the directors of this thesis, but also an academic and personal advisor ever since my stay in Tongji University. I would also like to thank Professor José Antonio Lozano, who has given me advice every time that I was stamped with a problem with the thesis. Finally, I am also grateful to Professor Gonzalo Ramos, who has been part of this project and has given me support when I needed it. To all of them, I am really thankful for their continuous support during my study and research. They have contributed to a rewarding master degree experience by demanding a high quality of work in all my endeavours, engaging me in new ideas and supporting me both personally and institutionally. It has been their strictness and exigency with me that has made me gain knowledge not only about the master thesis topic, but also about other issues concerning my academic future, but it has also been their closeness and kindness that have made me feel encouraged with what I was doing.

I am also thankful to Lei Jun and Marc Reina, who have shared the office with me this year and whose assistance and friendliness has always helped me to move forward.

Definitely, this thesis has needed academic support, but more important has been the emotional support that my university mates have provided me. This master's thesis is not only the culmination of the last year's master, but of the six years that the career in UPC has lasted. Hence, I would like to name here and express my gratitude to Alberto, Rosa Maria, Martinet, Albert, Bernat, Gerard, Helena, Marta and to all those who have shared this long –but enriching– path with me.

There are four people who I absolutely appreciate and admire and without whose support I would probably have not been able to bear the difficulties I have encountered. Thank you Alícia for being always there when I needed a few kind words, thank you Laia for being such an inspiring example of effort and success, thank you Eulàlia for being a constant light of joy. And thank you Alejandro; my success during the last years is unimaginable without your source of inspiration and your stable and strong support.

Lastly, I am indebted to Josep, whose company during our long trip I deeply appreciate and who has been a constant pillar of support during my last master's year. Thank you UC2.

'The secret of change is to focus all of your energy,
not on fighting the old, but on building the new'

— *Socrates*

Contents

List of Tables

List of Figures

Chapter 1

Introduction

1.1 Introduction

Continuously knowing the integrity of in-service structures through its lifetime is a very important objective for manufacturers, end-users and maintenance teams.

This is the function of Structural Health Monitoring (SHM), which aims to give, at every moment during the life of a structure, a diagnosis of the state of the constituent materials, of the different parts, and of the full assembly of these parts constituting the structure as a whole. The state of the structure must remain in the domain specified in the design, although this can be altered by normal ageing due to usage, by the action of the environment, and by accidental events. As it allows performing monitoring in a time-dimension, SHM can also provide prognosis (evolution of damage, residual life, etc.).

Structural System Identification (SSI) lies one of its applications on SHM. However, it is not the only one. When the structural response of a civil structure is modelled, mechanical and geometrical properties of the structural elements are assumed to be known. Nevertheless, in most of the cases the actual characteristics are unknown due to uncertainties in the procedures, stress state and damage. As an example, there exists a high uncertainty in concrete's Young's modulus, as it has dependence on concrete age, humidity and concrete strength, among other factors.

The research on SSI is increasingly becoming more important, as it allows anticipating possible failures of structures; it can be applied to all kinds of structures. For example, to structures operating under

continually changing environments (such as wind turbines, which are under wind induced vibrations or pedestrian bridges), or to deteriorating and ageing infrastructures.

The present document presents a study on SSI and, more particularly, on SSI based on dynamic measurements.

1.2 Objectives

The global objective of this work is to propose a SSI method based on dynamic measurements and to study its performance. With this aim, the following two partial objectives are defined:

1. Developing an algorithm in Matlab able to perform a direct dynamic analysis over any type of structures. Namely, a program that carries out a modal analysis over the eigenvalue equation of structural dynamics to calculate the frequencies of vibration and modal displacements.

2. Developing an algorithm in Matlab able to perform an inverse analysis over any type of structures. This is, writing a code that is able to estimate the mechanical characteristics of a structure (Young's modulus, area, inertia, shear parameter and mass) by using as inputs the modal frequencies and displacements.

1.3 Methodology

In order to accomplish the aforementioned objectives, the methodology intended to be used is related in the following steps:

1. Reviewing the research done in SSI and separating it between the one done using static and/or dynamic measurements. Also, study how the observability method works.

2. Studying the SSI based on the observability method and deepen the knowledge on the studies around static SSI.

3. Reviewing the theory of dynamic of structures in order to be able to propose a method of dynamic SSI based on observability. Specially, work with modal analysis, both theoretically and experimentally.

4. Proposing a SSI method based on observability with dynamic measurements.

5. Studying the performance of the proposed method in both simple and complex structures. Also, validating the method by verifying the equations and applying it to simple structures numerically.

1.4 Thesis organisation

With the above objectives and methodology the thesis is organised in seven chapters. Each chapter is intended to deal with several specific topics –SSI, observability, static and dynamic SSI, etc.–, but with the main objective of approaching the reader to the particularities of dynamic SSI as much as possible.

In Chapter 2, a literature review is presented. This review starts with an introduction about Structural System Identification and its growing importance since it was first studied. Then, the characteristics of the different types of SSI are presented – this is, the research on SSI is divided into the one based on static measurements, on dynamic measurements and on the combination of two. Next, the observability method is presented as a means of identifying a subset of variables which are sufficient to estimate the state of a system. Although it has several applications, the thesis will focus in the one that refers to SSI.

Chapter 3 deals with the Structural System Identification based on the observability method and using static measurements. Even though the main focus of this thesis is the dynamic SSI, it has been considered as necessary to include a chapter presenting the characteristics and principles of the static SSI. Therefore, this chapter addresses the theoretical basis of the method as well as presents the mathematical algorithm used to implement the method with computer tools. Finally, an example is presented of the application of the static identification over a simple structure: a frame.

In Chapter 4 the problem of the direct dynamic observability is dealt with. To do so, first of all the theoretical modal analysis is explained as it is the first step to perform a dynamic SSI. Next, some methods of the experimental modal analysis are presented since they are necessary when applying the dynamic SSI to real structures. Since there are many methods whose goal is to obtain natural frequencies and modal shapes, only three are presented in this thesis: the Peak Picking method, the Frequency Domain Decomposition and the Stochastic Subspace Identification.

In Chapter 5 the inverse dynamic observability is presented. First, a method is proposed to obtain the structure's parameters using dynamic measurements; this is, by measuring displacements, velocities

and accelerations on-site, the natural frequencies and modal shapes might be obtained. With these, the proposed method bases its formulation on the dynamics of structures and the dynamic eigenvalue equation in order to apply the observability method and be able to estimate the structure's characteristics. Next, an algorithm to be applied as a computer tool is proposed.

In Chapter 6 applications of the proposed method are presented. Firstly, three symbolic examples are presented in order to let an easier understanding of the functioning of the program. The examples are done upon a cantilever beam using only one mode of vibration, a cantilever beam using two modes of vibration and a simple frame. Next, a step-by-step numerical application is done in order to verify that the equations leading to the final results are correct. To do so, two cases are presented: the study on a cantilever beam based using one mode of vibration and the study on a simple frame using also one vibration mode. Thirdly, the method is applied to two structures numerically (a cantilever beam and a frame). Then, a symbolic application on a more complex structure is performed. The structure which is dealt with is a 13-story frame; this structure is studied performing both a global SSI and a local SSI.

Finally, in Chapter 7, the main conclusions and major contributions of this thesis are summarised as well as a set of possible future research lines are proposed.

Chapter 2

State of the Art

2.1 Structural system identification

System identification can be defined [26] as "the process of developing or improving a mathematical model of a physical system using experimental data to describe the input, output or response, and noise relationship".

The range of possible uses of system identification is wide. Any process can be characterised by a set of inputs and outputs and therefore, any system can be simulated with a more or less accurate model that reproduces its behaviour (no matter if financial, mathematical, engineering, biological, structural, etc.).

When system identification is performed in order to model a structural system, it can be done by [24]:

(a) Identifying structural parameters such as stiffness, vibration signatures (frequencies, mode shapes, damping ratios) and stress and strain energies.

(b) Structural response.

Among all the subfields of SSI, the estimation of the physical characteristics of a structural system is of particular interest, as finding these parameters can be used to monitor the "health" of a structural system.

As the SSI has been deeply studied, there exist several methods to perform the identification of the parameters of these systems. These methods can be classified according to how the approach relates

the inputs and the outputs. Non-parametric methods adjust outputs to inputs creating a mathematical model to characterise the system. Hence, the established relationship has no explicit physical meaning and they actually tend to require a larger amount of data. On the other hand, parametric methods relate inputs to outputs on the basis of an actual physical meaning. Due to this physical basis, these kinds of methods make it possible to obtain parametric equations of the identified variables, driving to a better understanding of the problem and of the sensitivity to certain parameters. These parametric identification algorithms, however, depend strongly on the accuracy of the measured data. They cannot provide the required accuracy and reliability needed for complex system identifications of real life structures due to complicated nonlinear nature of behaviour of civil structures, and incomplete, incoherent, and noise-contaminated measurements of structural response to strong ground motions. They are particularly effective for large-scale structures due to their complicated nonlinear behaviour and the incomplete, incoherent, and noise-contaminated measurements of structural response under extreme loadings. In the nonparametric approach, the input-output map is characterised and determined by a system model that may not have any explicit physical meaning. In general, the system model does not represent any physical quantity directly, but it is trained to approximate a physical structure and predict the structural responses. As such, the approach does not require complete and coherent measurements of the structural response to strong ground motions. It has better adaptability than the parametric methods.

Besides the parametric/non-parametric classification, SSI can be classified depending on the nature of the excitation test; this is dynamic and static ones, according to whether or not they engage inertial effects.

Recently, there has been many studies endeavour for damage detection, assessment of structures and health monitoring by using either the dynamic approach from dynamic test data or the static approach from static test data. Dynamic approaches have been developed more actively, although static approaches do have advantages as they are simpler and comparatively cheaper than the dynamic ones according to some authors [1]. However, there are researchers that argue that from a practical point of view, estimation of parameters from static response is less appealing than doing it from modal or dynamic response. This is so because it is much easier to dynamically excite a large structure than it is to do it statically. Moreover, it is easier to measure accelerations than displacements because of the simplicity of establishing an inertial reference frame for measuring accelerations.

Structural system identification finds applications in:

1. Determination of structural properties such as the stiffness and natural periods and measurements.

2. Nondestructive damage evaluations, where input-output measurements are used to assess nondestructively the damage severity and location in an existing structure.

3. Health monitoring of the global or local conditions of structures.

4. Structural control of smart structures, which requires evaluation of dynamic response of structures with various structural rigidities, masses and damping.

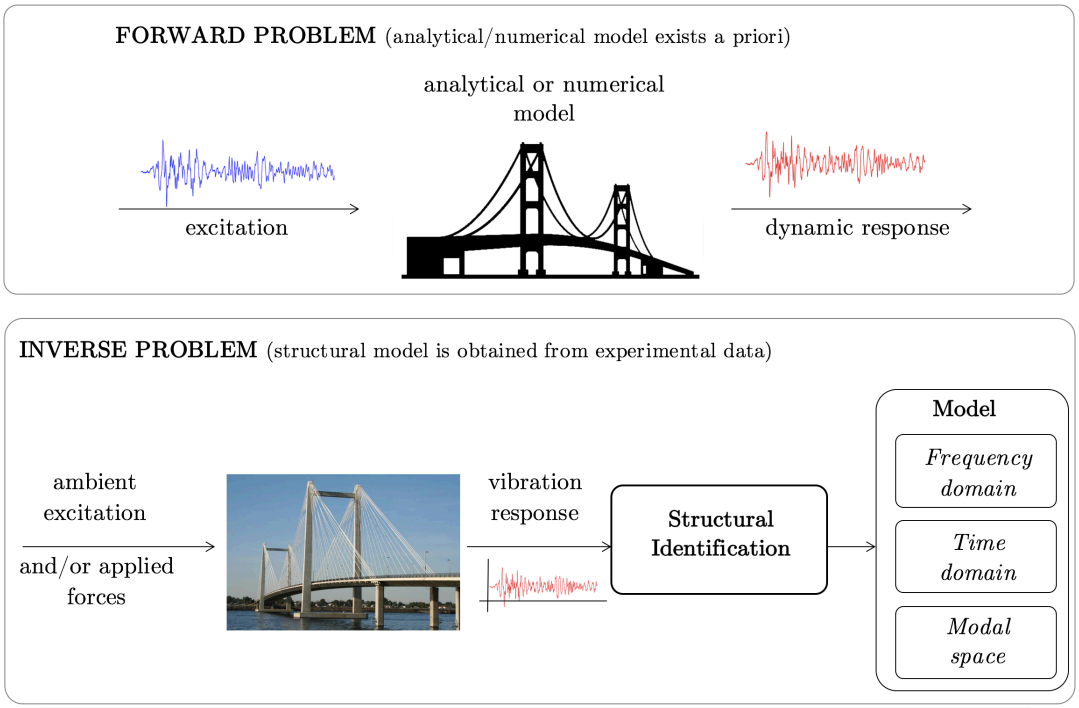

Figure 2.1: Inverse and forward problem in system identification

2.1.1 Static SSI

The beginning of literature on parameter estimation of structural systems based on static response dates back to 1982, when Sheena and Zalmanovich [51] presented a method for improving the analytical stiffness matrix from noise free static measurements. From measurements at certain degrees of freedom, they used spline functions to predict the remaining unmeasured degrees of freedom. All the elements of the stiffness matrix were adjusted in order to minimize the difference between the actual and analytical stiffness matrices subject to measured displacement constraints.

Sanayei and Nelson [46] and Sanayei and Scampoli [49] estimated structural stiffnesses at the element

level by minimizing the difference between the applied and internal forces (equation error approach). However, for their method, deformations measured at the same degrees of freedom that the external loads were applied were required. This drawback was eliminated in 1991, when Sanayei and Onipede used a condensation procedure for this purpose [47]. At the same time, Hjelmstad described an approach to parameter estimation of complex linear structures based on the principle of virtual work for static and modal experiments. In order to deal with the incompletely measured systems, a condensation procedure was used; they studied the behavior of the method in a noisy environment using numerical simulations. Just before, in 1989, Hajela and Soeiro [18] had classified the parameter estimation techniques into the equation error, output error and minimum deviation approaches. They assumed that the mass matrix did not change and lumped all elemental parameters into a single parameter. They used both measured static and modal responses to assess stiffness change on element-by-element basis in structural systems. When dealing with parameter estimation of large structures, they proposed some substructuring and order reduction techniques.

In 1996, Sanayei [48] presented a method for structural parameter identification using elemental strain measurements. It was an optimization-based parameter estimation method to adjust the parameters of a finite element model with simulated static strain measurements. Forces were applied at a subset of DOFs and strains were measured on a limited number of structural elements. By using the Gauss-Newton method or the steepest descent method, an iterative approach was established to solve for the structural stiffnesses at the element level.

In 1997, Hejelmstad and Shin proposed an adaptive parameter-grouping algorithm to localize damage in a structural system for which the measured data are sparse [20]. The algorithm can evaluate the sensitivity of each member parameter simultaneously with the process of damage detection, but requires much computation due to the number of perturbation trials involved in the algorithm.

Some years later, in 2000, Cui [12] developed a damage detection algorithm based on static displacement and static strain. The identified result is ideal, but this method requires sufficient measurement information and load cases. A year later, Wang presented a damage identification algorithm [54] using both static test data and natural frequencies, which is very effective in the case of single damage, but only the location important to the structural deformation can be identified in the case of multiple damages.

In 2005 a method was developed for structural damage identification using limited test static displacement based on grey system theory. The damages were first localized by using the node grey relation

coefficient, and then, a based on the quadratic programming technique iterative procedure for solving nonlinear programming problems was used to identify the extent of the damage.

The essential expression of the grey relation coefficient (GRC) was first formulated by Deng ([14]). The grey relational space is one that describes the posture relationships between one main factor and all the other factors in a given system.

2.1.2 Dynamic SSI

In 2012, Sirca and Adeli reviewed the representative research reported in articles published in journals since 1995 in the field of SI when the structure is subject to dynamic loading [24]. They divided the references according to the approach used:

i. Conventional modal-based approaches.

ii. Biologically-inspired approaches (such as neural network and genetic algorithm).

iii. Signal processing-based approaches (such as wavelets).

iv. Chaos theory.

v. Multi-paradigm approaches.

The first approach typically uses a computer model of the structure (such a FE model) to identify the structural parameters primarily from field or laboratory data.

The advantages of using this approach are modeling and estimating the physical properties and convenience. The main disadvantage is that it does not produce accurate results for large and complex real-life structures.

Model-based system identification methods cannot be used effectively for large and complicated real-world structures with nonlinear behaviour. For such cases, biologically-inspired or softcomputing techniques such as Neural Networks, Genetic Algorithms, or particle swarm optimization have been proposed as a more effective approach.

The accuracy of the NN models depends on how it is trained to solve new problems. A poorly trained model using sparse and/or corrupted data leads to inaccurate results. Some researchers have used biologically inspired methods to enhance model-based methods in an attempt to reduce the shortcomings of the traditional model based approach.

Thirdly, wavelets have been used increasingly in the past two decades to solve complicated time series pattern recognition problems.

Wavelet representation is based on a fundamental concept of representing arbitrary functions in terms of the translations and dilations of a single localized small wave or wavelet function. Unlike the Fourier basis functions, the wavelet basis functions are localized both in space and in frequency so the wavelet analysis can provide time-frequency information about a function that in many practical situations is more pertinent than the standard Fourier analysis. Wavelets also provide a powerful approximation tool that can be used to synthesise economically, using a minimal number of basis elements, functions which are difficult to approximate by other methods.

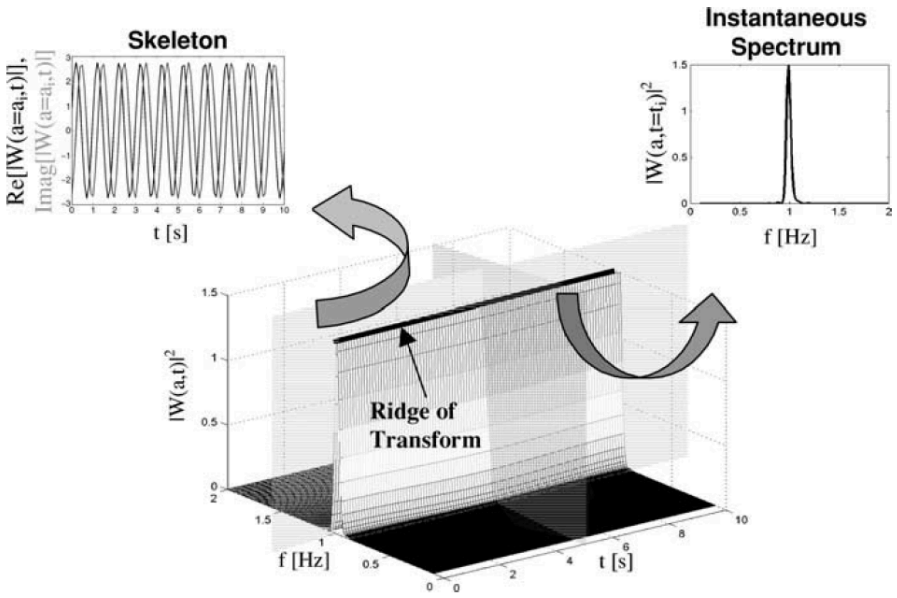

Figure 2.2: Wavelet time-frequency system identification concept [29]

It has increasingly been used in transportation engineering, like in [27] and [28], where they were used for detection of freeway incidents or for estimating the work zone capacity and queue length and delay. Wavelets have also been used in structural engineering, such as in [57], were the basis wavelet function was generated by records of ground motion with the objective of investigating the characteristics of accelerograms recorded on various types of sites and their effects on several structures or in [2], where dynamic environmental disturbance signals due to winds and earthquakes were used in order to build an algorithm for structures control.

Kijewski and Kareem (2003) discussed the considerations to be taken when working with wavelets in the system identification field [29].

In 2005 Huang also used a wavelet-based approach for structural parameters identification [21]. They proposed a procedure that performed wavelet transformation on earthquake responses or free vibration responses of a structure in order to directly determine its natural frequencies, damping rations and mode shapes without extracting impulse response functions. It applied a discrete wavelet transformation to discrete equations of motion. Then, the parameters of the equations of motion were determine by least-squares approach and directly used to determine the dynamic characteristics of the structure. They proved its applicability by applying it on measured dynamic responses of a five-story steel frame and of a five-span arch bridge.

Chaos theory has been employed by some researchers to model structural dynamics for system identification.

Briefly, polynomial chaos is a non-sampling-based method to determine evolution of uncertainty in a dynamical system, when there is probabilistic uncertainty in the system parameters.

It has been used, for example, in 2011 by Schoefs [50]. He used polynomial chaos representation for identification of mechanical characteristics of complex instrumented structures such as harbor structures. A decomposition of random variableson Polynomial Chaos was selected and it was shown to represent better the basic variables in comparison to preselected distribution functions, when considering maximum likelihood estimate. The decomposed variables were used for a stochastic analysis to be further updated with available monitoring data. The model could be used to follow the structure behavior during in-service or extreme conditions and to perform a reliability analysis.

This theory was also used the same year by Li [31] through Katzs Fractal Dimension measure of displacement mode shape for damage localization in beams.

Finally, multi-paradigm approaches integrate two or more computing paradigms such as neural networks, fuzzy logic, evolutionary computing, signal processing (such as wavelets) and chaos theory to come up with more powerful approaches especially for nonlinear and complex problems.

Until 2003, wavelets had not been used for nonparametric system identification of structures. Hung [22] used the neural network model (WNN) for signal processing for system identification of a five-story test framed subjected to simulated earthquake loadings on a shaking table. However, Adeli and Jiang pointed out (2006) that WNN method for SSI suffered from [1]:

(1) Lack of an efficient constructive model.

(2) In order to find the modal parameters the method is trial and error.

(3) When there is noise in the measured data, the convergence rate is slow.

(4) When there exists imprecision in the measured data the identification accuracy is low.

This is why they presented a new multiparadigm dynamic time-delay fuzzy WNN model for nonparametric identification of structures with nonlinear behavior using the nonlinear autoregressive moving average with exogenous inputs (NARMAX approach). The model was based in the integration of four different computing concepts: dynamic time delay neural network, wavelet, fuzzy logic, and the reconstructed state space concept from the chaos theory.

2.1.3 SSI by combination of dynamic and static data

As it has been seen, usually static identification methods are simpler than dynamic ones; however, there is less information that can be used in static damage identification techniques compared with dynamic ones. This makes it more difficult to obtain the perfectly accurate identification result.

On the one hand, dynamic characteristics (modal parameters) give information about the global response of structures and, therefore, they lack of sensitivity to local phenomena. On the other hand, static measurements (such as strains and displacements) do have more sensitivity to the response in their vicinity, which makes them more suitable for local defects determination.

So, taking into account that in every load-bearing structure damage manifests itself because of structural degradation both in changes in dynamic and in static properties, a few researchers have considered the option of combining static and dynamic measurements, as it might lead to better knowledge of the structure.

The first studies combining dynamic and static SSI where made in 1990 [19]. They developed a damage assessment algorithm based on modes, frequencies and static displacements for simulating higher modes. The algorithm consisted in an iterative nonlinear programming method to solve an unconstrained optimization problem. Measurements of static deflections and vibration modes were used in the identification procedure.

Then, in 2001, Wang defined a damage location signature by using changes in the static deformations and natural frequencies [54]. First, to detect the damage location, the Damage Signature Matching

(DSM) technique was improved through defining two damage signatures using the first order approximation of changes in static displacements and natural frequencies. Then, an iterative procedure for solving non-linear programming problems, based on the quadratic programming technique, was proposed to predict the damage extents of possible damaged components detected in the first step.

Finally, in 2013 a group of researchers [41] presented a damage identification methodology that permitted to combine static and dynamic measurements through a model updating procedure by using evolutionary algorithms. Until the moment, the methods had been multi-stage procedures, but this one was simplified to one stage. They defined an objective function according to the results of different test conditions. As the majority of the research done until the moment, they assumed that there was no mass alteration before and after damage. Then, they parameterized the damage by a reduction factor or damage index related to the element bending stiffness. This index allowed to estimate the damage severity and, also, its location since the the damage identification was performed at the element level.

2.2 Observability

The observability analysis refers to the problem of identifying if a set of available measurements is sufficient to estimate the state of a system or of a part of it.

It is said that a subset of variables is observable when the system of equations implies a unique solution for this subset [35], even though the remaining variables remain undetermined. When the system state is observable, it might be relevant to identify critical measurements; this is, those measurements that, if unknown, render the state of the system unobservable. Contrary, if the state of the system is unobservable, it is relevant to identify observable islands; this is, those areas of the system whose respective states can be estimated, and it is also important to identify the minimum set of additional measurements that render the whole system observable.

Observability analysis is the previous step to the estimation of the system. It addresses the question: *do we have enough measurements to estimate the state of a system?*

The observability problem is closely linked to the counter location problem in traffic networks. The aim of

2.2.1 The observability technique

Consider the system of linear equations,

$$[A]\{x\} = \{b\} \tag{2.1}$$

where it is assumed that a subset x_1 of x and a subset b_1 of b are observed (this is, known) and the remaining subsets x_0 of x and b_0 of b are not.

Then, the system in eq. (2.1) can be partitioned as:

$$[A]\{x\} = \begin{pmatrix} A_{00}^{p\times r} & A_{01}^{p\times s} \\ A_{10}^{q\times r} & A_{11}^{q\times s} \end{pmatrix} \begin{Bmatrix} x_0^{r\times 1} \\ x_1^{s\times 1} \end{Bmatrix} = \begin{Bmatrix} b_0^{p\times 1} \\ b_1^{q\times 1} \end{Bmatrix} = \{b\} \tag{2.2}$$

where $A_{00}^{p\times r}$, $A_{01}^{p\times s}$, $A_{10}^{q\times r}$ and $A_{11}^{q\times s}$ are the partitioned matrices of $[A]$ with their dimensions given as superindices and $x_0^{r\times 1}$, $x_1^{s\times 1}$, $b_0^{p\times 1}$ and $b_1^{q\times 1}$ are the partitioned matrices of $\{x\}$ and $\{b\}$, respectively. The subindices 0 and 1 refer to unknown and known variables, respectively.

This is a system of $p + q$ equations. In order to join the unknowns, eq. (2.2) can be written in the alternative equivalent form as:

$$[B]\{z\} = \begin{pmatrix} A_{10}^{q\times r} & 0^{q\times p} \\ A_{00}^{p\times r} & -I^{p\times p} \end{pmatrix} \begin{Bmatrix} x_0^{r\times 1} \\ b_0^{p\times 1} \end{Bmatrix} = \begin{Bmatrix} b_1^{q\times 1} - A_{11}^{q\times s} x_1^{s\times 1} \\ -A_{01}^{p\times s} x_1^{s\times 1} \end{Bmatrix} = \{D\} \tag{2.3}$$

which is a system of $p + q$ equations in $r + p$ unknowns. These unknowns now appear on the left-hand side of the equation and the observations on the right-hand side, whose coefficient matrix is $[B]$ and the independent term column matrix is $\{D\}$.

In eq. (2.3), $0^{q\times p}$ and $I^{p\times p}$ are the null and identity matrices of the indicated dimensiones. In general, this system does not need to be compatible (to have a solution). Actually, matrix $\{D\}$ must satisfy some conditions for the system in eq. (2.3) to have a solution. In order to check whether the system has got a solution, it is sufficient to calculate the null space $[V]$ of $[B]$ and check that $[V]^T\{D\} = 0$. If this holds, the system is compatible; otherwise, it has no solution.

The general solution of eq. (2.3) has the structure (see [9]:

$$\begin{Bmatrix} x_0^{r\times 1} \\ b_0^{p\times 1} \end{Bmatrix} = \begin{Bmatrix} x_{00}^{r\times 1} \\ b_{00}^{p\times 1} \end{Bmatrix} + [V]\{\rho\} \tag{2.4}$$

where $\begin{Bmatrix} x_0^{r\times 1} \\ b_0^{p\times 1} \end{Bmatrix}$ is a particular solution of the system eq. (2.3) and $[V]\{\rho\}$ is the set of all solutions of the associated homogeneous system of equations (which is a linear space of solutions, where the column of $[V]$ is a basis and the elements of the column matrix $\{\rho\}$ are arbitrary real values that represent the coefficients of all possible linear combinations).

It is interesting to note that a variable has a unique solution not only when matrix $[V]$ has zero dimensions (it does not exist), but also when the associated row in matrix $[V]$ is null. Therefore, examination of matrix $[V]$ and identification of its null rows leads to identification of the observable variables (subset of variables with a unique solution).

In order to obtain matrix $[V]$, we need to obtain the null space of matrix $[B]$, which can easily be done with the aid of functions provided by Matlab, for example.

2.2.2 Application of observability to SSI

It has to be noted that not all systems arising in engineering problems are linear as in eq. (2.3). Then, alternative methods need to be used. As it has been previously been said, this thesis faces the problem of Structural System Identification, SSI, using observability techniques.

The following chapter presents an application of SSI based on observability using static measurements, which is a face a nonlinear problem. To solve this observability problem, we can work with a linear system of products of variables, which allows us to use the linear case tools and methods for these variables.

Chapter 3

Static observability

3.1 Observability over the stiffness matrix method

As it has been stated previously in 2.2, many applications can be derived from the observability techniques. One of them was proposed by Lozano-Galant [35], it lies inside the field of civil engineering and is directly related to Structural System Identification.

In his method, Lozano-Galant presents a methodology to be applied over the stiffness matrix method. The stiffness matrix method main objective is to compute the static displacement of a structure given a set of forces and structural parameters; it bases his formulation on equilibrium equations and strength of materials theory, which are written in terms of node forces and displacements. The structure is discretised into bar elements made up of two nodes each. Then, for a structure in 2D, each node has three degrees of freedom (these are the horizontal displacement u_i, the vertical one v_i and the rotation w_i). Hence, if N_N is the total number of nodes of the structure, the stiffness method provides a system of $(3 \times N_N)$ linear equations. These equations might be written in matrix form as:

$$[K]^{(3N_N \times 3N_N)} \times \{\delta\}^{(3N_N \times 1)} = \{f\}^{(3N_N \times 1)} \tag{3.1}$$

equation in which $[K]$ stands for the stiffness matrix of the structure, $\{\delta\}$ for the vector of displacements and $\{f\}$ for the vector of forces; the sizes of these matrices are indicated by the corresponding superindices.

A set of variables might be found in each of the matrices in eq. (3.1); this is:

- The components of the stiffness matrix $[K]$ depend on the characteristics of all the elements of the structures (this is, the N_B beams). If a 2D problem is considered, the characteristics of a beam j are its length, L_j, area, A_j, inertia, I_{Z_j}, and the Young's modulus, E_j.
- Those elements in vector $\{\delta\}$ refer to the deflections of the N_N nodes. In a 2D problem, each node k has got a certain horizontal deflection, u_k, a vertical deflection, v_k, and a rotation, w_k.
- Vector $\{f\}$ includes the forces applied in all N_N nodes. In the case of a 2D problem, there is a force applied in each k in the x-axis direction, H_k, and in the y-axis direction, V_k, as well as a bending moment in the z-axis direction M_k.

The previous information about the different variables in the matrices can be summarised as:

$$[K] = [K(L_j, A_j, I_{Z_j}, E_j)],\ j = 1, N_B \tag{3.2}$$

$$\{\delta\} = \{\delta(u_k, v_k, w_k)\},\ k = 1, N_N \tag{3.3}$$

$$\{f\} = \{f(H_k, V_k, M_k)\},\ k = 1, N_N \tag{3.4}$$

Traditionally, when the stiffness matrix method is used, the variables inside of matrix $[K]$ are assumed as known. With this assumption, the unknown variables might only be found in $\{\delta\}$ and $\{f\}$. Therefore, after defining the boundary conditions and applied forces, it can be assumed that a subset δ_1 of $\{\delta\}$ (which corresponds to the null deflections at the boundary conditions) and a subset f_1 of $\{f\}$ (which corresponds to the forces applied in all the nodes except in the boundary conditions) are known, while the remaining subset δ_0 of $\{\delta\}$ (deflections at the nodes except at the boundary conditions) and f_0 of $\{f\}$ (reactions at the boundary conditions) are not.

However, in most of the structures the values of the mechanical and geometric properties are unknown because of uncertainties in the materials, construction methods, stress state or damage. In these cases, new unknowns appear in matrix $[K]$ apart from those in $\{\delta\}$ and $\{f\}$.

In most 2D problems cases, L_j is assumed to be known whereas the flexural stiffness, E_jI_j, the inertia, I_j, the axial stiffness, E_jA_j, the Young's modulus, E_j, and/or the area, A_j, of the different elements of the structure are considered as unknown. The SSI method is the basis for the determination of these unknown mechanical properties. Since in this case the unknown mechanical properties are multiplied by the displacements of each of the nodes, the problem appears to be a nonlinear one instead of linear, because of the products of variables, such as E_jI_j, E_jA_j, A_jv_k, E_ju_k or I_jw_k. If the nonlinear products

of variables are considered to be linear variables, the system of equations can be solved linearly.

When the unknowns are found in the three matrices $[K]$, $\{\delta\}$ and $\{f\}$, the system in eq. (3.1) can be partitioned as it was presented in eq. (2.2), in a system of $p+q$ equations. Then, the resulting system is the following one:

$$[K]\{\delta\} = \begin{bmatrix} K_{00}^{p\times r} & K_{01}^{p\times s} \\ K_{10}^{q\times r} & K_{11}^{q\times s} \end{bmatrix} \begin{Bmatrix} \delta_0^{r\times 1} \\ \delta_1^{s\times 1} \end{Bmatrix} = \begin{Bmatrix} f_0^{p\times 1} \\ f_1^{q\times 1} \end{Bmatrix} = \{f\} \tag{3.5}$$

With the objective of joining all the unknowns, the system in eq. (3.5) can be written in the following equivalent form as it was presented in eq. (2.3):

$$[B]\{z\} = \begin{bmatrix} K_{10}^{q\times r} & 0^{q\times p} \\ K_{00}^{p\times r} & -I^{p\times p} \end{bmatrix} \begin{Bmatrix} \delta_0^{r\times 1} \\ f_0^{p\times 1} \end{Bmatrix} = \begin{Bmatrix} f_1^{q\times 1} - K_{11}^{q\times s}\delta_1^{s\times 1} \\ -K_{01}^{p\times s}\delta_1^{s\times 1} \end{Bmatrix} = \{D\} \tag{3.6}$$

Then, the observability of eq. (3.6) can be analysed as it was presented in the previous sections.

3.2 Algorithm of the static identification

An algorithm of how the static identification can be computationally implemented is shown in fig. 3.1.

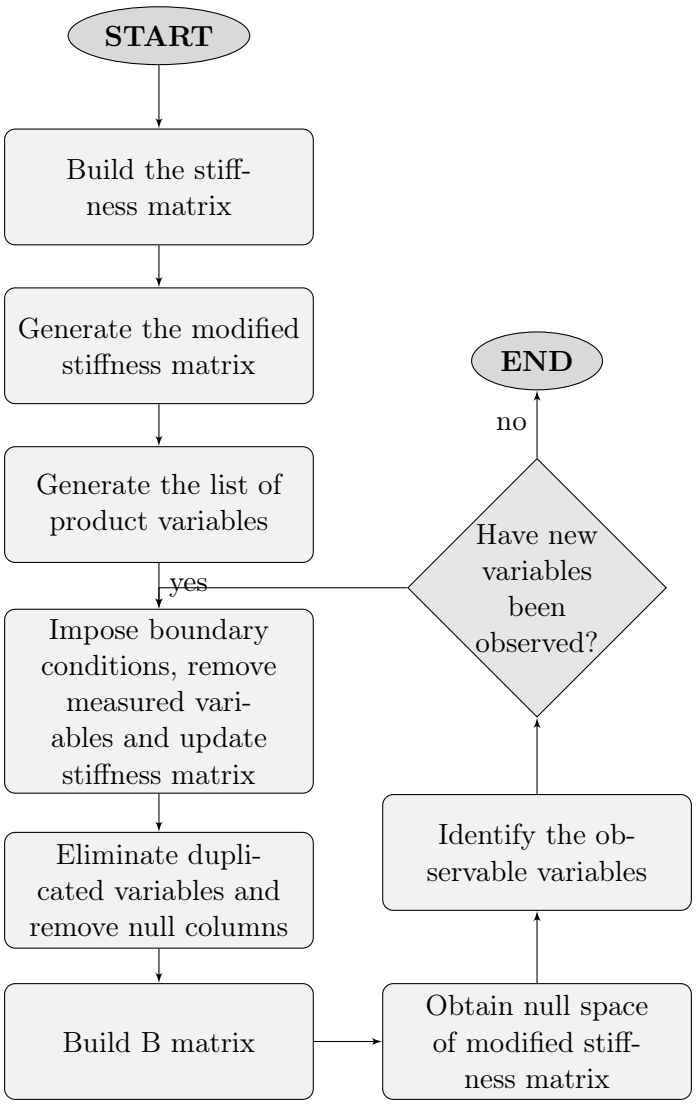

Figure 3.1: Flow chart of the static algorithm

3.3 Example of application of the static identification

An example is presented now in order to better understand the algorithm for static identification using observability shown in fig. 3.1.

The example proposed is based on the simple frame structure that can be seen in fig. 3.2. On the left, the known variables are shown. These are the vertical displacement at node 2 and the horizontal displacement at node 3. On the right and in red, the unknown variables can be seen. These are the three mechanical properties of both elements of the structure: Young's modulus, E, area, A, and inertia, I; also, the rotations at the three nodes are unknown and the horizontal displacement at node 2.

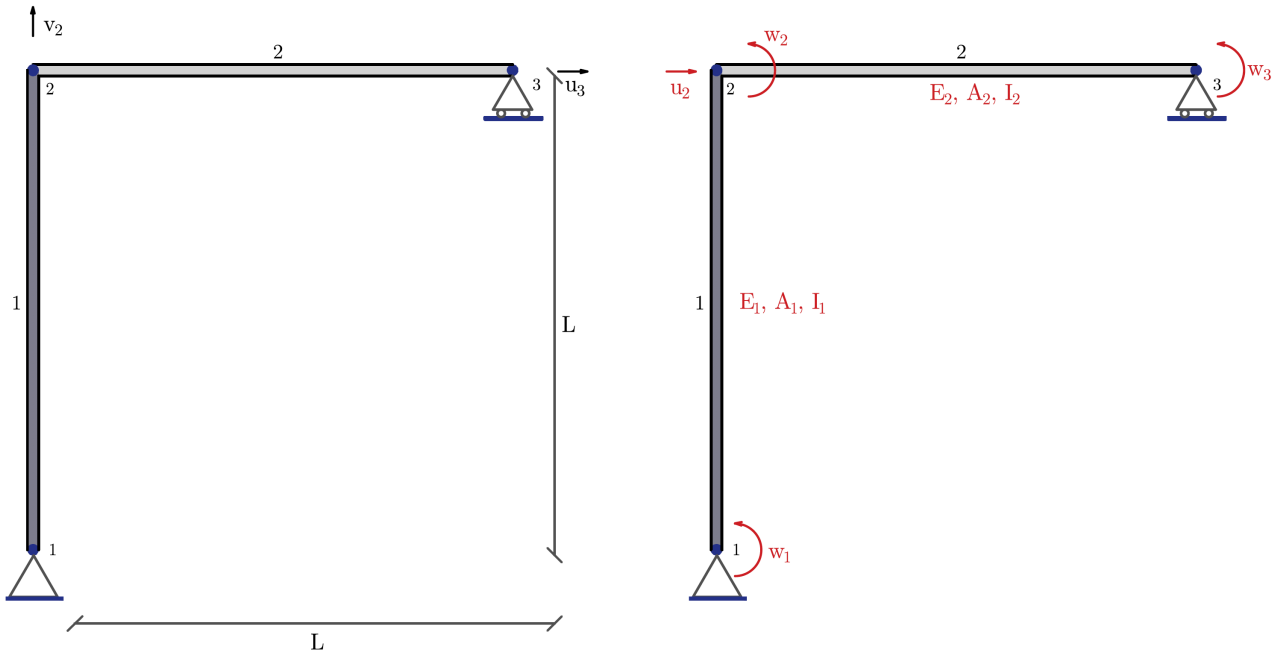

Figure 3.2: Illustration of the frame used in the example of the static SSI algorithm

Step 1. Building stiffness matrix of the structure

In this initial step the stiffness matrix K of the structure is built based on its topology.

$$\begin{Bmatrix} H_1 \\ V_1 \\ M_1 \\ H_2 \\ V_2 \\ M_2 \\ H_3 \\ V_3 \\ M_3 \end{Bmatrix} = \begin{bmatrix} \frac{12E_1I_1}{L_1^3} & 0 & \frac{6E_1I_1}{L_1^2} & -\frac{12E_1I_1}{L_1^3} & 0 & \frac{6E_1I_1}{L_1^2} & 0 & 0 & 0 \\ 0 & \frac{E_1A_1}{L_1} & 0 & 0 & -\frac{E_1A_1}{L_1} & 0 & 0 & 0 & 0 \\ \frac{6E_1I_1}{L_1^2} & 0 & \frac{4E_1I_1}{L_1} & -\frac{6E_1I_1}{L_1^2} & 0 & \frac{2E_1I_1}{L_1} & 0 & 0 & 0 \\ -\frac{12E_1I_1}{L_1^3} & 0 & -\frac{6E_1I_1}{L_1^2} & -\frac{12E_1I_1}{L_1^3}+\frac{E_2A_2}{L_2} & 0 & -\frac{6E_1I_1}{L_1^2} & -\frac{E_2A_2}{L_2} & 0 & 0 \\ 0 & -\frac{E_1A_1}{L_1} & 0 & 0 & \frac{E_1A_1}{L_1}+\frac{12E_2I_2}{L_2^3} & \frac{6E_2I_2}{L_2^2} & 0 & -\frac{12E_2I_2}{L_2^3} & \frac{6E_2I_2}{L_2^2} \\ \frac{6E_1I_1}{L_1^2} & 0 & \frac{2E_1I_1}{L_1} & -\frac{6E_1I_1}{L_1^2} & \frac{6E_2I_2}{L_2^2} & \frac{4E_1I_1}{L_1}+\frac{4E_2I_2}{L_2} & 0 & -\frac{6E_2I_2}{L_2^2} & \frac{2E_2I_2}{L_2} \\ 0 & 0 & 0 & -\frac{E_2A_2}{L_2} & 0 & 0 & \frac{E_2A_2}{L_2} & 0 & 0 \\ 0 & 0 & 0 & 0 & -\frac{12E_2I_2}{L_2^3} & -\frac{6E_2I_2}{L_2^2} & 0 & \frac{12E_2I_2}{L_2^3} & -\frac{6E_2I_2}{L_2^2} \\ 0 & 0 & 0 & 0 & \frac{6E_2I_2}{L_2^2} & \frac{2E_2I_2}{L_2} & 0 & -\frac{6E_2I_2}{L_2^2} & \frac{4E_2I_2}{L_2} \end{bmatrix} \begin{Bmatrix} u_1 \\ v_1 \\ w_1 \\ u_2 \\ v_2 \\ w_2 \\ u_3 \\ v_3 \\ w_3 \end{Bmatrix}$$

Figure 3.3: Step 1

Step 2. Generating the modified stiffness matrix of the structure

Now the modified stiffness matrix of the structure, K^* is built. This is done by separating those columns of the matrix that are made up of summands such that each summand belongs to one column.

See that the corresponding rows of the vector of displacements δ are duplicated in order to keep verifying the equations.

$$\begin{Bmatrix} H_1 \\ V_1 \\ M_1 \\ H_2 \\ V_2 \\ M_2 \\ H_3 \\ V_3 \\ M_3 \end{Bmatrix} = \begin{bmatrix} \frac{12E_1I_1}{L_1^3} & 0 & \frac{6E_1I_1}{L_1^2} & -\frac{12E_1I_1}{L_1^3} & 0 & 0 & 0 & \frac{6E_1I_1}{L_1^2} & 0 & 0 & 0 & 0 \\ 0 & \frac{E_1A_1}{L_1} & 0 & 0 & 0 & -\frac{E_1A_1}{L_1} & 0 & 0 & 0 & 0 & 0 & 0 \\ \frac{6E_1I_1}{L_1^2} & 0 & \frac{4E_1I_1}{L_1} & -\frac{6E_1I_1}{L_1^2} & 0 & 0 & 0 & \frac{2E_1I_1}{L_1} & 0 & 0 & 0 & 0 \\ -\frac{12E_1I_1}{L_1^3} & 0 & -\frac{6E_1I_1}{L_1^2} & -\frac{12E_1I_1}{L_1^3} & \frac{E_2A_2}{L_2} & 0 & 0 & -\frac{6E_1I_1}{L_1^2} & 0 & -\frac{E_2A_2}{L_2} & 0 & 0 \\ 0 & -\frac{E_1A_1}{L_1} & 0 & 0 & 0 & \frac{E_1A_1}{L_1} & \frac{12E_2I_2}{L_2^3} & 0 & \frac{6E_2I_2}{L_2^2} & 0 & -\frac{12E_2I_2}{L_2^3} & \frac{6E_2I_2}{L_2^2} \\ \frac{6E_1I_1}{L_1^2} & 0 & \frac{2E_1I_1}{L_1} & -\frac{6E_1I_1}{L_1^2} & 0 & 0 & \frac{6E_2I_2}{L_2^2} & \frac{4E_1I_1}{L_1} & \frac{4E_2I_2}{L_2} & 0 & -\frac{6E_2I_2}{L_2^2} & \frac{2E_2I_2}{L_2} \\ 0 & 0 & 0 & 0 & -\frac{E_2A_2}{L_2} & 0 & 0 & 0 & 0 & \frac{E_2A_2}{L_2} & 0 & 0 \\ 0 & 0 & 0 & 0 & 0 & 0 & -\frac{12E_2I_2}{L_2^3} & 0 & -\frac{6E_2I_2}{L_2^2} & 0 & \frac{12E_2I_2}{L_2^3} & -\frac{6E_2I_2}{L_2^2} \\ 0 & 0 & 0 & 0 & 0 & 0 & \frac{6E_2I_2}{L_2^2} & 0 & \frac{2E_2I_2}{L_2} & 0 & -\frac{6E_2I_2}{L_2^2} & \frac{4E_2I_2}{L_2} \end{bmatrix} \begin{Bmatrix} u_1 \\ v_1 \\ w_1 \\ u_2 \\ u_2 \\ v_2 \\ v_2 \\ w_2 \\ w_2 \\ u_3 \\ v_3 \\ w_3 \end{Bmatrix}$$

Figure 3.4: Step 2

Step 3. Generating the list of product variables

At this stage the set of all product variables corresponding to each column is to be identified and moved to the column matrix δ of displacements. A modified column matrix δ^* is obtained.

After this step, the matrix K^* becomes a matrix of constant terms, since all the variables (E, I and A) have been moved out.

It can be seen that the list of product variables corresponds now to the vector δ^*.

$$\begin{Bmatrix} H_1 \\ V_1 \\ M_1 \\ H_2 \\ V_2 \\ M_2 \\ H_3 \\ V_3 \\ M_3 \end{Bmatrix} = \begin{bmatrix} \frac{12}{L_1^3} & 0 & \frac{6}{L_1^2} & -\frac{12}{L_1^3} & 0 & 0 & 0 & \frac{6}{L_1^2} & 0 & 0 & 0 & 0 \\ 0 & \frac{1}{L_1} & 0 & 0 & 0 & -\frac{1}{L_1} & 0 & 0 & 0 & 0 & 0 & 0 \\ \frac{6}{L_1^2} & 0 & \frac{4}{L_1} & -\frac{6}{L_1^2} & 0 & 0 & 0 & \frac{2}{L_1} & 0 & 0 & 0 & 0 \\ -\frac{12}{L_1^3} & 0 & -\frac{6}{L_1^2} & -\frac{12}{L_1^3} & \frac{1}{L_2} & 0 & 0 & -\frac{6}{L_1^2} & 0 & -\frac{1}{L_2} & 0 & 0 \\ 0 & -\frac{1}{L_1} & 0 & 0 & 0 & \frac{1}{L_1} & \frac{12}{L_2^3} & 0 & \frac{6}{L_2^2} & 0 & -\frac{12}{L_2^3} & \frac{6}{L_2^2} \\ \frac{6}{L_1^2} & 0 & \frac{2}{L_1} & -\frac{6}{L_1^2} & 0 & 0 & \frac{6}{L_2^2} & \frac{4}{L_1} & \frac{4}{L_2} & 0 & -\frac{6}{L_2^2} & \frac{2}{L_2} \\ 0 & 0 & 0 & 0 & -\frac{1}{L_2} & 0 & 0 & 0 & 0 & \frac{1}{L_2} & 0 & 0 \\ 0 & 0 & 0 & 0 & 0 & 0 & -\frac{12}{L_2^3} & 0 & -\frac{6}{L_2^2} & 0 & \frac{12}{L_2^3} & -\frac{6}{L_2^2} \\ 0 & 0 & 0 & 0 & 0 & 0 & \frac{6}{L_2^2} & 0 & \frac{2}{L_2} & 0 & -\frac{6}{L_2^2} & \frac{4}{L_2} \end{bmatrix} \begin{Bmatrix} E_1I_1u_1 \\ E_1A_1v_1 \\ E_1I_1w_1 \\ E_1I_1u_2 \\ E_2A_2u_2 \\ E_1A_1v_2 \\ E_2I_2v_2 \\ E_1I_1w_2 \\ E_2I_2w_2 \\ E_2A_2u_3 \\ E_2I_2v_3 \\ E_2I_2w_3 \end{Bmatrix}$$

Figure 3.5: Step 3

Step 4. Imposing boundary conditions, removing measured variables and updating modified stiffness matrix

In this step all the columns of K^* that are associated with boundary conditions are multiplied by their corresponding values and the associated factors are removed from δ^*. In this case, the boundary

conditions are $u_1 = v_1 = 0$ for the first node and $v_3 = 0$ for the third one. Therefore, the corresponding columns become zero.

Apart from this, also the measured variables are introduced into K^* and their factor removed from δ^*. In this example, it is the case of v_2 and u_3. It is shown in fig. 3.6.

$$\begin{Bmatrix} H_1 \\ V_1 \\ M_1 \\ H_2 \\ V_2 \\ M_2 \\ H_3 \\ V_3 \\ M_3 \end{Bmatrix} = \begin{bmatrix} 0 & 0 & \frac{6}{L_1^2} & -\frac{12}{L_1^3} & 0 & 0 & 0 & \frac{6}{L_1^2} & 0 & 0 & 0 & 0 \\ 0 & 0 & 0 & 0 & 0 & -\frac{v_2}{L_1} & 0 & 0 & 0 & 0 & 0 & 0 \\ 0 & 0 & \frac{4}{L_1} & -\frac{6}{L_1^2} & 0 & 0 & 0 & \frac{2}{L_1} & 0 & 0 & 0 & 0 \\ 0 & 0 & -\frac{6}{L_1^2} & -\frac{12}{L_1^3} & \frac{1}{L_2} & 0 & 0 & -\frac{6}{L_1^2} & 0 & -\frac{u_3}{L_2} & 0 & 0 \\ 0 & 0 & 0 & 0 & 0 & \frac{v_2}{L_1} & \frac{12v_2}{L_2^3} & 0 & \frac{6}{L_2^2} & 0 & 0 & \frac{6}{L_2^2} \\ 0 & 0 & \frac{2}{L_1} & -\frac{6}{L_1^2} & 0 & 0 & \frac{6v_2}{L_2^2} & \frac{4}{L_1} & \frac{4}{L_2} & 0 & 0 & \frac{2}{L_2} \\ 0 & 0 & 0 & 0 & -\frac{1}{L_2} & 0 & 0 & 0 & 0 & \frac{u_3}{L_2} & 0 & 0 \\ 0 & 0 & 0 & 0 & 0 & 0 & -\frac{12v_2}{L_2^3} & 0 & -\frac{6}{L_2^2} & 0 & 0 & -\frac{6}{L_2^2} \\ 0 & 0 & 0 & 0 & 0 & 0 & \frac{6v_2}{L_2^2} & 0 & \frac{2}{L_2} & 0 & 0 & \frac{4}{L_2} \end{bmatrix} \begin{Bmatrix} 0 \\ 0 \\ E_1 I_1 w_1 \\ E_1 I_1 u_2 \\ E_2 A_2 u_2 \\ E_1 A_1 \\ E_2 I_2 \\ E_1 I_1 w_2 \\ E_2 I_2 w_2 \\ E_2 A_2 \\ 0 \\ E_2 I_2 w_3 \end{Bmatrix}$$

Figure 3.6: Step 4

Step 5. Eliminating duplicated variables and removing null columns

The variables that appear duplicated are now put together and matrix K^* is compacted by adding the columns corresponding to these duplicated variables. The vector δ^* is then replaced by the non-duplicated variable list.

As it has been previously seen, when some displacements, measured or coming from boundary conditions, are null, they generate null columns in K^*. These columns can be removed together with its associated variables in the list.

In this example, there are no duplicated variables in the variable list and therefore it is only necessary to remove the null columns.

$$\begin{Bmatrix} H_1 \\ V_1 \\ M_1 \\ H_2 \\ V_2 \\ M_2 \\ H_3 \\ V_3 \\ M_3 \end{Bmatrix} = \begin{bmatrix} \frac{6}{L_1^2} & -\frac{12}{L_1^3} & 0 & 0 & 0 & \frac{6}{L_1^2} & 0 & 0 & 0 \\ 0 & 0 & 0 & -\frac{v_2}{L_1} & 0 & 0 & 0 & 0 & 0 \\ \frac{4}{L_1} & -\frac{6}{L_1^2} & 0 & 0 & 0 & \frac{2}{L_1} & 0 & 0 & 0 \\ -\frac{6}{L_1^2} & -\frac{12}{L_1^3} & \frac{1}{L_2} & 0 & 0 & -\frac{6}{L_1^2} & 0 & -\frac{u_3}{L_2} & 0 \\ 0 & 0 & 0 & \frac{v_2}{L_1} & \frac{12v_2}{L_2^3} & 0 & \frac{6}{L_2^2} & 0 & \frac{6}{L_2^2} \\ \frac{2}{L_1} & -\frac{6}{L_1^2} & 0 & 0 & \frac{6v_2}{L_2^2} & \frac{4}{L_1} & \frac{4}{L_2} & 0 & \frac{2}{L_2} \\ 0 & 0 & -\frac{1}{L_2} & 0 & 0 & 0 & 0 & \frac{u_3}{L_2} & 0 \\ 0 & 0 & 0 & 0 & -\frac{12v_2}{L_2^3} & 0 & -\frac{6}{L_2^2} & 0 & -\frac{6}{L_2^2} \\ 0 & 0 & 0 & 0 & \frac{6v_2}{L_2^2} & 0 & \frac{2}{L_2} & 0 & \frac{4}{L_2} \end{bmatrix} \begin{Bmatrix} EI_1w_1 \\ EI_1u_2 \\ EA_2u_2 \\ EA_1 \\ EI_2 \\ EI_1w_2 \\ EI_2w_2 \\ EA_2 \\ EI_2w_3 \end{Bmatrix}$$

Figure 3.7: Step 5

Step 6. Building B matrix

In the sixth step, matrix B is built by grouping together the unknown variables on the left-hand side of the equation.

$$[B]\{z\} = \begin{bmatrix} \frac{6}{L_1^2} & -\frac{12}{L_1^3} & 0 & 0 & 0 & \frac{6}{L_1^2} & 0 & 0 & 0 & 0 & 0 & 0 \\ 0 & 0 & 0 & -\frac{v_2}{L_1} & 0 & 0 & 0 & 0 & 0 & 0 & 0 & 0 \\ \frac{4}{L_1} & -\frac{6}{L_1^2} & 0 & 0 & 0 & \frac{2}{L_1} & 0 & 0 & 0 & 0 & 0 & 0 \\ -\frac{6}{L_1^2} & -\frac{12}{L_1^3} & \frac{1}{L_2} & 0 & 0 & -\frac{6}{L_1^2} & 0 & -\frac{u_3}{L_2} & 0 & 0 & 0 & 0 \\ 0 & 0 & 0 & \frac{v_2}{L_1} & \frac{12v_2}{L_2^3} & 0 & \frac{6}{L_2^2} & 0 & \frac{6}{L_2^2} & 0 & 0 & 0 \\ \frac{2}{L_1} & -\frac{6}{L_1^2} & 0 & 0 & \frac{6v_2}{L_2^2} & \frac{4}{L_1} & \frac{4}{L_2} & 0 & \frac{2}{L_2} & 0 & 0 & 0 \\ 0 & 0 & -\frac{1}{L_2} & 0 & 0 & 0 & 0 & \frac{u_3}{L_2} & 0 & -1 & 0 & 0 \\ 0 & 0 & 0 & 0 & -\frac{12v_2}{L_2^3} & 0 & -\frac{6}{L_2^2} & 0 & -\frac{6}{L_2^2} & 0 & -1 & 0 \\ 0 & 0 & 0 & 0 & \frac{6v_2}{L_2^2} & 0 & \frac{2}{L_2} & 0 & \frac{4}{L_2} & 0 & 0 & -1 \end{bmatrix} \begin{Bmatrix} EI_1w_1 \\ EI_1u_2 \\ EA_2u_2 \\ EA_1 \\ EI_2 \\ EI_1w_2 \\ EI_2w_2 \\ EA_2 \\ EI_2w_3 \\ H_1 \\ V_1 \\ V_3 \end{Bmatrix} = \begin{Bmatrix} M_1 \\ H_2 \\ V_2 \\ M_2 \\ H_3 \\ M_3 \\ 0 \\ 0 \\ 0 \end{Bmatrix} = \{D\}$$

Figure 3.8: Step 6

Step 7. Obtaining null space of matrix B

In order to find out which variables are observable, the null space of matrix B has to be obtained.

It is shown in fig. 3.9.

$$NullSpace = \begin{pmatrix} 0 & 1 & 0 & 0 & 0 & 0 & 0 & 0 \\ 0 & L & 0 & 0 & 1 & \frac{-L}{2} & \frac{-L}{2} & 0 \\ 1 & 0 & 0 & 0 & 0 & 0 & 0 & 0 \\ 0 & 0 & 0 & 0 & 0 & 0 & 0 & 0 \\ 0 & 0 & \frac{-L}{u_2} & 1 & 0 & 0 & \frac{-L}{2u_2} & \frac{-L}{2u_2} \\ 0 & 1 & 0 & 0 & 0 & 0 & 0 & 0 \\ 0 & 0 & 1 & 0 & 0 & 0 & 0 & 0 \\ \frac{1}{u_3} & 0 & 0 & 0 & 0 & 0 & 0 & 0 \\ 0 & 0 & 1 & 0 & 0 & 0 & 0 & 0 \\ 0 & 0 & 0 & 0 & 0 & 0 & 0 & 0 \\ 0 & 0 & 0 & 0 & 0 & 0 & 0 & 0 \\ 0 & 0 & 0 & 0 & 0 & 0 & 0 & 0 \end{pmatrix}$$

Figure 3.9: Step 6

Step 8. Identifying the observable variables

Finally, the observable variables can be identified. The null rows of the matrix with generators of the null space have to be identified; their corresponding associated product variable is the observable variable.

From fig. 3.9 it can be seen that the fourth, tenth, eleventh and twelfth rows are null. This means that the variables from their corresponding rows of vector δ^* are the observable variables. Therefore (see fig. 3.10):

$$Observable = \begin{pmatrix} EA_1 \\ H_1 \\ V_1 \\ V_3 \end{pmatrix}; \quad Unobservable = \begin{pmatrix} EI_1 w_1 \\ EI_1 u_2 \\ EA_2 u_2 \\ EI_2 \\ EI w_2 \\ EI_2 w_2 \\ EA_2 \\ EI_2 w_3 \end{pmatrix}$$

Figure 3.10: Step 6

Step 9. Testing for convergence

The final step is done only if new variables have been observed in step 8. If so, the recursive process starts again from *step 4*. Otherwise, the process is stopped and the program returns the list of all variables.

Chapter 4

Direct dynamic observability

4.1 Theoretical modal analysis

The simplest model of a Single Degree of Freedom system (SDOF system) subjected to an external source of excitation or dynamic loading is generally defined by a set of properties concentrated in a single physical element. This set of properties includes its mass, its elastic properties (flexibility or stiffness) and the energy-loss mechanism or damping. The sketch of this system is presented in fig. 4.1.

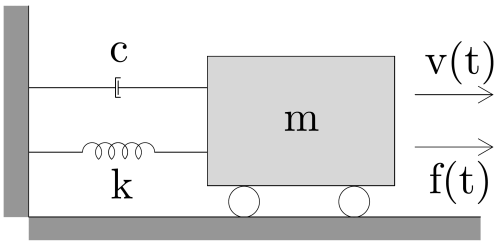

Figure 4.1: Basic Single Degree of Freedom system

The total mass, m, is concentrated in the rigid block. This block is constrained by rollers and it can therefore only move in one direction; this means that the velocity *v(t)* completely defines its position. In the sketch, the elastic resistance is represented by a weightless spring of stiffness k, while the mechanism of energy loss is represented by a damper c. Finally, the external dynamic loading that produces the response of the system is a time-varying force *f(t)*.

The equation of motion of this SDOF can be derived to (see [11]):

$$m\ddot{x} + c\dot{x} + kx = f(t) \tag{4.1}$$

However, this equation holds only if the physical properties of the system are such that its motion might be described by a single coordinate and no other motion is possible. If the structure has in fact more than one mode of displacement possible, the above presented equation will not be a good approximation of the true dynamic behaviour.

This is the reason why the equations of motion of a Multiple Degree of Freedom system (MDOF system) need to be developed. The typical example of this type of system is shown in fig. 4.2, and it is a general simple beam. However, the formulation applies equally to any type of structure.

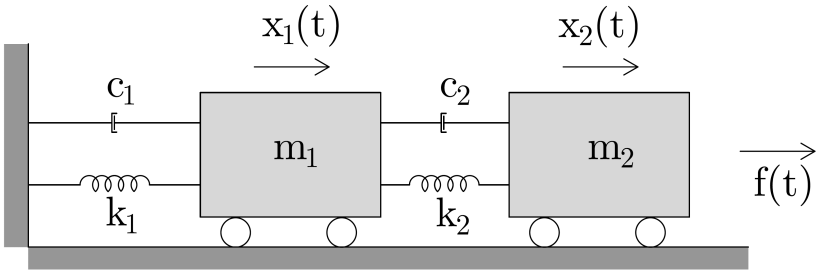

Figure 4.2: Basic Multiple Degree of Freedom system

Then, the complete dynamic equilibrium of the structure, considering all degrees of freedom is:

$$[M]\{\ddot{x}\} + [C]\{\dot{x}\} + [K]\{x\} = \{f\} \tag{4.2}$$

which is equivalent to eq. (4.1) with the only difference that each term of the SDOF equation is represented by a matrix in eq. (4.2). The order of the matrix corresponds then to the number of degrees of freedom used in describing the displacements of the structure. Namely, eq. (4.2) expresses the N equations of motion which serve to define the response of the MDOF system.

In this equation, matrix $[K]$ is expressed as the traditional stiffness matrix:

$$K = \begin{bmatrix} \frac{EA}{L} & 0 & 0 & -\frac{EA}{L} & 0 & 0 \\ 0 & \frac{12EI}{L^3} & \frac{6EI}{L^2} & 0 & -\frac{12EI}{L^3} & \frac{6EI}{L^2} \\ 0 & \frac{6EI}{L^2} & \frac{4EI}{L} & 0 & -\frac{6EI}{L^2} & -\frac{2EI}{L} \\ -\frac{EA}{L} & 0 & 0 & \frac{EA}{L} & 0 & 0 \\ 0 & -\frac{12EI}{L^3} & -\frac{6EI}{L^2} & 0 & \frac{12EI}{L^3} & -\frac{6EI}{L^2} \\ 0 & \frac{6EI}{L^2} & -\frac{2EI}{L} & 0 & -\frac{6EI}{L^2} & \frac{4EI}{L} \end{bmatrix} \tag{4.3}$$

And the mass matrix $[M]$ might refer to the consistent mass matrix (eq. (4.4)) or to the lumped one

(eq. (4.5)).

$$M_{consistent} = \frac{\rho AL}{420}\begin{bmatrix} 140 & 0 & 0 & 70 & 0 & 0 \\ 0 & 156 & 22L & 0 & 54 & -13L \\ 0 & 22L & 4L^2 & 0 & 13L & -3L^2 \\ 70 & 0 & 0 & 140 & 0 & 0 \\ 0 & 54 & 13L & 0 & 156 & -22L \\ 0 & -13L & -3L^2 & 0 & -22L & 4L^2 \end{bmatrix} \tag{4.4}$$

$$M_{lumped} = \frac{\rho AL}{2}\begin{bmatrix} 1 & 0 & 0 & 0 & 0 & 0 \\ 0 & 1 & 0 & 0 & 0 & 0 \\ 0 & 0 & \frac{L^2}{12} & 0 & 0 & 0 \\ 0 & 0 & 0 & 1 & 0 & 0 \\ 0 & 0 & 0 & 0 & 1 & 0 \\ 0 & 0 & 0 & 0 & 0 & \frac{L^2}{12} \end{bmatrix} \tag{4.5}$$

If a freely vibrating undamped system is considered, the equations of motion for the corresponding displacements might be obtained by omitting the damping matrix and the applied loads vector from eq. (4.2) as follows:

$$[M]\{\ddot{x}\} + [K]\{x\} = 0 \tag{4.6}$$

where 0 is a zero vector.

If the free vibration motion is assumed to be simple harmonic, it may be expressed for a MDOF system as:

$$x(t) = \hat{x}\sin(\omega t + \theta) \tag{4.7}$$

where $\hat{x}$ represents the shape of the system, which does not change with time, and θ is the phase angle.

If the second time derivative is taken from eq. (4.7), the accelerations in free vibration are obtained, which are:

$$\ddot{x} = -\omega^2\hat{x}\sin(\omega t + \theta) = -\omega^2 x \tag{4.8}$$

And substituting eqs. (4.7) and (4.8) into eq. (4.6) yields into:

$$-\omega^2[M]\hat{x}\sin(\omega t + \theta) + [K]\hat{x}\sin(\omega t + \theta) = 0 \tag{4.9}$$

and since the trigonometric term may be omitted, the expression in eq. (4.9) may be written as:

$$[K - \omega^2 M]\phi = 0 \tag{4.10}$$

Equation (5.1) is one of the ways of expressing what is called the **eigenvalue** or **characteristic value** problem. The quantities ω^2 are the eigenvalues or characteristic values, and they represent the square of the free-vibration frequencies. On the other hand, the corresponding displacement vectors ϕ express the displacement shapes of the vibrating system and they are usually referred to as the eigenvectors or mode shapes.

The solution to this set of simultaneous equations is of the form:

$$\phi = \frac{0}{\|K - \omega^2 M\|} \tag{4.11}$$

Therefore, a nontrivial solution is only possible when the denominator determinant vanishes. In other words, finit-amplitude vibrations are only possible when:

$$\|K - \omega^2 M\| = 0 \tag{4.12}$$

Equation (5.3) is the so-called **frequency equation** of the system. If the determinant is expanded, it will give an algebraic equation with N roots for a system having N degrees of freedom. The roots represent the frequencies of the several modes of vibration that are possible in the system.

The mode with the lowest frequency is the first mode, the next higher frequency is the second mode, and so on. The frequency vector is made up of the total set of modal frequencies, arranged in sequence:

$$\omega = \begin{Bmatrix} \omega_1 \\ \omega_2 \\ \omega_3 \\ \vdots \\ \omega_N \end{Bmatrix} \tag{4.13}$$

Another way of writing eq. (5.1) is the following one, where the square frequency ω^2 is written as λ:

$$[K]\{\Phi\}_i = \lambda_i [M]\{\Phi\}_i \tag{4.14}$$

4.2 Experimental modal analysis

Modal analysis is a key step in the estimation of the axial force of a structural member as knowing the natural frequencies of the system is fundamental in many formulations regarding dynamic analysis of structures.

The modal parameter estimation technique has evolved over the years, developing several methods. However, some of these methods can lead to inaccuracies due to its simplicity, and some of them can be highly complex.

From all the existing methods three have been chosen to be explained with more detail in this chapter in order to better understand how experimental modal analysis works.

In Peak Picking the power spectra of time histories measurements are computed by discrete Fourier transform. This technique directly uses the peaks of the spectra to determine modal frequencies.

For the cases of lightly damped structures, a derived relationship between response spectral density and modal parameters provides a basis for the Frequency Domain Decomposition method. In application of the FDD identification algorithm, the power spectral density (PSD) of the output measurements are estimated and then decomposed by taking the Singular Value Decomposition (SVD) of the PSD matrix.

Stochastic subspace identification is a time-domain identification method which can determine linear models from column and row spaces of the matrices computed from the input-output data.

4.2.1 Peak Picking

One of the first techniques of modal parameter extraction that was developed was the peak picking technique. Its implementation is based in the fact that the peak of the frequency response function is directly related to the mode shape of the system.

The natural frequencies are picked directly from the power spectral density plot (PSD) and the damping rate corresponds to the sharpness of each peak through application of the half power method.

However, under operational conditions the results obtained from this method strongly depend on user experience and intuition for peak choosing and distinction.

The relationship between the unknown inputs x(t) and the measured responses y(t) to the excitations can be expressed as (Bendat, Julius S., and Piersol, Allan G., Random Data, Analysis and Measurement Procedures, John Wiley and Sons, 1986.):

$$[G_{yy}(j\omega] = [H(j\omega)]^*[G_{xx}(j\omega)][H(j\omega)]^T \tag{4.15}$$

where $G_{xx}(j\omega)$ is the input Power Spectral Density matrix of the input, whose dimensions are $r \times r$ being r the number of inputs. This matrix is constant in case of a stationary zero mean white noise input; this constant will be called C in the following mathematical derivation. $G_{yy}(j\omega)$ is the output PSD matrix with dimensions $m \times m$, where m is the number of responses. $H(j\omega)$ is the frequency response function (FRF) matrix with dimensions $m \times r$.

The FRF matrix can be written in a typical partial fraction form (used in classical modal analysis), in terms of poles and residues:

$$[H(j\omega)] = \frac{Y(\omega)}{H(\omega)} = \sum_{k=1}^{m} \frac{[R_k]}{j\omega - \lambda_k} + \frac{[R_k]^*}{j\omega - \lambda_k^*} \tag{4.16}$$

with

$$\lambda_k = -\sigma_k + j\omega_{dk} \tag{4.17}$$

m being the total number of modes, λ_k being the pole of the k^{th} mode, σ_k the modal damping and ω_{dk} the damped natural frequency of the k^{th} mode:

$$\omega_{dk} = \omega_{0k}\sqrt{1 - \zeta_k^2} \tag{4.18}$$

with

$$\zeta_k = \frac{\sigma_k}{\omega_{0k}} \tag{4.19}$$

ζ_k being the critical damping and ω_{0k} the undamped natural frequency, both for mode k.

$[R_k]$ is called the residue matrix and is expressed in an outer product form:

$$[R_k] = \psi_k \gamma_k^T \tag{4.20}$$

where psi_k is the mode shape and γ_k is the modal participation vector. All those parameters are specified for the k^{th} mode.

The transfer function $[H]$ is symmetric and an element $H_{pq}(j\omega)$ of this matrix is then written in terms of the component $r_{kpq}(j\omega)$ of the residue matrix as follows:

$$H_{pq}(j\omega) = \sum_{k=1}^{m} \frac{r_k(p,q)}{j\omega - \lambda_k} + \frac{r_k(p,q)^*}{j\omega - {\lambda_k}^*} \tag{4.21}$$

Using eq. (4.15) for the matrix G_{yy} and the heaviside partial fraction theorem or polynomial expansions, we obtain the following expression for the matrix output PSD, matrix G:

$$G_{yy}(j\omega) = \sum_{k=1}^{m} \frac{[A_k]}{j\omega - \lambda_k} + \frac{[A_k]^*}{j\omega - {\lambda_k}^*} + \frac{[B_k]}{-j\omega - \lambda_k} \frac{[B_k]^*}{-j\omega - {\lambda_k}^*} \tag{4.22}$$

where $[A_k]$ is the k^{th} residue matrix of the matrix G_{yy}. The matrix G_{xx} is assumed to be a constant value C, since the excitation signals are assumed to be uncorrelated zero mean white noise in all the measured DOFs. This matrix is Hermitian and is described in the form:

$$[A_k] = [R_k]C \sum_{s=1}^{m} \frac{[R_s]^H}{-\lambda_k - {\lambda_s}^*} + \frac{[R_s]^T}{-\lambda_k - \lambda_s} \tag{4.23}$$

The contribution of the residue has the following expression:

$$[A_k] = \frac{[R_k]C[R_k]^H}{2\sigma_k} \tag{4.24}$$

At this point, the peak picking technique can be performed by simply choosing the peaks from the matrix output PSD.

Figure 4.3 shows two examples of the Peak Picking method. They have been obtained from the same experiment, but using sensors in two different locations. The graphs shown have already been converted to the frequency domain. One of them shows the first five modes as very clear peaks, while in the other one some peaks are not very clear.

This proves the effectiveness of the PP technique in some cases, but it can lead to errors sometimes. In the next subsection, a more accurate method is presented.

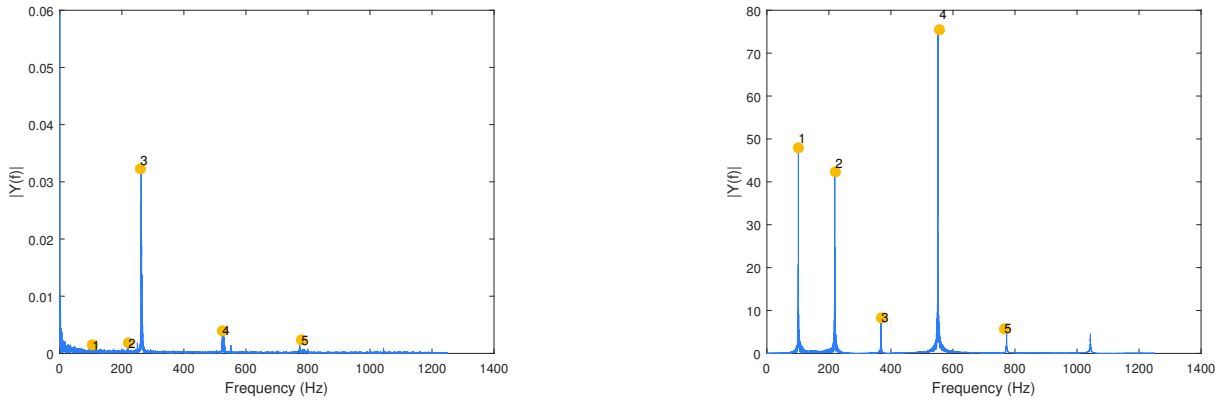

Figure 4.3: Graph examples of the functioning of the Peak Picking method

4.2.2 Frequency Domain Decomposition

The frequency domain decomposition technique follows the first steps of the peak picking technique. Then, it considers a lightly damped model for its formulation.

Considering a lightly damped model, we have the following relationship:

$$\lim_{damping \to light}[A_k] = [R_k]C[R_k]^T = \psi_k \gamma_k^T C \gamma_k \psi_k^T = d_k \psi_k \psi_k^T \tag{4.25}$$

where d_k is a scalar constant.

The contribution of the modes at a particular frequency is limited to a finite number (usually 1 or 2). The response spectral density matrix can then be written as the following final form:

$$[G_{yy}(j\omega)] = \sum_{k \in Sub(\omega)} \frac{d_k \psi_k \psi_k^H}{j\omega - \lambda_k} + \frac{d_k^* \psi_k^* \psi_k^H}{j\omega - \lambda_k^*} \tag{4.26}$$

where $Sub(\omega)$ is the set of modes that contribute at the particular frequency.

This final form of the matrix is then decomposed into a set of singular values and singular vectors using the Singular Value Decomposition technique (SVD). This decomposition is performed to identify single degree of freedom models of the problem.

The singular value decomposition of an $m \times n$ complex matrix A is the following factorization:

$$A = U \Sigma V^H \tag{4.27}$$

where U and V are unitary and Σ is a diagonal matrix that contains the real singular values.

$$\Sigma = diag(s_1, \cdots, s_r) \tag{4.28}$$

$$r = min(m, n) \tag{4.29}$$

The superscript H on the matrix V denotes a Hermitian transformation (transpose and complex conjugate). In the case of real valued matrices, the V matrix is only transposed. The s_i elements in the matrix Σ are called the singular values and their following singular vectors are contained in the matrices U and V.

This singular value decomposition is performed for each of the matrices at each frequency and for each measurement (see fig. 4.4). The spectral density matrix is then approximated to the following expression after SVD decomposition:

$$[G_{yy}(j\omega)] = [\Phi][\Sigma][\Phi]^H \tag{4.30}$$

with

$$[\Phi]^H[\Phi] = [I] \tag{4.31}$$

Σ being the singular value matrix and Φ the singular vectors unitary matrix:

$$[\Sigma] = diag(s_1, \cdots, s_r) = \begin{bmatrix} s_1 & 0 & 0 & . & . & 0 \\ 0 & s_2 & 0 & . & . & . \\ 0 & 0 & s_3 & . & . & . \\ . & . & . & . & . & 0 \\ . & . & . & . & s_r & 0 \\ 0 & . & . & 0 & 0 & 0 \end{bmatrix} \tag{4.32}$$

$$[\Phi] = [\{\varphi_1\}\{\varphi_2\}\{\varphi_3\}\cdots\{\varphi_r\}] \tag{4.33}$$

The number of nonzero elements in the diagonal of the singular matrix corresponds to the rank of each spectral density matrix. The singular vectors correspond to an estimation of the mode shapes and the corresponding singular values are the spectral densities of the SDOF system expressed in eq. (4.26).

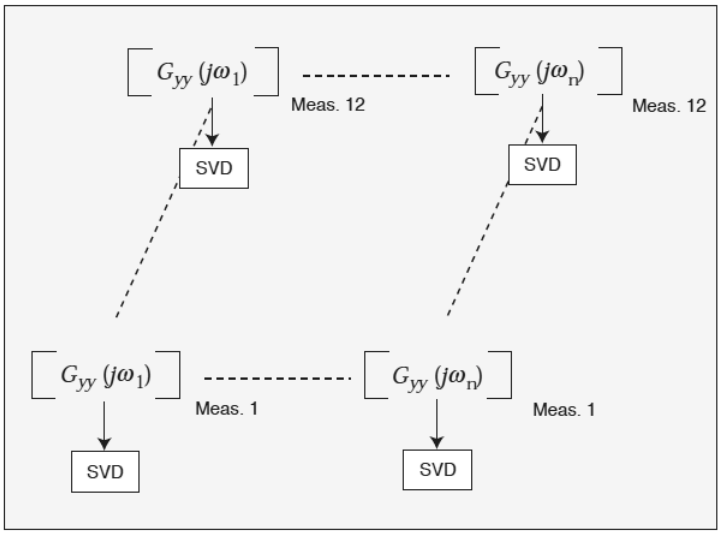

Figure 4.4: Singular value decomposition procedure for the spectral density matrix at each frequency [13]

In the following figure, fig. 4.5, two examples of how the Frequency Domain Decomposition works are shown. The graphs shown have been constructed using exactly the same experiment data as in fig. 4.3. It can be seen how, with the same available information (acceleration measurements), the FDD gives clearer results for both cases.

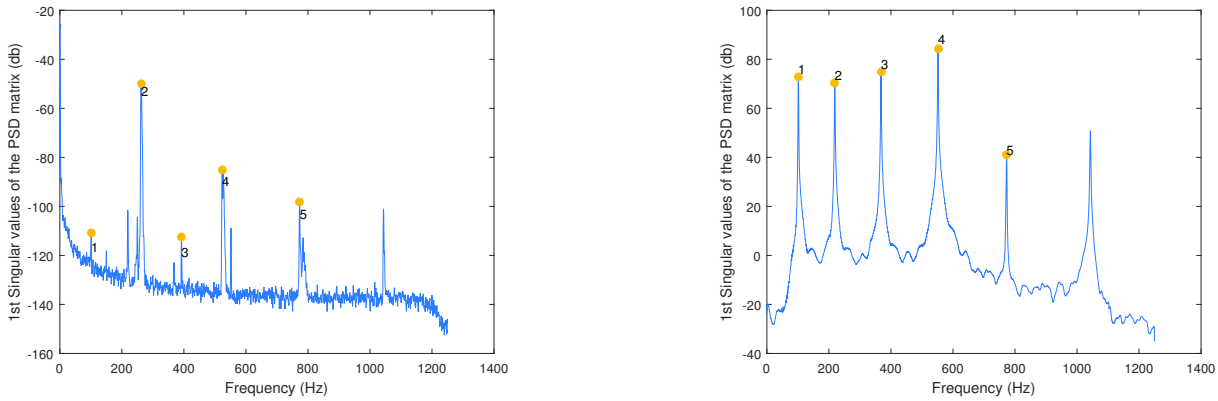

Figure 4.5: Graph examples of the functioning of the Frequency Domain Decomposition method

4.2.3 Stochastic Subspace Identification

The third technique presented is, as it has been aforementioned, the stochastic subspace identification. This section firstly makes a brief overview on the stochastic state space models (section 4.2.3.1) so that, secondly, the stochastic subspace identification technique can be better understood (section 4.2.3.2).

Stochastic state space models

It is, for instance, shown in Peeters and De Roeck [40] that a vibrating structure excited by white noise can be modelled by following stochastic state space model:

$$\begin{matrix} x_{k+1} = Ax_k + w_k \\ y_k = Cx_k + v_k \end{matrix}, \quad E\left[\begin{pmatrix} w_p \\ v_p \end{pmatrix}\begin{pmatrix} w_q^T & v_q^T \end{pmatrix}\right] = \begin{pmatrix} Q & S \\ S^T & R \end{pmatrix}\delta_{pq} \tag{4.34}$$

where $y_k \in \mathbb{R}^{l\times 1}$ are the measurements of l outputs at discrete time instant k ($t = k\Delta t,\ k \in \mathbb{N}$ with Δt the sample time); $x_k \in \mathbb{R}^{n\times 1}$ is the state vector. The number of elements of the state space vector is the number of independent variables needed to describe the state of a system: if the state space model represents a structure with n_2 degrees of freedom (DOFs), than $n = 2n_2$. The vector $w_k \in \mathbb{R}^{n\times 1}$ is the process noise due to disturbances and modelling inaccuracies and models also the white noise input; $v_k \in \mathbb{R}^{l\times 1}$ is the measurement noise due to sensor inaccuracy and, in case that accelerations are measured, models also the direct transmission of the white noise inputs. They are both unmeasurable vector signals assumed to be zero mean, white and with covariance matrices given by the second part of eq. (4.34); where E is the expected value operator; δ_{pq} is the Kronecker delta; p, q are two arbitrary time instants. $A \in \mathbb{R}^{n\times n}$ is the state matrix, describing the dynamics of the system. $C \in \mathbb{R}^{l\times n}$ is the output matrix that describes how the internal states are transferred to the outside world.

Some important properties of stochastic state space systems are briefly resumed. These properties are well-known [**?**]. Also some notations are clarified. The stochastic process is assumed to be stationary with zero mean $\mathbf{E}\left[x_k x_k^T\right] = \Sigma$, $\mathbf{E}\left[x_k\right] = 0$ where the state covariance Σ is independent of the time k. w_k, v_k are independent of the actual state $\mathbf{E}\left[x_k w_k^T\right] = \Sigma$, $\mathbf{E}\left[x_k v_k^T\right] = 0$. The output covariance matrix of lag i, Λ_i, and the "next-state-output" covariance matrix G are defined as:

$$\Lambda_i = \mathbf{E}\left[y_{k+1} y_k^T\right], \quad G = \mathbf{E}\left[x_{k+1} y_k^T\right] \tag{4.35}$$

From these definitions the following properties are easily deduced:

$$\Sigma = A\Sigma A^T + Q, \quad G = A\Sigma^T + S, \quad \Lambda_0 = C\Sigma C^T + R \tag{4.36}$$

$$\Lambda_i = CA^{i-1}G \tag{4.37}$$

Equation (4.37) is an important property and means that the output covariances can be considered as

impulse responses of the deterministic linear time variant system A, G, C, Λ_0. Therefore the classical realization theory applies. Also in mechanical engineering, this observation (eq. (4.37)) is used to feed classical algorithms that normally work with impulse responses, with output covariances instead: polyreference LSCE, ERA, Ibrahim time domain.

Although the computation of the covariance matrices Λ_i can be avoided in the data-driven stochastic subspace algorithms, property from eq. (4.37) is important for the derivation of the algorithms [38].

It is assumed that the state covariance matrix Σ is independent of time. This can put a severe constraint on the applicability of the identification method. For covariance-driven subspace algorithms (which are highly related to the data-driven algorithms of this paper), it has been shown by Benveniste and Fuchs [6] that they also work in the non-stationary white noise case.

Principles of the Stochastic Subspace Identification

In this subsection only the main principles of stochastic subspace identification (SSI) are discussed. These can be found in Van Overschee and De Moor [**?**].

The output measurements are gathered in a block Hankel matrix $H \in \mathbb{R}^{2li \times j}$ with $2i$ block rows and j columns. Every block consists of l rows. For statistical reasons, it is assumed that $j \to \inf$. The Hankel matrix can be divided into a past and a future part:

$$H = \frac{1}{\sqrt{j}} \left(\begin{array}{cccc} y_0 & y_1 & \cdots & y_{j-1} \\ y_1 & y_2 & \cdots & y_j \\ \cdots & \cdots & \cdots & \cdots \\ y_{i-1} & y_i & \cdots & y_{i+j-2} \\ \hline y_i & y_{i+1} & \cdots & y_{i+j-1} \\ y_{i+1} & y_{i+2} & \cdots & y_{i+j} \\ \cdots & \cdots & \cdots & \cdots \\ y_{2i-1} & y_{2i} & \cdots & y_{2i+j-2} \end{array} \right) = \left(\frac{Y_{0|i-1}}{Y_{i|2i-1}} \right) = \left(\frac{Y_p}{Y_f} \right) \begin{array}{l} \updownarrow li \\ \updownarrow li \end{array} \begin{array}{l} "past" \\ "future" \end{array} \tag{4.38}$$

Remark that the output data need to be scaled by a factor of $1/\sqrt{(}j)$ to be consistent with the definition of the output covariances Λ_i. Thanks to the scaling, the first l rows and first l columns of the matrix

product $Y_f Y_p^T$ can be written as:

$$Y_f Y_p^T(1:l,1:l) = \sum_{k=0}^{j-1} \frac{1}{\sqrt{j}} y_{k+i} \frac{1}{\sqrt{j}} y_k^T = \frac{1}{\sqrt{j}} \sum_{k=0}^{j-1} y_{k+i} y_k^T = \Lambda_i \tag{4.39}$$

where the last equation only holds if the data are ergodic and if an infinite number of data is available $j \to \inf$. If one of the two conditions is not fulfilled, not the true covariance Λ_i but only an estimate is obtained.

The algorithm proceeds with projecting the row space of the future outputs into the row space of the past outputs. This projection is noted and defined as:

$$\mathcal{P}_i = Y_f / Y_p = Y_f Y_p^T (Y_f Y_p^T)^\dagger Y_p \tag{4.40}$$

where $(\bullet)^\dagger$ represents the pseudo-inverse of a matrix. The idea behind this projection is that it retains all the information in the past that is useful to predict the future. The main theorem of stochastic subspace identification states that the $\mathcal{P}_i$ can be factorized as the product of the observability matrix O_i and the Kalman filter state sequence $\hat{X}_i$:

$$\mathcal{P}_i = \begin{pmatrix} C \\ CA \\ CA^2 \\ \cdots \\ CA^{i-1} \end{pmatrix} = \begin{pmatrix} \hat{x}_i & \hat{x}_{i+1} & \cdots & \hat{x}_{i+j-1} \end{pmatrix} = O_i \hat{X}_i \tag{4.41}$$

Classically, the aim of the Kalman filter is to produce an optimal prediction for the vector x_{k+1} by making use of observations of the outputs up to time k and the available system matrices together with the known noise covariances. These optimal predictions are denoted by a hat $\hat{x}_{k+1}$. More details on the Kalman filter can be found in literature [34] [25].

Both factors of eq. (4.41), the observability matrix O_i and the state sequence $\hat{X}_i$, are obtained by applying the singular value decomposition (SVD) to the projection matrix:

$$\mathcal{P}_i = USV^T = \begin{pmatrix} U_1 & U_2 \end{pmatrix} \begin{pmatrix} S_1 & 0 \\ 0 & 0 \end{pmatrix} \begin{pmatrix} V_1^t \\ V_2^T \end{pmatrix} = U_1 S_1 V_1^T \tag{4.42}$$

where $U \in \mathbb{R}^{li \times li}$ and $V \in \mathbb{R}^{ri \times ri}$ are orthonormal matrices: $U^T U = UU^T = I_{li}$ and $V^T V = VV^T = I_{ri}$; $S \in \mathbb{R}^{li \times ri}$ is a diagonal matrix containing the singular values in descending order. Since the inner dimension of the product $O_i \hat{X}_i$ equals n and since we assume that $li \geq n$, the rank of the product cannot exceed n. The rank of the matrix is found as the number of non-zero values. In the last equality of eq. (4.42), the zero singular values and corresponding singular vectors have been omitted. Combining eq. (4.41) and eq. (4.42) gives:

$$O_i = U_1 S_1^{1/2}, \ \hat{X}_i = O_i^{\dagger} \mathcal{P}_i \tag{4.43}$$

Up to now we found the order of the system n (as the number of nonzero singular values in eq. (4.42)), the observability matrix O_i and the state sequence $\hat{X}_i$. However, the main aim is to recover the system matrices A, C, Q, R and S. If the separation between past and future outputs is shifted one block row down in eq. (4.38), another projection can be defined:

$$\mathcal{P}_{i-1} = Y_f^- / Y_p^+ = Y_{i+1|2i-1} / Y_{0|i} = O_{i-1} \hat{X}_{i+1} \tag{4.44}$$

where the last equation is similar to the main theorem (eq. (4.41)). O_{i-1} is obtained after deleting the last l rows of O_i computed as in eq. (4.43). The shifted state sequence is obtained as:

$$\hat{X}_{i+1} = O_{i-1}^{\dagger} \mathcal{P}_{i-1} \tag{4.45}$$

At this moment the Kalman state sequences $\hat{X}_i$, $\hat{X}_{i+1}$ are calculated using only the output data of eq. (4.43) and eq. (4.46). Next, the system matrices can be recovered from the following overdetermined set of linear equations, obtained by extending eq. (4.34):

$$\begin{pmatrix} \hat{X}_{i+1} \\ Y_{i|i} \end{pmatrix} = \begin{pmatrix} A \\ C \end{pmatrix} \begin{pmatrix} \hat{X}_i \end{pmatrix} + \begin{pmatrix} W_i \\ V_i \end{pmatrix} \tag{4.46}$$

where $Y_{i|i}$ is a Hankel matrix with only one block row; W_i, V_i are the least squares residuals. Since the Kalman state sequences and the outputs are known and the residuals $\left(W_i^T V_i^T\right)^T$ are uncorrelated with $\hat{X}_i$, the set of equations can be solved for A, C in a least square sense:

$$\begin{pmatrix} A \\ C \end{pmatrix} = \begin{pmatrix} \hat{X}_{i+1} \\ Y_{i|i} \end{pmatrix} \hat{X}_i^{\dagger} \tag{4.47}$$

Finally, the noise covariances Q, R, S are recovered as the covariances of the residuals in eq. (4.47). Using eq. (4.36), A, C, Q, R and S can be transformed into A, G, C and Λ_0. At this point the identification problem is theoretically solved: based on the outputs, the system order n and the system matrices A, G, C and Λ_0 are found.

4.3 Patch tests of the direct dynamic observability

An algorithm that performs an analysis to obtain the modal shapes and frequencies has been implemented. In the following subsections this algorithm is validated by analysing its performance for several different structures.

4.3.1 Testing of the connectivity

First of all several tests have been carried out with the objective of testing whether the connectivities between elements -which is implemented through the order of the different elements of the matrices- is correct.

In order to do so, a cantilever beam has been taken under study. Since modal frequencies and deflections do not change depending on the

(a) Order of the elements

(b) Direction of the structure

(c) Connectivity labelling

the results should be the same if the aforementioned variables are varied.

In fig. 4.6 a cantilever is shown. The difference between cantilevers A, B and C is the enumeration order of the elements that comprise the whole structure and the connectivity between the nodes.

Then, fig. 4.7 shows all the cases that have been tested through the program. Cases *1* to *6* differ from each other in the position of the structure itself.

The analysis has been done for all the possible combinations between cases A, B and C and cases *1*, *2*, *3*, *4*, *5* and *6*. Therefore 18 different analysis have been carried out. The modal shapes and the natural frequencies obtained for all the cases were the same (see table 4.1 for the frequencies obtained

and table 4.2 for the modal shapes). Hence, the feasibility of the program has been proved as it has been seen how the order in which the elements and nodes are taken into account does not affect the results.

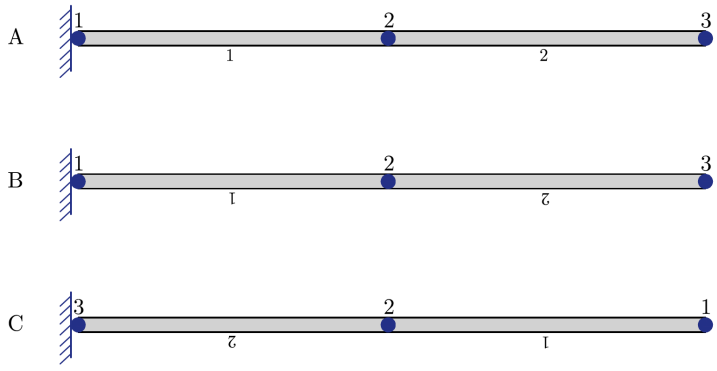

Figure 4.6: Different order of the elements and connectivities

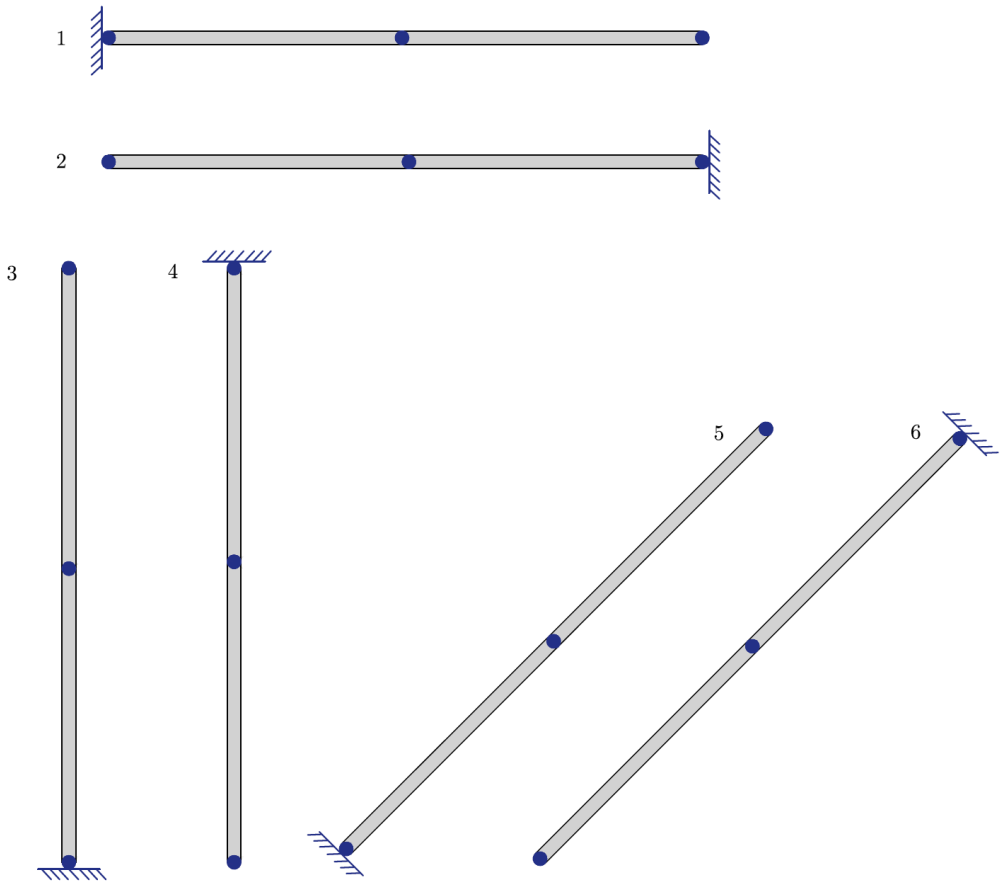

Figure 4.7: Different location of the boundary conditions and direction of the elements

The results obtained for all the cases are presented in table 4.1 (frequencies) and in table 4.2 (modal shapes).

Mode	**Frequency (Hz)**	
	Consistent mass matrix	*Lumped mass matrix*
1	8,340	5,283
2	82,168	25,314
3	1416,691	1156,723

Table 4.1: Numerical frequencies for the cantilever beams using a consistent or a lumped mass matrix

	Modal shapes					
	Consistent mass matrix			*Lumped mass matrix*		
	Mode 1	Mode 2	Mode 3	Mode 1	Mode 2	Mode 3
u_1	0,000	0,000	0,000	0,000	0,000	0,000
v_1	0,000	0,000	0,000	0,000	0,000	0,000
w_1	0,000	0,000	0,000	0,000	0,000	0,000
u_2	0,000	0,000	1,957	0,000	0,000	1,598
v_2	-2,282	3,181	0,000	-1,454	-0,664	0,000
w_2	-3,144	24,245	0,000	-2,301	5,036	0,000

Table 4.2: Numerical modal shapes for the cantilever beams using a consistent or a lumped mass matrix

4.3.2 Testing of the matrix assemblage

The correct assemblage of the matrices has been verified by checking step-by-step that the matrices were the same both in the program and when calculating them by hand.

This has been checked for three structures: a cantilever beam, a one-floor frame and a two-floor one.

4.3.3 Cantilever beam

After having tested the performance of the program related to connectivity and position, a patch test is carried out for a cantilever beam with the characteristics shown in table 4.3. An image of the structural element is presented in section 4.3.3.

As it will be seen afterwards, one of the variables that has been taken into account is the number of elements in which the structure is discretised. This is the reason why the length of the beam is considered to be $\frac{1}{n}$, because the total length of the beam is 1 m, but each of the fractions' length is $\frac{1\ m}{n}$.

In this first case, two analysis are performed: the theoretical one and the numerical one. The first one

is derived from existing equations and the second one is developed through FEM softwares.

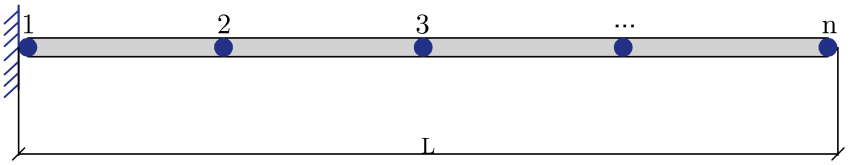

Figure 4.8: Cantilever used in the patch testing. The number of elements in which it discretised is n

L	$\frac{1}{n}\ m$	**A**	$0,0001\ m^2$
E	$2,068E+11\ N/m^2$	$\boldsymbol{\rho}$	$7830\ kg/m^3$
I	$8,33E-10\ m^4$	$\boldsymbol{\nu}$	$0,33$

Table 4.3: Properties of the cantilever beam used for the patch tests

Theoretical modal analysis

The equation, based on the assumptions under Euler-Bernoulli hypotheses, describing the transverse vibrations $w = w(y,t)$ of a beam is given by the formula:

$$\frac{\partial^2 w}{\partial t^2} + \frac{EI}{\rho A}\frac{\partial^4 w}{\partial x^4} \tag{4.48}$$

where E is the Young's modulus, I the moment of inertia, ρ the material's density and A the area of cross-section. Using the method of separation of variables, the solution of the transverse beam vibration equation might be written as:

$$w(y,t) = W(y)T(t) \tag{4.49}$$

where $W(y)$ is the eigenfunction and $T(t)$ a function describing beam displacement as a function of time t. If eq. (4.49) is inserted into eq. (4.48), the following equation might be obtained:

$$W^{IV} - \beta^4 W = 0 \tag{4.50}$$

where

$$\beta^4 = \omega^2 \frac{\rho A}{EI} \tag{4.51}$$

and the $\cdot^{IV}$ symbol designates the derivative with respect to the y coordinate. Then, the solution to the equation is the following function:

$$W(y) = C_1 (\cos \beta y + \cosh \beta y) + C_2 (\cos \beta y - \cosh \beta y) + C_3 (\sin \beta y + \sinh \beta y) + C_4 (\sin \beta y - \sinh \beta y) \tag{4.52}$$

The constants C_1, C_2, C_3 and C_4 are determined after the appropriate boundary conditions have been accounted for and they are unique for a certain set of boundary conditions. However, the solution for the displacement is not unique, and it depends on the modal frequency. Therefore, the solution is typically written as:

$$W(y) = C_1 (\cos \beta_n y + \cosh \beta_n y) + C_2 (\cos \beta_n y - \cosh \beta_n y) + C_3 (\sin \beta_n y + \sinh \beta_n y) + C_4 (\sin \beta_n y - \sinh \beta_n y) \tag{4.53}$$

where $n = 1, 2, \ldots, k$ corresponds to each of the k modes of vibration and $\beta_n L = n\pi$.

For the cantilever beam under consideration, the boundary conditions that apply are the following ones:

$$w(y,t)|_{y=0} = 0 \tag{4.54}$$

$$\frac{\partial w(y,t)}{\partial y}|_{y=0} = 0 \tag{4.55}$$

$$- EI \frac{\partial^2 w(y,t)}{\partial y^2}|_{y=L} = 0 \tag{4.56}$$

$$- EI \frac{\partial^3 w(y,t)}{\partial y^3}|_{y=L} = 0 \tag{4.57}$$

If the previous conditions are applied, it is observed that non-trivial solutions are only found if the following equation is satisfied:

$$\cosh \beta_n L \cos \beta_n L + 1 = 0 \tag{4.58}$$

This nonlinear equation can be solved numerically leading to the circular natural frequency ω_n for the *n-th* mode, which can be written as:

$$\omega_n = \alpha_n^2 \sqrt{\frac{EI}{\rho A L^4}} \tag{4.59}$$

with $\alpha_n = n\pi$. To get the frequencies in *Hz*:

$$\omega = 2\pi f \rightarrow f = \frac{\omega}{2\pi} \tag{4.60}$$

So finally this leads to the natural frequencies as:

$$f_n = \frac{\alpha_n^2}{2\pi}\sqrt{\frac{EI}{\rho A L^4}} \tag{4.61}$$

Also, the boundary conditions in eqs. (4.54) to (4.57) can be used to determine the modal shapes from the solution for the displacement. Its expression is the one that follows:

$$W(y) = C_1\left[(\cosh\beta_n y - \cos\beta_n y) + \frac{\cos\beta_n L + \cosh\beta_n L}{\sin\beta_n L + \sinh\beta_n L}(\sin\beta_n y - \sinh\beta_n y)\right] \tag{4.62}$$

The unknown constant A_1 (which is actually constants, since there is one for each mode n) is in general complex and is determined by the initial conditions at $t = 0$ on the displacements and velocity of the beam. Typically, a value of $A_1 = 1$ is used when plotting modal shapes.

Then, using the equations above, the modal frequencies are the ones shown in table 4.4.

Mode	**Frequency (Hz)**
1	8,2993
2	52,0144
3	145,6563

Table 4.4: Theoretical frequencies for the structure in section 4.3.3

Numerical modal analysis

In order to check the accuracy of the programmed code, the cantilever beam has also been analysed through the finite element method. For this purpose, three softwares have been used to be able to adequately carry out the verification of the results.

- Midas Civil
- SAP2000
- ANSYS

It is significant to highlight the importance of the number of nodes in which the structure is discretised. The accuracy changes gradually with an increase of the number of elements of the structure. This is the reason why the analysis that has been carried out has been based on the same structure (a cantilever)

but the level of discretisation has varied in order to see how it affects the results. In the same way, the yielded results are not the same depending on the mass matrix being used. Namely, using a consistent mass matrix and a lumped mass matrix provide different results. Hence, the analysis has also been performed for the two mentioned types of mass matrices.

First of all, table 4.5 shows the results for the first three modes of vibration for the cantilever previously described. Table 4.5 only shows the results for the cantilever discretised into 2 elements - but the results have been obtained for discretisation levels of 1, 2, 4, 6, 8, 16, 32, 64 and 128 elements. For a better comprehension the results are shown graphically in figs. 4.9 and 4.10.

From the graphs, it can be seen that the higher number of elements in which the structure is discretised, the lower the error is. As for the first mode, the error drops very quickly before reaching a number of elements equal to 10. Both Ansys and Matlab result in lower errors than Midas. These errors are under 0,025. As for the next modes, it can be seen how they need more elements to achieve low errors, although after 20 elements they all converge to errors close to 0%.

Also the results obtained using a lumped mass matrix are analysed. They are shown in table 4.6 and fig. 4.10. As it happened with the consistent mass matrix case, the higher the mode, the more elements needed for the error to drop to values around 0%.

However, in this case, it is seen that in general a higher discretisation is needed. In the first mode, it is not until a number of elements of 60 that the errors become stable; this is high compared to the 5 elements needed in the case of a consistent mass matrix for the first mode. It happens the same with the second and third modes. It has to be noted, anyway, that the errors achieved with the three methods are rather low, reaching minimum values under 0,05% for all the cases.

Mode	**Frequency (Hz)**		
	ANSYS	*MIDAS*	*MATLAB*
1	8,3040	8,3059	8,3042
2	52,4510	52,4683	52,458
3	177,3500	177,4573	177,4218

Table 4.5: Numerical frequencies for the structure in section 4.3.3 discretised into 2 elements and using a consistent mass matrix

Next, the convergence of the frequencies is analysed to compare how the calculations with different types of matrices behave. Figure 4.11 shows the frequencies obtained with each of the methods and

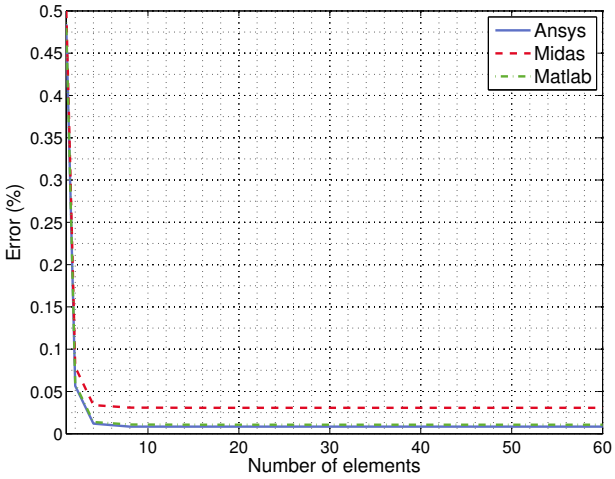

(a) Errors in the frequencies for the first mode

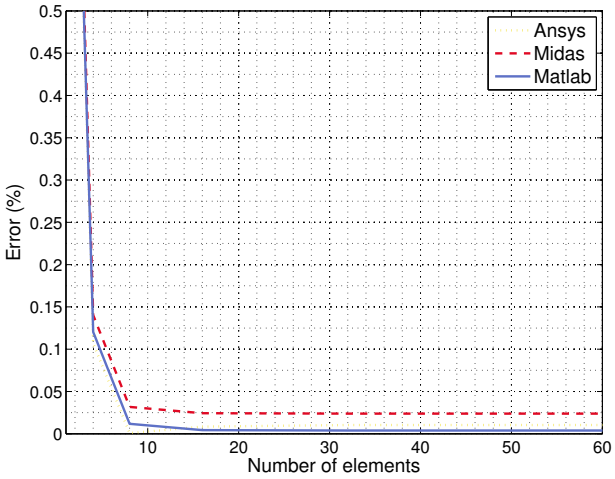

(b) Errors in the frequencies for the second mode

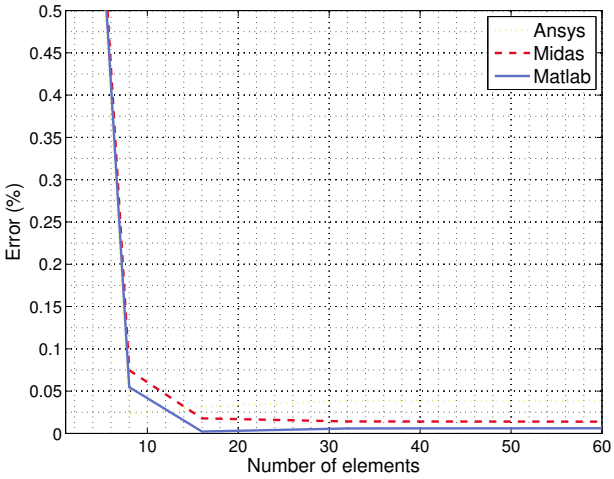

(c) Errors in the frequencies for the third mode

Figure 4.9: Errors in the frequencies of the cantilever for the modes 1, 2 and 3 and using a consistent mass matrix

Mode	**Frequency (Hz)**		
	ANSYS	*MIDAS*	*MATLAB*
1	7,4509	7,4523	7,4509
2	38,3800	38,3877	38,3800
3	1252,0000	1252,0284	1252,0284

Table 4.6: Numerical frequencies for the structure in section 4.3.3 discretised into 2 elements and using a lumped mass matrix

using different number of discretisation levels.

On the other hand, the two graphs in fig. 4.12 show the same results but for the consistent mass matrix and lumped mass matrix separately, so that the results can be seen more clearly.

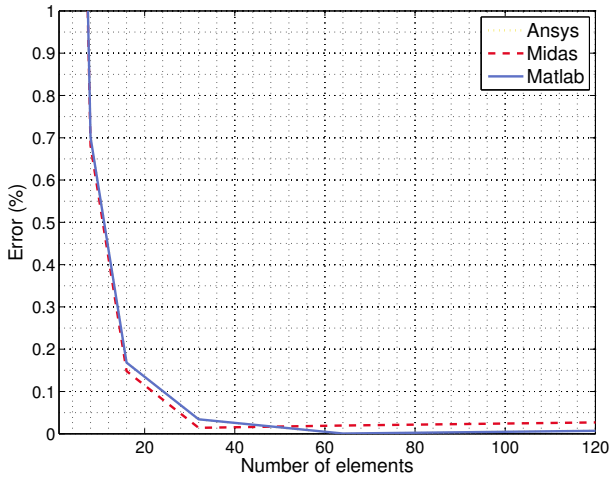

(a) Errors in the frequencies for the first mode

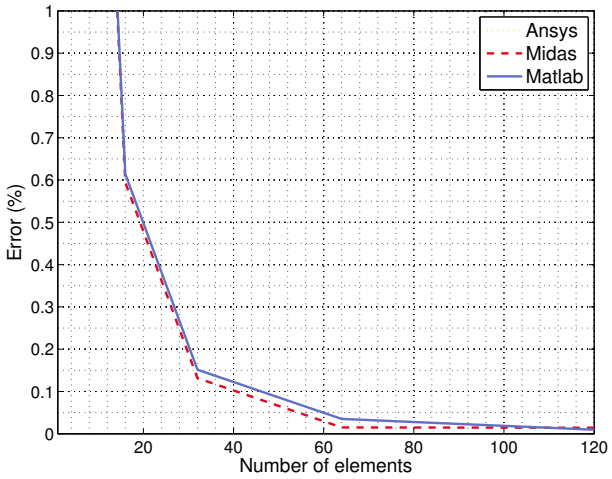

(b) Errors in the frequencies for the second mode

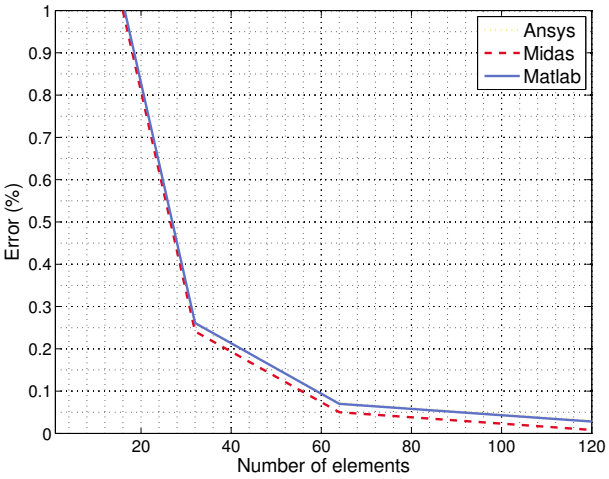

(c) Errors in the frequencies for the third mode

Figure 4.10: Errors in the frequencies of a cantilever for the modes 1, 2 and 3 and using a lumped mass matrix

The frequencies calculated with consistent mass matrices tend to be higher, while the ones with lumped mass matrices, tend to be lower. As well, the frequencies with lumped matrices tend to converge more slowly than those calculated with consistent matrices.

The very same happens when calculating the following modes (see figs. 4.13 and 4.14 for the second mode and figs. 4.15 and 4.16 for the third one).

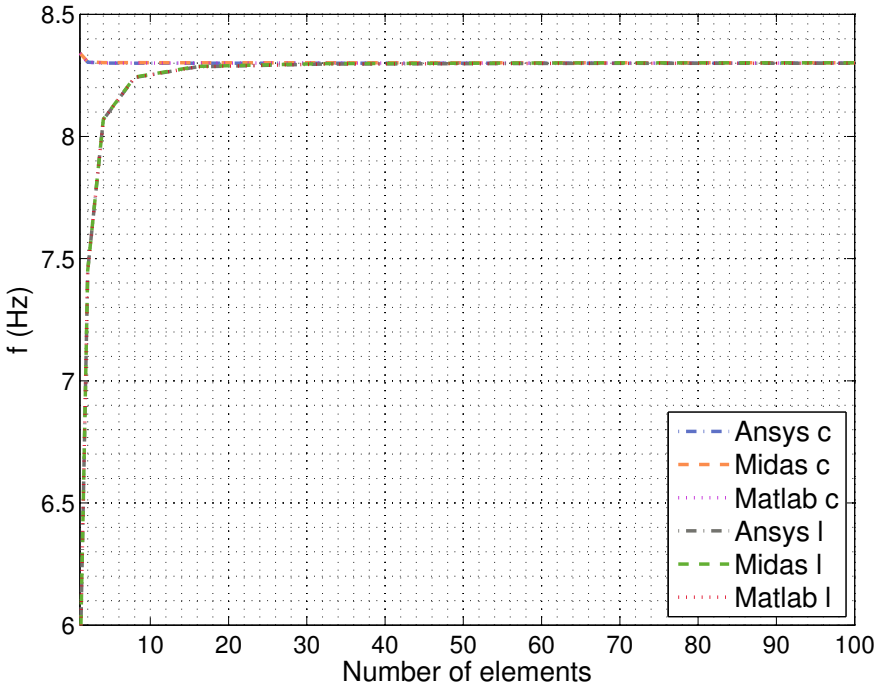

Figure 4.11: Natural frequencies of the cantilever for the first mode using different levels of discretisation, programs and mass matrices

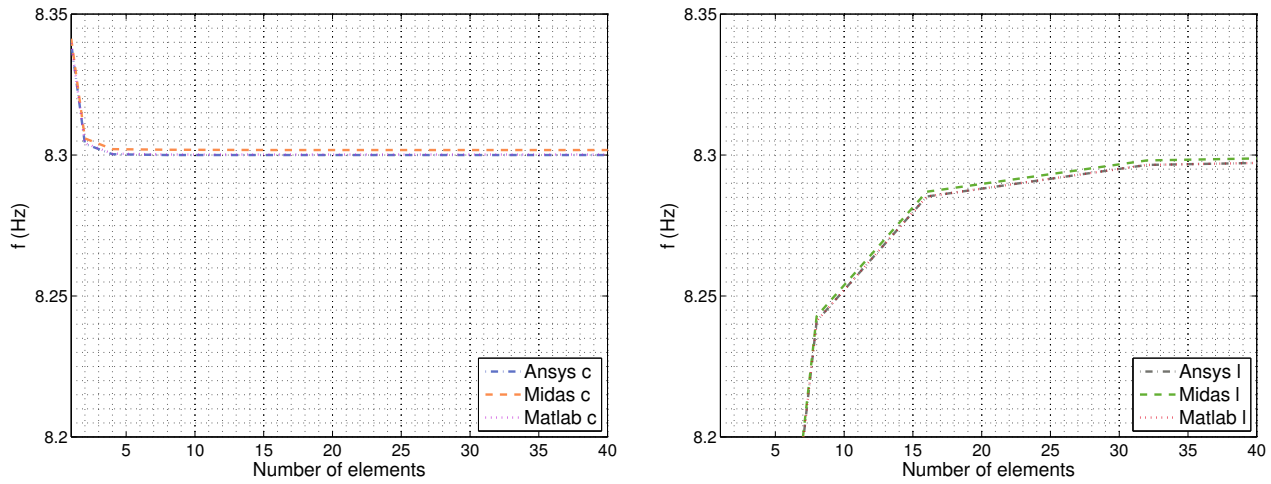

(a) (b)

Figure 4.12: Frequencies of the two-floor frame in section 4.3.3 for the first mode and using consistent (a) and lumped (b) mass matrices and three different programs

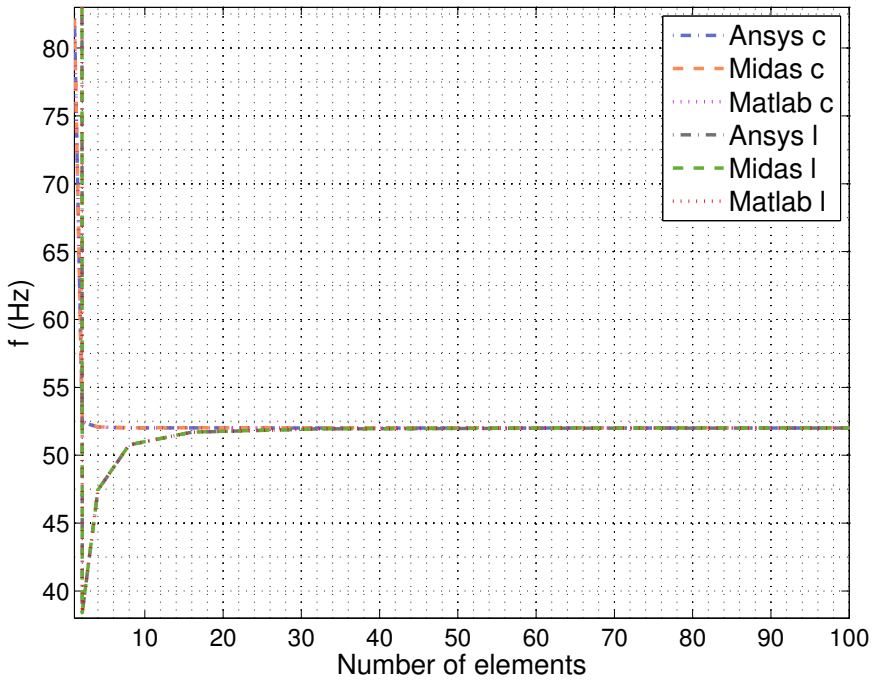

Figure 4.13: Natural frequencies of the cantilever for the second mode using different levels of discretisation, programs and mass matrices

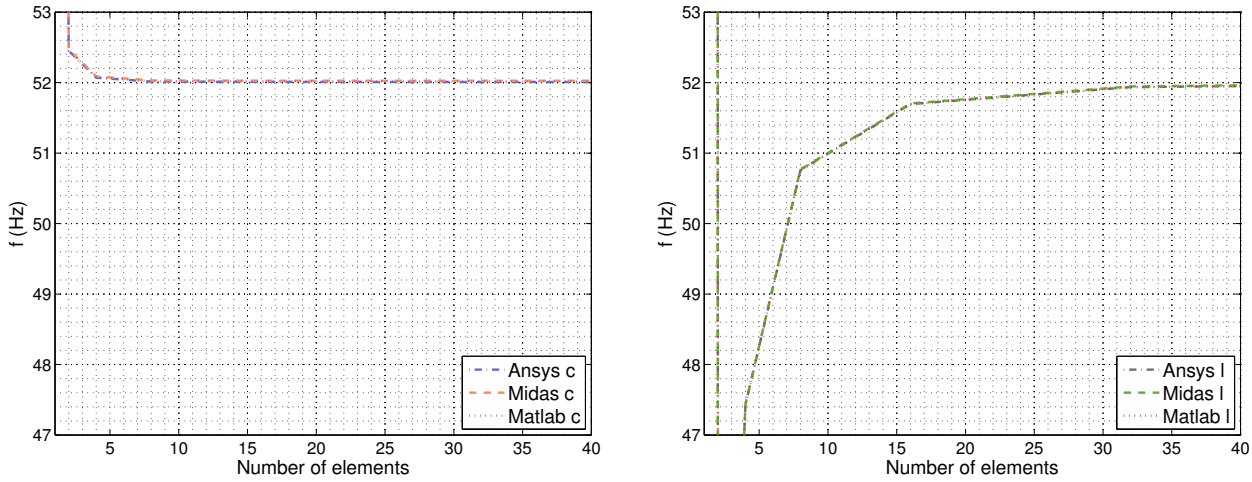

(a) (b)

Figure 4.14: Frequencies of the cantilever in section 4.3.3 for the second mode and using consistent (a) and lumped (b) mass matrices and three different programs

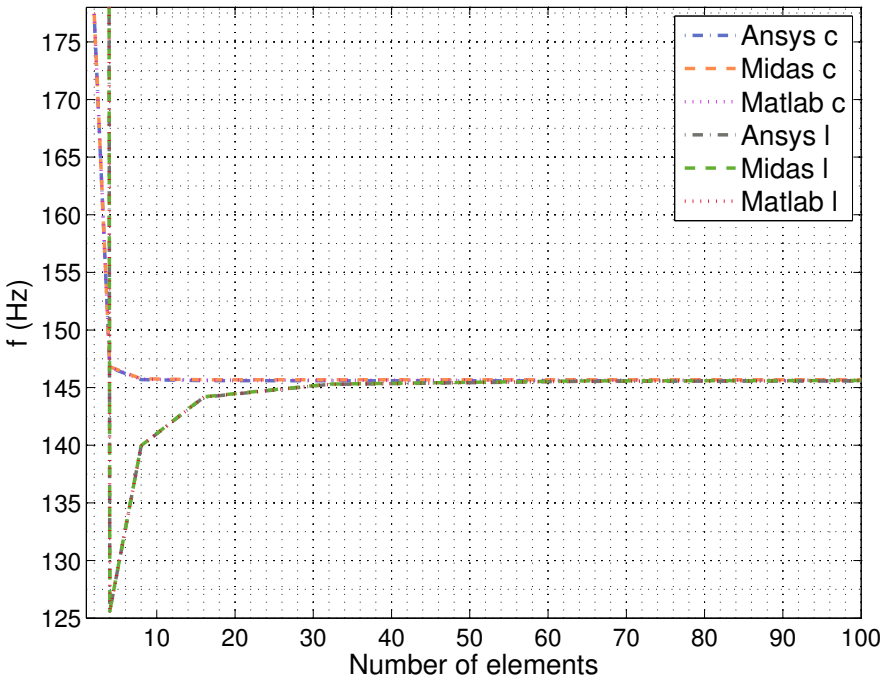

Figure 4.15: Natural frequencies of the cantilever for the third mode using different levels of discretisation, programs and mass matrices

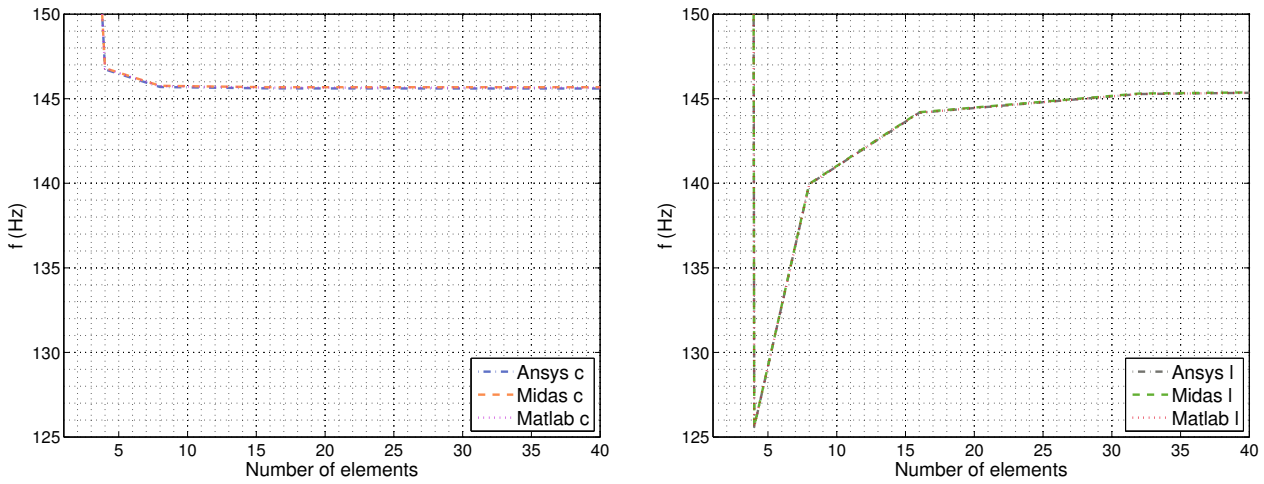

(a) (b)

Figure 4.16: Frequencies of the cantilever in section 4.3.3 for the third mode and using consistent (a) and lumped (b) mass matrices and three different programs

4.3.4 Simple frame

In the same way as before, a simple frame has been analysed through the three softwares Ansys, MidasCivil and Matlab. The analysed structure might be seen in fig. 4.17. The properties of the elements are the same as the previous section - they can be seen in table 4.3.

The number of elements in which the structure is discretised is varied in order to see how the accuracy is related to the number of elements.

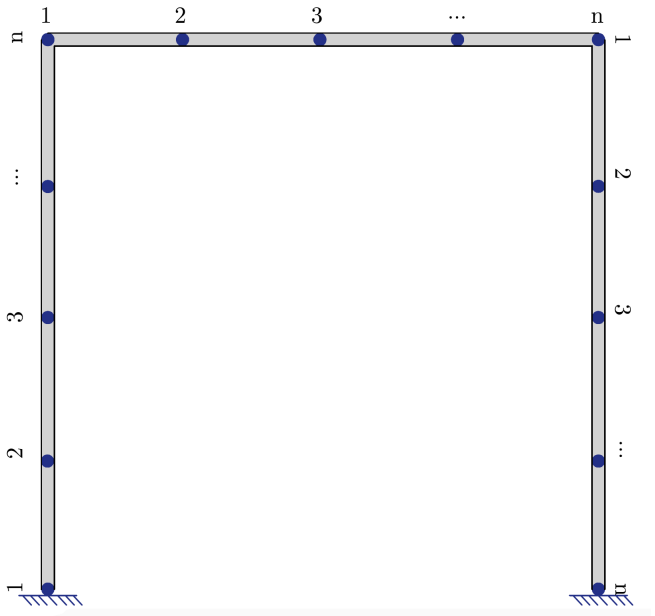

Figure 4.17: Simple frame used for the patch test

First of all, tables 4.7 and 4.8 show the frequencies obtained through the three different methods when each element of the structure is discretised into two parts (three nodes).

Mode	**Frequency (Hz)**		
	ANSYS	*MIDAS*	*MATLAB*
1	0,8407	0,8409	0,8407
2	3,3386	3,3393	3,3387
3	5,4724	5,4735	5,4724

Table 4.7: Numerical frequencies for the frame in fig. 4.17 with each bar discretised into 2 elements and using a consistent mass matrix

Mode	**Frequency (Hz)**		
	ANSYS	*MIDAS*	*MATLAB*
1	0,8278	0,8279	0,8278
2	3,2508	3,2514	3,2508
3	4,7807	4,7816	4,7807

Table 4.8: Numerical frequencies for the frame in fig. 4.17 with each bar discretised into 2 elements and using a lumped mass matrix

Since the theoretical frequency can not be found in this case, the graphs that have been drawn relate frequency and number of elements in order to see if the different methods converge to the same frequencies and how many elements are needed for the frequencies to converge.

Figures 4.18, 4.20 and 4.22 show all the obtained data for modes 1, 2 and 3 respectively. This is, they show the obtained frequencies through the three different methods (Ansys, Midas and Matlab) and using the two different mass matrices: the consistent one and the lumped one. The frequency data is plotted against the number of elements in which each element of the structure is discretised.

Then, figs. 4.19, 4.21 and 4.23 show the same data as figs. 4.18, 4.20 and 4.22 but with more detail, since the data related to consistent and lumped mass matrices is plotted in different graphs.

One can see how, as it happened with the cantilever beam, the frequencies obtained using a consistent mass matrix tend to be higher in the first discretisation levels and the ones obtained using a lumped mass matrix have a tendency of being lower than the real one.

Also, in the first modes the frequencies obtained from the different methods converge more quickly than in higher modes.

Frequencies obtained with the developed program are in general closer to those obtained with Ansys, although the difference between all of them is not greater than 0,00025 Hz.

Finally, it can also be noted that if the results are compared to those obtained with the cantilever beam, the frequencies of the frame converge more quickly than the ones of the cantilever beam do. It appears that the more complex the structure, quicker the convergence to the same value using different methods is.

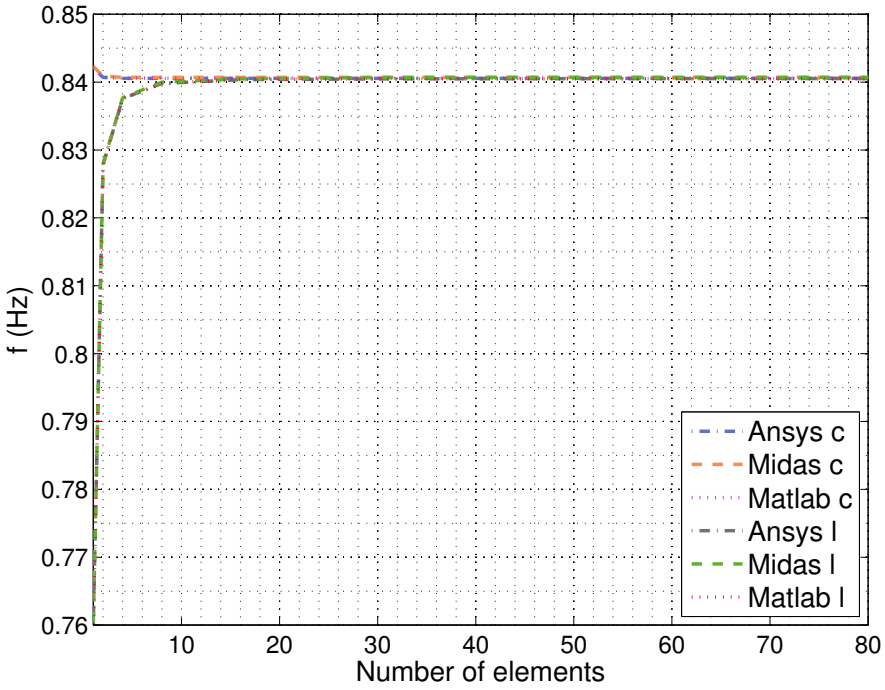

Figure 4.18: Natural frequencies of the one-floor frame for the first mode using different levels of discretisation, programs and mass matrices

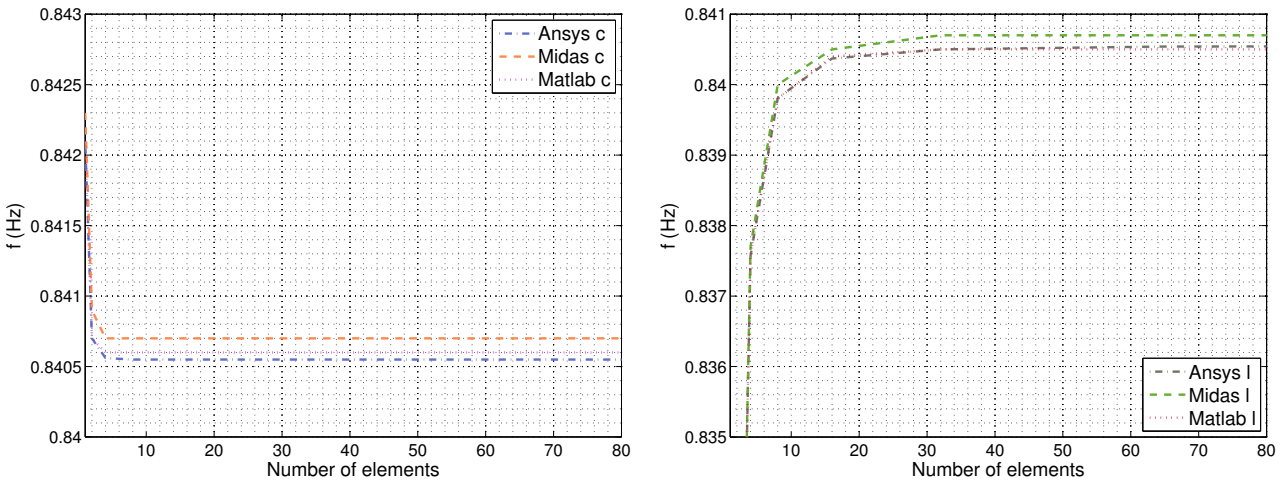

(a) (b)

Figure 4.19: Frequencies of the simple frame in fig. 4.17 for the first mode and using consistent (a) and lumped (b) mass matrices and three different programs

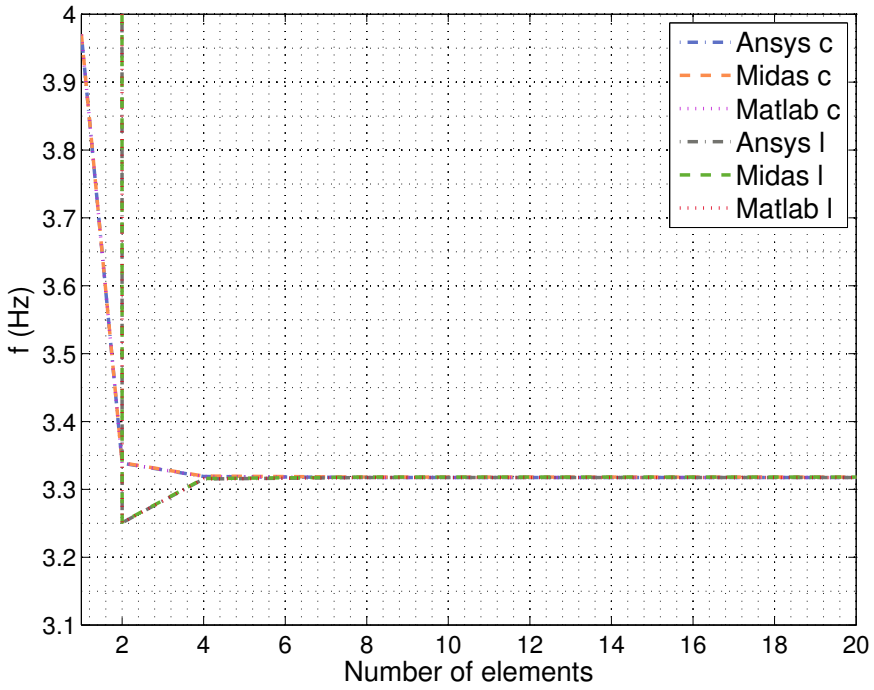

Figure 4.20: Natural frequencies of the one-floor frame for the second mode using different levels of discretisation, programs and mass matrices

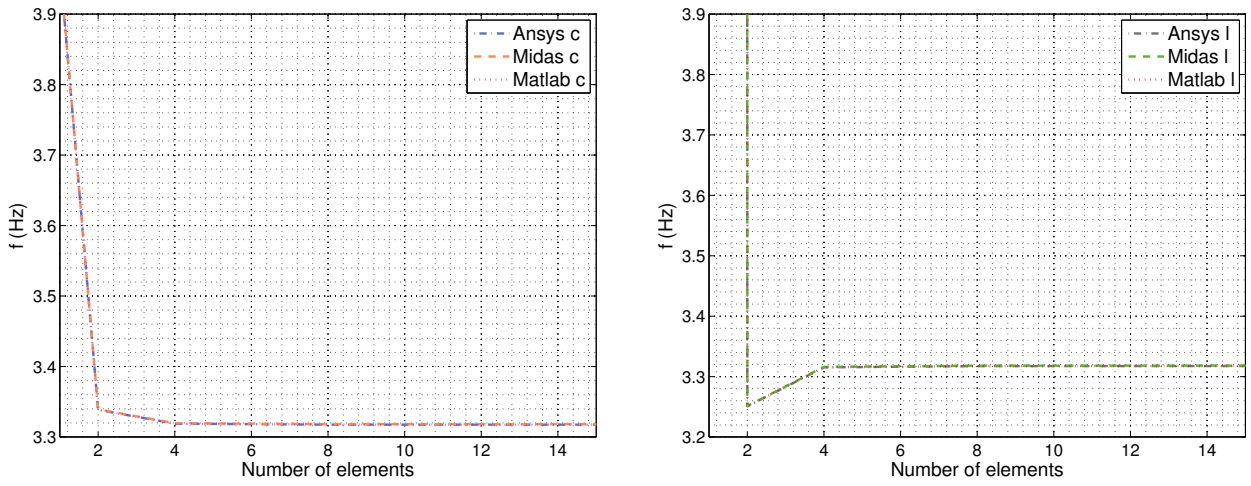

(a) (b)

Figure 4.21: Frequencies of the simple frame in fig. 4.17 for the second mode and using consistent (a) and lumped (b) mass matrices and three different programs

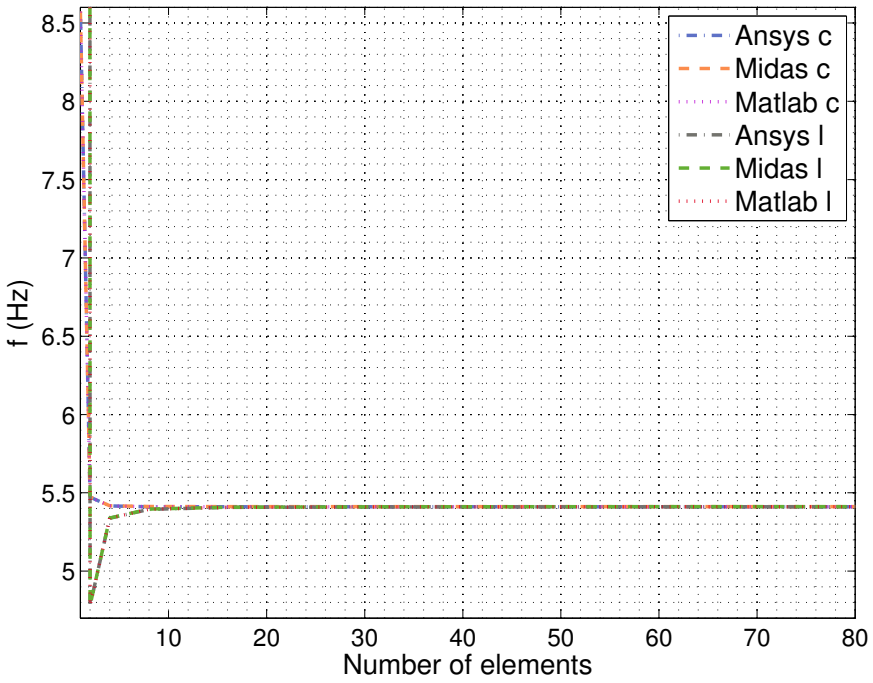

Figure 4.22: Natural frequencies of the one-floor frame for the third mode using different levels of discretisation, programs and mass matrices

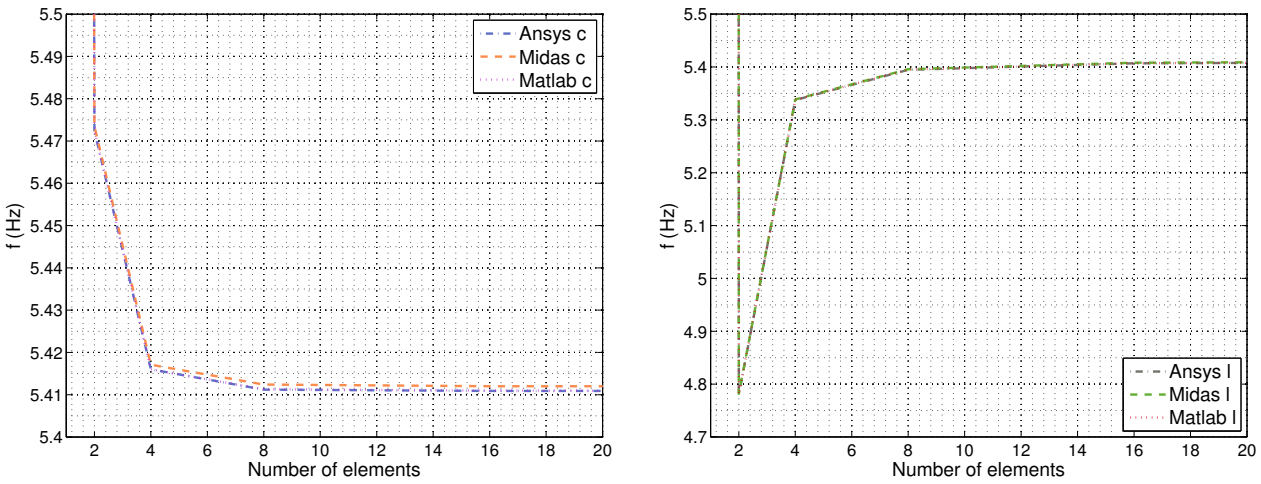

(a) (b)

Figure 4.23: Frequencies of the simple frame in fig. 4.17 for the third mode and using consistent (a) and lumped (b) mass matrices and three different programs

4.3.5 Two-floor frame

Finally, the analysis of a two floor frame (fig. 4.24) has been carried out. One of the reasons of verifying the results of a third structure has been to check whether connectivities between three elements (one node from which three elements derive) had been correctly implemented.

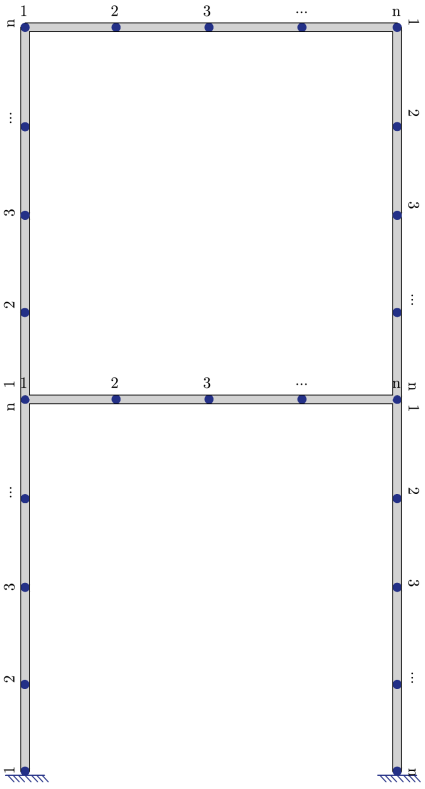

Figure 4.24: Two-floor frame used for the patch test

First of all, as for the frequencies obtained from doing the analysis with mass matrices of type consistent, the results when $n = 2$ (number of elements in which each element is divided) are shown in table 4.9. For the ease of comprehension, also some graphs are shown that correspond to the frequencies obtained through each of the three methods (Ansys, MidasCivil and Matlab) and relative to the number of elements and modes.

Mode	**Frequency (Hz)**		
	ANSYS	*MIDAS*	*MATLAB*
1	0,3930	0,3931	0,3930
2	1,2907	1,2909	1,2907
3	2,8499	2,8505	2,8499

Table 4.9: Numerical frequencies for the frame in fig. 4.24 with each bar discretised into 2 elements and using a consistent mass matrix

Mode	Frequency (Hz)		
	ANSYS	*MIDAS*	*MATLAB*
1	0,3917	0,3918	0,3917
2	1,2716	1,2718	1,2716
3	2,8053	2,8058	2,8053

Table 4.10: Numerical frequencies for the frame in fig. 4.24 with each bar discretised into 2 elements and using a lumped mass matrix

Next, the results of the natural frequencies corresponding to the two-floor frame have been plotted in the same way as it was done with the cantilever beam and the one-floor frame.

On the one hand, figs. 4.25, 4.27 and 4.29 show the values obtained for the frequencies when discretising each of the bars of the frame into a different number of elements. Moreover, these frequencies are also separated depending on whether they have been calculated with Ansys, Midas or Matlab and whether a consistent mass matrix or a lumped mass matrix has been used.

On the other hand, figs. 4.26, 4.28 and 4.30 show the very same data as in figs. 4.25, 4.27 and 4.29 but showing more detail in those parts that are of more interest of the graph; this is, the first part in which the frequencies have not yet converged. In these graphs, the data is shown by mass matrix type.

In the same way as in the two previous cases, when the frequencies have not converged yet, those that have been calculated using a consistent mass matrix tend to be higher, while those using a lumped mass matrix tend to be lower than the real one.

Furthermore, it can be seen that the convergence is now more quickly than that in the cantilever beam and one-frame floor, which leads to think that the more complex the structure the more quickly the frequencies converge to the real value.

Although the different methods yield into frequencies that are not exactly the same, the maximum differences between the methods are of 0,0001.

Also, it must be noted that the frequencies obtained through the developed program coincide with those obtained with Ansys, while the values obtained through Midas are usually a bit higher.

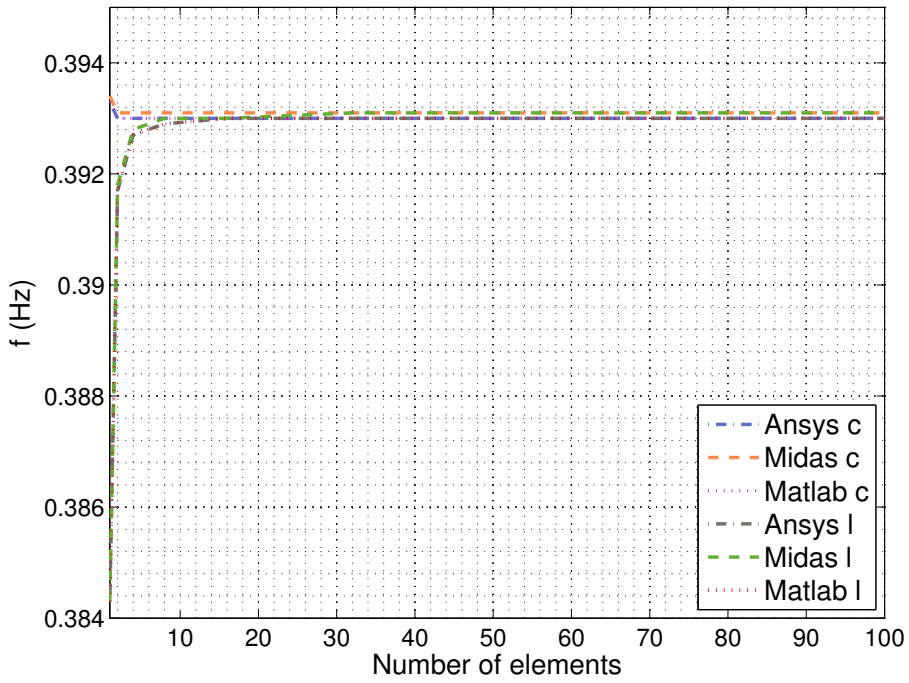

Figure 4.25: Natural frequencies of the two-floor frame for the first mode using different levels of discretisation, programs and mass matrices

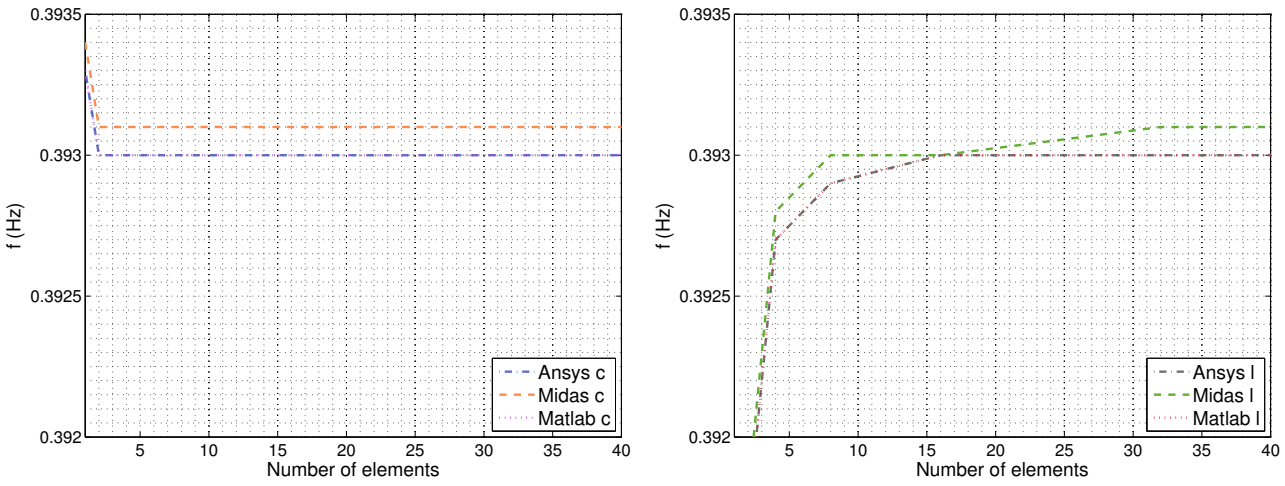

Figure 4.26: Frequencies of the two-floor frame in fig. 4.24 for the first mode and using consistent (a) and lumped (b) mass matrices and three different programs

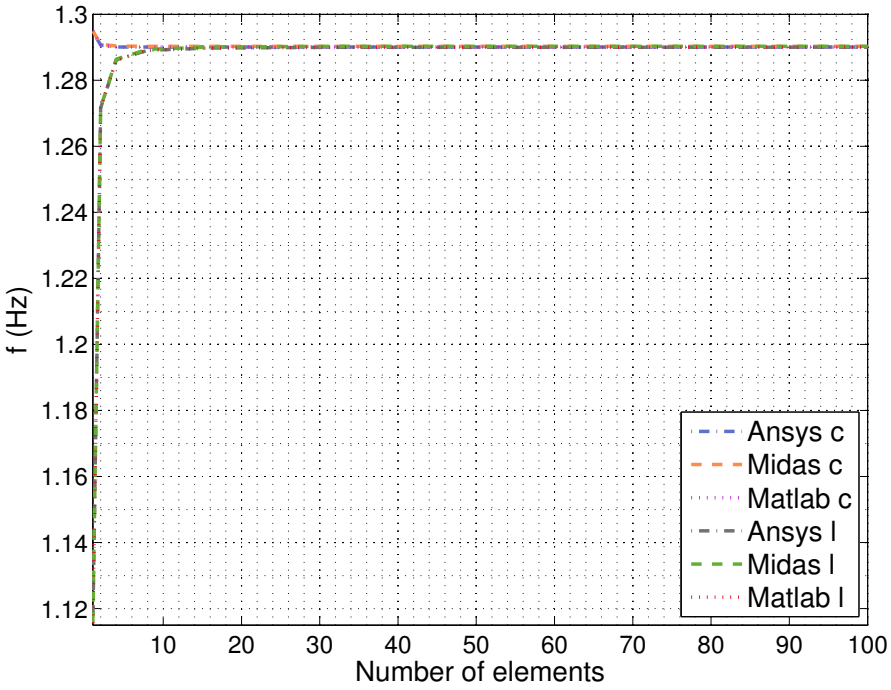

Figure 4.27: Natural frequencies of the two-floor frame for the second mode using different levels of discretisation, programs and mass matrices

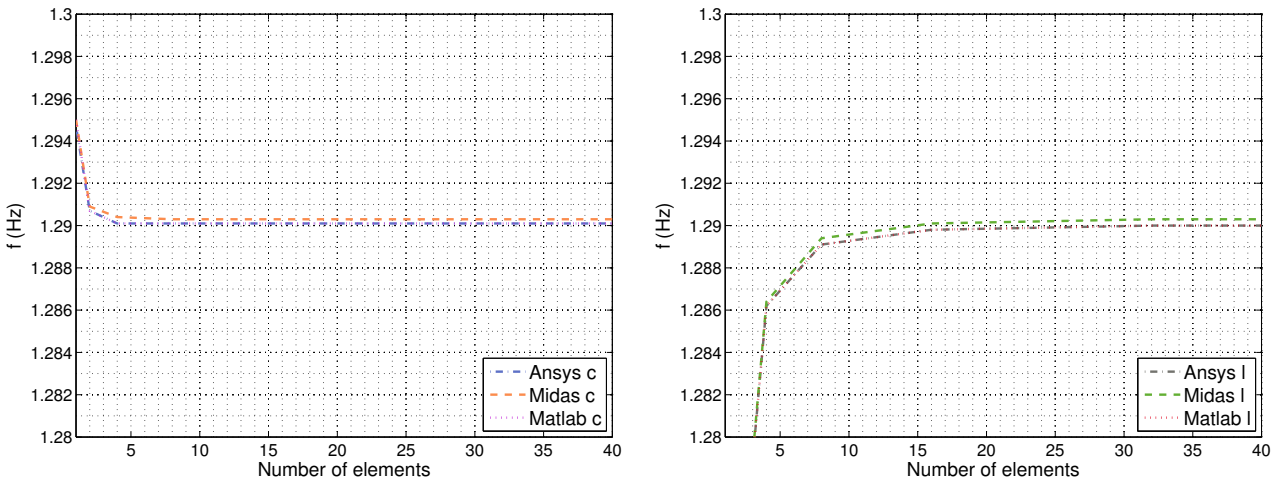

(a) (b)

Figure 4.28: Frequencies of the two-floor frame in fig. 4.24 for the second mode and using consistent (a) and lumped (b) mass matrices and three different programs

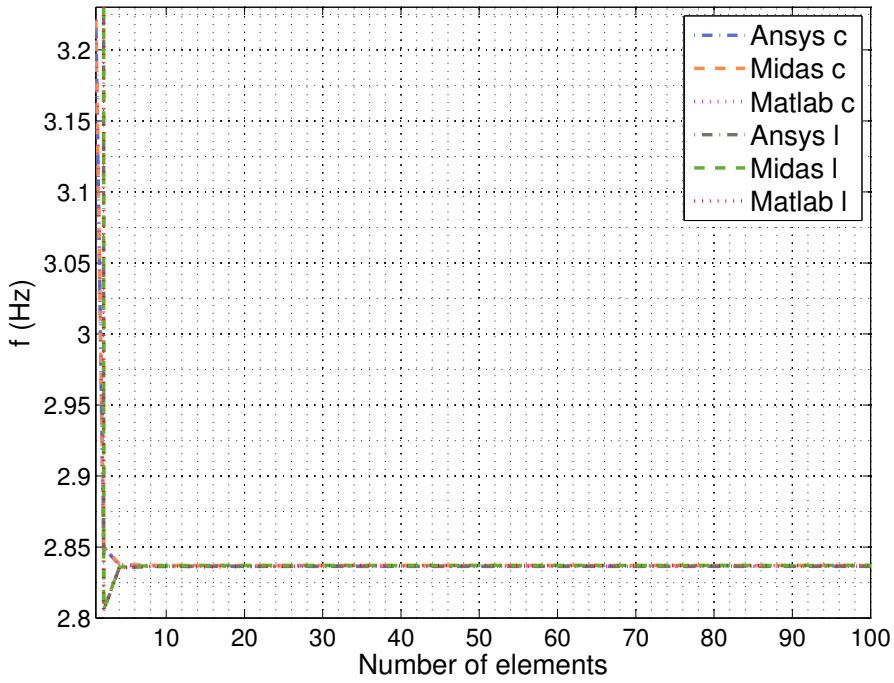

Figure 4.29: Natural frequencies of the two-floor frame for the third mode using different levels of discretisation, programs and mass matrices

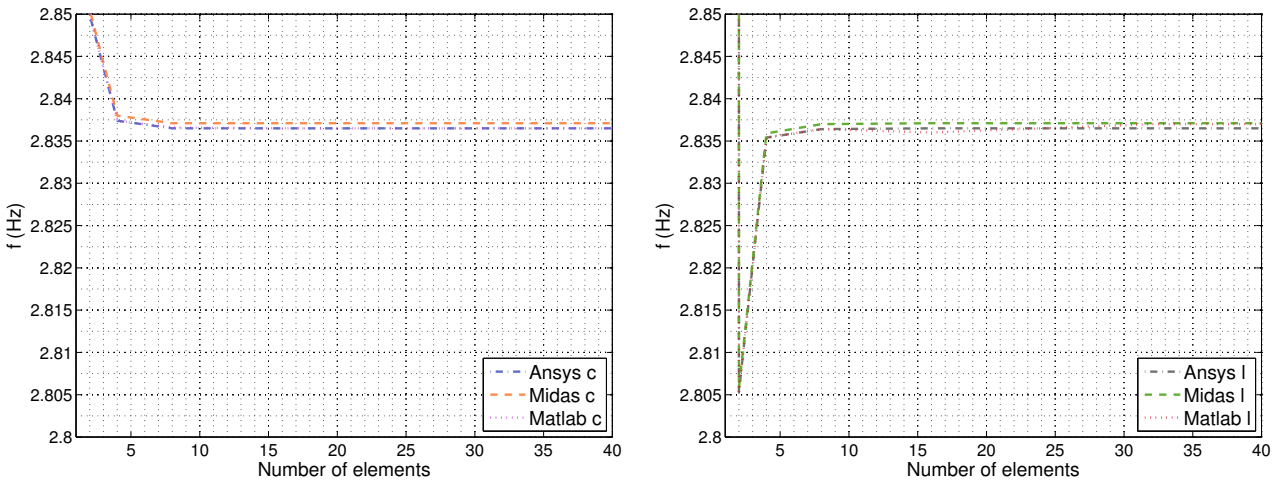

(a) (b)

Figure 4.30: Frequencies of the two-floor frame in fig. 4.24 for the third mode and using consistent (a) and lumped (b) mass matrices and three different programs

Chapter 5

Inverse dynamic observability

5.1 Observability over the dynamic equation

As it has been seen, there are several methods for estimating the modal parameters of a structural system. On the one hand, there is theoretical modal analysis, which computes the modal parameters by solving the dynamic equilibrium equations as an eigenvalue problem. Although this is the traditional way of carrying out the dynamic analysis in structural design, it has got a drawback: all the terms of the stiffness $[K]$, mass $[M]$ and damping $[C]$ matrices are assumed as known. On the other hand, experimental modal analysis uses the system response and modal identification techniques are used to compute the modal parameters. The main advantage of this method is that it does not require previous information about the mechanical properties of the structure since it is only based on the analysis of the response measurements.

In the formulation of the observability over the dynamic equations, it is assumed that a set of modal parameters of the structure (frequency $\{\omega_1\}$, mode shape $\{\Phi_1\}$ and damping ratio $\{c_1\}$) have been obtained from experimental modal analysis. Then, the observability techniques can be used to identify the unknown mechanical properties of the structure, which are found in the stiffness $[K]$, mass $[M]$ and damping $[C]$ matrices, and the unknown modal parameters $\{\omega_0\}$, $\{\Phi_0\}$ and $\{c_0\}$.

5.1.1 SSI from several vibration modes - general case

One way of applying the observability method over eq. (4.14) consists of analysing together multiple vibration modes. This is the general case, since all the R vibration modes are taken into account.

If several modes of vibration are taken into study, eq. (4.14) might be formulated as in eqs. (5.1) and (5.2). In these equations, the stiffness and mass matrices of the R vibration modes are located in the main diagonal of matrices $[K]$ and $[M]$ respectively. Then, for instance, $[K_1]$ and $[M_1]$ correspond to the stiffness and mass matrices of the first mode of vibration and the first components of the modal vectors $[\Phi_{K_1}]$ and $[\Phi_{M_1}]$ contain the full set of vibration modes of this first mode. Finally, the scalar λ_1 is the natural frequency associated to it.

$$[K]\{\Phi\}_R = \lambda_i[M]\{\Phi\}_R \tag{5.1}$$

$$\begin{bmatrix} K_1 & \cdots & 0 & \cdots & 0 \\ \vdots & \ddots & 0 & \cdots & 0 \\ 0 & 0 & K_i & 0 & 0 \\ \vdots & \vdots & 0 & \ddots & 0 \\ 0 & 0 & 0 & \cdots & K_R \end{bmatrix} \begin{Bmatrix} \Phi_1 \\ \vdots \\ \Phi_i \\ \vdots \\ \Phi_R \end{Bmatrix} = \begin{Bmatrix} \lambda_1 \cdots \lambda_i \cdots \lambda_R \end{Bmatrix} \begin{bmatrix} M_1 & \cdots & 0 & \cdots & 0 \\ \vdots & \ddots & 0 & \cdots & 0 \\ 0 & 0 & M_i & 0 & 0 \\ \vdots & \vdots & 0 & \ddots & 0 \\ 0 & 0 & 0 & \cdots & M_R \end{bmatrix} \begin{Bmatrix} \Phi_1 \\ \vdots \\ \Phi_i \\ \vdots \\ \Phi_R \end{Bmatrix} \tag{5.2}$$

If the unknown mechanical properties of [K] and [M] are moved to its respective vectors of modes of vibration, eq. (5.1) might be rewritten as presented in eq. (5.3).

$$\begin{bmatrix} K^*_{00} & K^*_{01} \\ K^*_{10} & K^*_{11} \end{bmatrix} \begin{Bmatrix} \Phi^*_{K,0} \\ \Phi^*_{K,1} \end{Bmatrix} = \begin{bmatrix} \lambda_{00} & \lambda_{01} \\ \lambda_{10} & \lambda_{11} \end{bmatrix} \begin{bmatrix} M^*_{00} & M^*_{01} \\ M^*_{10} & M^*_{11} \end{bmatrix} \begin{Bmatrix} \Phi^*_{M,0} \\ \Phi^*_{M,1} \end{Bmatrix} \tag{5.3}$$

In this new configuration of the system, subindices 0 and 1 refer to unknown and known parameters respectively.

When modifying eq. (5.1) into eq. (5.3), the vector of eigenfrequencies becomes a matrix on the basis of the relationships between known and unknown frequencies and known and unknown mass modal displacements for each mode of vibration. Therefore, all the possible combinations between eigenfrequencies and modal displacements with regard to the fact of being known or not are considered. This is why each of the submatrices of the eigenfrequencies are set with a double subindex. The first subindex refers to the knowledge of the eigenfrequency, while the second one to the knowledge of the associated subset of displacements. Hence, a double 0 means that the submatrix is made up of unknown eigenfrequencies that are multiplying a subset of unknown modal displacements $\{\Phi_{M,0}\}$. On the other hand, a double 1 on the subindex means that all the eigenfrequencies of the submatrix $[\lambda_{11}]$ are known and are multiplying a subset of known mass modal displacements $\{\Phi_{M,1}\}$.

If the length of the elements is assumed to be known the modified stiffness modal vector $\{\Phi^*_K\}$ might include product variables of three terms (such as $E_jA_ju_{k,i}$, $E_jA_jv_{k,i}$, $E_jI_ju_{k,i}$, $E_jI_jv_{k,i}$ or $E_jI_jw_{k,i}$), of two terms (such as A_ju_{ik}, E_ju_{ik}, I_ju_{ik}, A_jv_{ik}, E_jv_{ik}, I_jv_{ik}, E_jw_{ik} or I_jw_{ik}) and a single term (such as A_j, I_j, E_j, u_{ik}, v_{ik} or w_{ik}). In the case of the modified mass modal vector $\{\Phi^*_M\}$ only product variables of two terms (such as m_ju_{ik}, m_jv_{ik} or m_jw_{ik}) and a single term (m_j, u_{ik}, v_{ik} or w_{ik}) might appear.

With the purpose of applying observability over eq. (5.3), the unknown variables must be moved to a vector $\{z\}$; also, the known variables are joined into a vector $\{D\}$. This way, the previous equation might be rewritten as presented in the following equation:

$$[B]\{z\} = \begin{bmatrix} K^*_{00} & K^*_{10} \\ -M^*_{00}\Phi^*_{M,1} & 0 \\ -M^*_{01} & 0 \\ 0 & -M^*_{11}\Phi^*_{M,1} \\ 0 & -M^*_{10} \end{bmatrix}^T \begin{Bmatrix} \Phi^*_{K,0} \\ \lambda_{00} \\ \lambda_{00}\Phi^*_{M,0} \\ \lambda_{01} \\ \lambda_{01}\Phi^*_{M,0} \end{Bmatrix} = \begin{Bmatrix} K^*_{01}\Phi^*_{K,1} - \lambda_{10}(M^*_{00} - M^*_{01})\Phi^*_{M,1} \\ K^*_{11}\Phi^*_{K,1} - \lambda_{11}(M^*_{11} - M^*_{10})\Phi^*_{M,1} \end{Bmatrix} \tag{5.4}$$

expression in which $[B]$ is a matrix of constant known coefficients, $\{D\}$ is a known vector of coefficients and $\{z\}$ contains the full set of unknown variables.

Variables in $\{z\}$ might be single (λ_k, u_{ik}, v_{ik} or w_{ik}) or coupled as a result of products of variables of stiffnesses and modal displacements ($E_jA_ju_{ik}$, $E_jI_jw_{ik}$), only stiffnesses (E_jA_j and E_jI_j), masses and modal displacements (m_jv_{ik}) or eigenfrequencies and modal displacements (λ_ku_{ik}, λ_kv_{ik} or λ_kw_{ik}).

Since vector $\{z\}$ contains the parameters to be observed, the study of the null space of $[B]$ allows to identify the set of observable variables as it has previously been done in the static measurements case.

eq. (B.6) could also be written in an expanded version, by writing the several equations it leads to; this can be done in this way:

$$\left.\begin{aligned} K^*_{00}\Phi^*_{K,0} + K^*_{01}\Phi^*_{K,1} &= (\lambda_{00}M^*_{00} + \lambda_{01}M^*_{10})\Phi^*_{M,0} + (\lambda_{00}M^*_{01} + \lambda_{01}M^*_{11})\Phi^*_{M,1} \\ K^*_{00}\Phi^*_{K,0} + K^*_{01}\Phi^*_{K,1} &= (\lambda_{10}M^*_{00} + \lambda_{11}M^*_{10})\Phi^*_{M,0} + (\lambda_{10}M^*_{01} + \lambda_{11}M^*_{11})\Phi^*_{M,1} \end{aligned}\right\} \tag{5.5}$$

5.1.2 SSI from a unique vibration mode - particular case

As a particular case of the SSI from multiple modes of vibration, the study of a single vibration mode can be considered. In this case, eq. (4.14) might be written as:

$$[K]\{\Phi\} = \lambda[M]\{\Phi\} \tag{5.6}$$

which in turn can be written as a system of partitioned matrices as follows:

$$\begin{bmatrix} K_{00} & K_{01} \\ K_{10} & K_{11} \end{bmatrix} \begin{Bmatrix} \Phi_{K,0} \\ \Phi_{K,1} \end{Bmatrix} = \lambda_0 \begin{bmatrix} M_{00} & M_{01} \\ M_{10} & M_{11} \end{bmatrix} \begin{Bmatrix} \Phi_{M,0} \\ \Phi_{M,1} \end{Bmatrix} \tag{5.7}$$

The two main differences with respect to the multiple modes formulation are the following ones:

1. The eigenfrequency is no longer a vector but a scalar.

2. The stiffness and mass matrices are not diagonal matrices made up of matrices in its diagonals anymore, but single matrices.

In the formulation, the square frequency of the mode shape, λ is assumed to be unknown (λ_0).

Again, unknown mechanical properties might be found in matrices [K] and [M]. In order to analyse the observability of the unknown variables, the unknown products of variables of the stiffness and mass matrices are moved to the corresponding modified vectors of modes of vibration $\{\Phi_K^*\}$ and $\{\Phi_M^*\}$. Doing so, modified stiffness and mass matrices $[K^*]$ and $[M^*]$ are matrices of known coefficients. The resulting system of equations is then written as:

$$[K^*]\{\Phi_K^*\} = \lambda_0[M]\{\Phi_M^*\} \tag{5.8}$$

$$\begin{bmatrix} K_{00}^* & K_{01}^* \\ K_{10}^* & K_{11}^* \end{bmatrix} \begin{Bmatrix} \Phi_{K,0}^* \\ \Phi_{K,1}^* \end{Bmatrix} = \lambda_0 \begin{bmatrix} M_{00}^* & M_{01}^* \\ M_{10}^* & M_{11}^* \end{bmatrix} \begin{Bmatrix} \Phi_{M,0}^* \\ \Phi_{M,1}^* \end{Bmatrix} \tag{5.9}$$

As it has previously been done, system in eq. (5.9) might be rearranged in order to join all the unknown variables in a vector $\{z\}$ and all the known ones in a vector of coefficients $\{D\}$ as it can be seen in

eq. (5.10).

$$[B]\{z\} = \begin{bmatrix} K^*_{00} & -M^*_{01}\Phi^*_{M,1} & -M^*_{00} \\ K^*_{10} & -M^*_{10}\Phi^*_{M,1} & -M^*_{11} \end{bmatrix} \begin{Bmatrix} \Phi^*_{K,0} \\ \lambda_0 \\ \lambda_0\Phi^*_{M,0} \end{Bmatrix} = \begin{Bmatrix} -K^*_{01}\Phi^*_{K,1} \\ -K^*_{11}\Phi^*_{K,1} \end{Bmatrix} = \{D\} \tag{5.10}$$

where $\{z\}$ includes three terms ($\Phi^*_{K,0}$, λ_0 and $\lambda_0\Phi^*_{M,0}$) that account for the unknown frequency and unknown variables coming from the modified stiffness and mass matrices.

It is to highlight that one of these terms is presents coupling between the eigenfrequency and the modified mass modal vector ($\lambda_0\Phi^*_{M,0}$). Since the eigenfrequency is multiplying the whole modified mass matrix, it is found coupled with each of the unknown parameters of Φ. Although this coupling generates an added complexity to the identification of the parameters of this vector, the experimental modal analysis is able to easily compute the eigenfrequencies of a structure. In consequence, the eigenfrequency might be assumed as known in most of the study cases.

Then, assuming the eigenfrequency as known, λ_0 can be written as λ_1 and eq. (5.10) can be written as eq. (5.11).

$$[B]\{z\} = \begin{bmatrix} K^*_{00} & -\lambda_1 M^*_{00} \\ K^*_{10} & -\lambda_1 M^*_{11} \end{bmatrix} \begin{Bmatrix} \Phi^*_{K,0} \\ \Phi^*_{M,0} \end{Bmatrix} = \begin{Bmatrix} \lambda_1 M^*_{01}\Phi^*_{M,1} - K^*_{00}\Phi^*_{K,1} \\ \lambda_1 M^*_{10}\Phi^*_{M,1} - K^*_{11}\Phi^*_{K,1} \end{Bmatrix} = \{D\} \tag{5.11}$$

Again, the previous matrices can be written as systems of individual equations as follows if the frequency is assumed to be unknown:

$$\left.\begin{aligned} K^*_{00}\Phi^*_{K,0} + K^*_{01}\Phi^*_{K,1} &= \lambda_0 \cdot M^*_{00}\Phi^*_{M,0} + \lambda_0 \cdot M^*_{01}\Phi^*_{M,1} \\ K^*_{10}\Phi^*_{K,0} + K^*_{11}\Phi^*_{K,1} &= \lambda_0 \cdot M^*_{10}\Phi^*_{M,0} + \lambda_0 \cdot M^*_{11}\Phi^*_{M,1} \end{aligned}\right\} \tag{5.12}$$

And as follows if the frequency is supposed to be known:

$$\left.\begin{aligned} K^*_{00}\Phi^*_{K,0} - \lambda_1 M^*_{00}\Phi^*_{M,0} &= \lambda_1 \cdot M^*_{01}\Phi^*_{M,1} - K^*_{00}\Phi^*_{K,1} \\ K^*_{10}\Phi^*_{K,0} - \lambda_1 M^*_{11}\Phi^*_{M,0} &= \lambda_1 \cdot M^*_{10}\Phi^*_{M,1} - K^*_{11}\Phi^*_{K,1} \end{aligned}\right\} \tag{5.13}$$

5.2 Algorithm of the dynamic identification

Following the path lines of the algorithm developed by Lozano et al [35], an algorithm has been developed in order to approach the dynamic observability problem. The proposed algorithm takes as inputs the topology of the structure (this is, the coordinates of the structure's nodes), the boundary conditions and the subset of measured parameters (letting this be the mechanical properties E, A, I and S, and the modal parameters, which correspond to the displacements u, v, w and the natural frequency f). Then, the outputs of the algorithm are the subset of observable variables and its values.

Similarly to the static algorithm, in the dynamic algorithm the method is applied repeatedly until no more variables are to be observed.

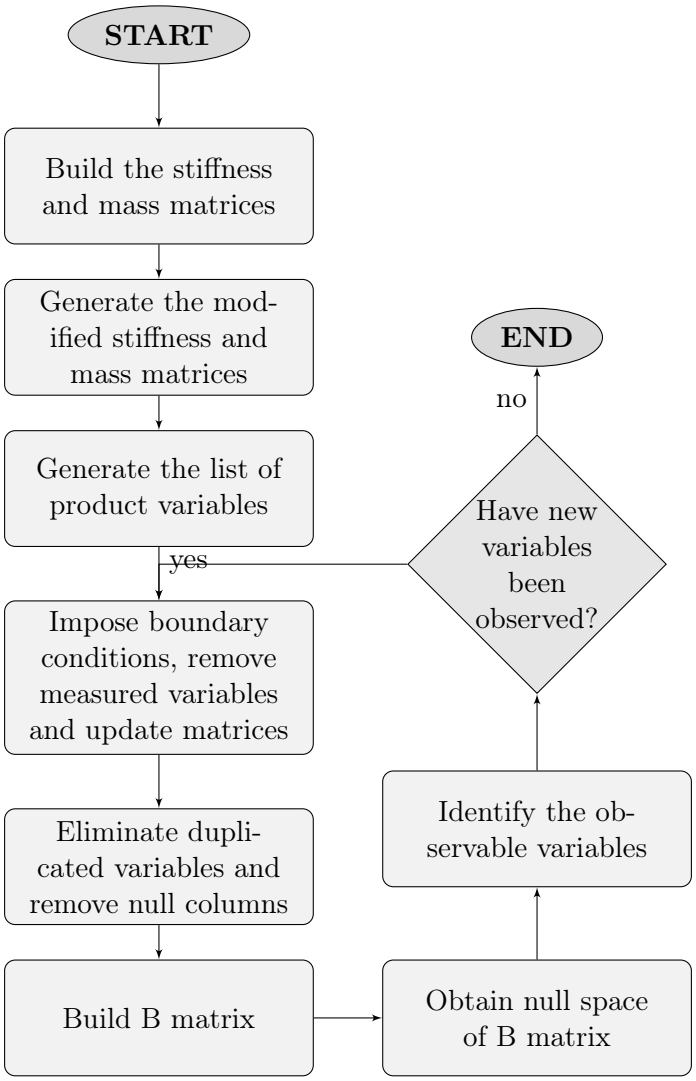

Figure 5.1: Flow chart of the dynamic algorithm

Figure 5.1 shows the flowchart of the dynamic algorithm. In the following sections the several steps of

the dynamic identification are explained with more detail by using some examples.

Chapter 6

Application of the dynamic observability

6.1 Symbolic application of the dynamic identification

6.1.1 Example 1: cantilever (single vibration mode)

In the first symbolic example a rather simple structure is taken under study. The cantilever in section 4.3.3 is considered. As it can be seen, it is discretised with only two nodes (one in each end). Since it is the first example, a single vibration mode is considered.

The variables that are assumed as known are the Young's modulus E, the length of the element L, the frequency squared $\omega^2 = \lambda$, the mass m and the vertical displacement of the second node, v_2.

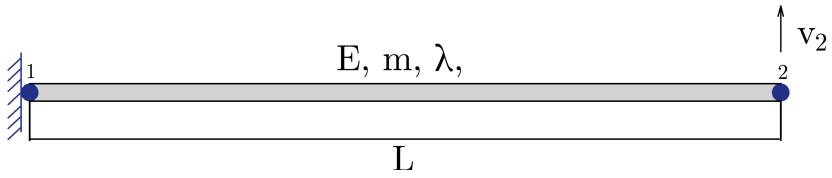

Figure 6.1: Illustration of the cantilever beam used in the example for the symbolic application and its known variables

Figure 6.2: Illustration of the cantilever beam used in the example for the symbolic application and its unknown variables

Step 1. Building stiffness and mass matrices

Firstly, the assemblage of the stiffness and mass matrices, $[K]$ and $[M]$ is carried out based on the topology of the structure. Then, the matrices are located in the from that has been presented in eq. (5.6), which corresponds to the expression of the eigenvalue equation.

$$\begin{bmatrix} \frac{EA}{L} & 0 & 0 & -\frac{EA}{L} & 0 & 0 \\ 0 & \frac{12EI}{L^3} & \frac{6EI}{L^2} & 0 & -\frac{12EI}{L^3} & \frac{6EI}{L^2} \\ 0 & \frac{6EI}{L^2} & \frac{4EI}{L} & 0 & -\frac{6EI}{L^2} & -\frac{2EI}{L} \\ -\frac{EA}{L} & 0 & 0 & \frac{EA}{L} & 0 & 0 \\ 0 & -\frac{12EI}{L^3} & -\frac{6EI}{L^2} & 0 & \frac{12EI}{L^3} & -\frac{6EI}{L^2} \\ 0 & \frac{6EI}{L^2} & -\frac{2EI}{L} & 0 & -\frac{6EI}{L^2} & \frac{4EI}{L} \end{bmatrix} \begin{Bmatrix} u_1 \\ v_1 \\ w_1 \\ u_2 \\ v_2 \\ w_2 \end{Bmatrix} = \lambda_0 \begin{bmatrix} \frac{mL}{3} & 0 & 0 & \frac{mL}{6} & 0 & 0 \\ 0 & \frac{13mL}{35} & \frac{11mL^2}{210} & 0 & \frac{9mL}{70} & -\frac{13mL^2}{420} \\ 0 & \frac{11mL^2}{210} & \frac{mL^3}{105} & 0 & \frac{13mL^2}{420} & -\frac{mL^3}{140} \\ \frac{mL}{6} & 0 & 0 & \frac{mL}{3} & 0 & 0 \\ 0 & \frac{9mL}{70} & \frac{13mL^2}{420} & 0 & \frac{13mL}{35} & -\frac{11mL^2}{210} \\ 0 & -\frac{13mL^2}{420} & -\frac{mL^3}{140} & 0 & -\frac{11mL^2}{210} & \frac{mL^3}{105} \end{bmatrix} \begin{Bmatrix} u_1 \\ v_1 \\ w_1 \\ u_2 \\ v_2 \\ w_2 \end{Bmatrix}$$

Figure 6.3: Step 1

Steps 2 and 3. Generating modified stiffness and mass matrices

In order to generate the modified stiffness and mass matrices $[K^*]$ and $[M^*]$, the terms made of summands should be separated. However, this does not apply to the studied structure since there are no compound terms.

Besides, the list of product variables is generated. The set of all different product variables is identified by moving the variables corresponding to each column to their respective column vectors of displacements, so that the modified vectors of displacements $\{\Phi_K^*\}$ and $\{\Phi_M^*\}$ are obtained.

After this step, it can be seen how matrices $[K^*]$ and $[M^*]$ are now built up by constant terms.

$$\begin{bmatrix} \frac{1}{L} & 0 & 0 & -\frac{1}{L} & 0 & 0 \\ 0 & \frac{12}{L^3} & \frac{6}{L^2} & 0 & -\frac{12}{L^3} & \frac{6}{L^2} \\ 0 & \frac{6}{L^2} & \frac{4}{L} & 0 & -\frac{6}{L^2} & -\frac{2}{L} \\ -\frac{1}{L} & 0 & 0 & \frac{1}{L} & 0 & 0 \\ 0 & -\frac{12}{L^3} & -\frac{6}{L^2} & 0 & \frac{12}{L^3} & -\frac{6}{L^2} \\ 0 & \frac{6}{L^2} & -\frac{2EI}{L} & 0 & -\frac{6}{L^2} & \frac{4}{L} \end{bmatrix} \begin{Bmatrix} EAu_1 \\ EIv_1 \\ EIw_1 \\ EAu_2 \\ EIv_2 \\ EIw_2 \end{Bmatrix} = \lambda_0 \begin{bmatrix} \frac{L}{3} & 0 & 0 & \frac{L}{6} & 0 & 0 \\ 0 & \frac{13L}{35} & \frac{11L^2}{210} & 0 & \frac{9L}{70} & -\frac{13L^2}{420} \\ 0 & \frac{11L^2}{210} & \frac{L^3}{105} & 0 & \frac{13L^2}{420} & -\frac{L^3}{140} \\ \frac{L}{6} & 0 & 0 & \frac{L}{3} & 0 & 0 \\ 0 & \frac{9L}{70} & \frac{13L^2}{420} & 0 & \frac{13L}{35} & -\frac{11L^2}{210} \\ 0 & -\frac{13L^2}{420} & -\frac{L^3}{140} & 0 & -\frac{11L^2}{210} & \frac{L^3}{105} \end{bmatrix} \begin{Bmatrix} mu_1 \\ mv_1 \\ mw_1 \\ mu_2 \\ mv_2 \\ mw_2 \end{Bmatrix}$$

Figure 6.4: Steps 2 and 3

Step 4. Imposing boundary conditions, removing measured variables and updating matrices

Now the columns of matrices $[K^*]$ and $[M^*]$ associated with boundary conditions and measured values are multiplied by their corresponding values and the associated factors are removed from the vectors of displacements.

In this case, the boundary conditions are $u_1 = 0$, $v_1 = 0$ and $w_1 = 0$ and the measured values are E, v_2, m and λ. Because the frequency is assumed to be known, now its corrsponding term is written as λ_1 instead of λ_0.

Figure 6.5 shows how the known displacements are introduced (the three displacements corresponding to the boundary conditions and v_2).

$$\begin{bmatrix} 0 & 0 & 0 & -\frac{1}{L} & 0 & 0 \\ 0 & 0 & 0 & 0 & -\frac{12v_2}{L^3} & \frac{6}{L^2} \\ 0 & 0 & 0 & 0 & -\frac{6v_2}{L^2} & -\frac{2}{L} \\ 0 & 0 & 0 & \frac{1}{L} & 0 & 0 \\ 0 & 0 & 0 & 0 & \frac{12v_2}{L^3} & -\frac{6}{L^2} \\ 0 & 0 & 0 & 0 & -\frac{6v_2}{L^2} & \frac{4}{L} \end{bmatrix} \begin{Bmatrix} 0 \\ 0 \\ 0 \\ EAu_2 \\ EIv_2 \\ EIw_2 \end{Bmatrix} = \lambda_1 \begin{bmatrix} 0 & 0 & 0 & \frac{L}{6} & 0 & 0 \\ 0 & 0 & 0 & 0 & \frac{9v_2L}{70} & -\frac{13L^2}{420} \\ 0 & 0 & 0 & 0 & \frac{13v_2L^2}{420} & -\frac{L^3}{140} \\ 0 & 0 & 0 & \frac{L}{3} & 0 & 0 \\ 0 & 0 & 0 & 0 & \frac{13v_2L}{35} & -\frac{11L^2}{210} \\ 0 & 0 & 0 & 0 & -\frac{11v_2L^2}{210} & \frac{L^3}{105} \end{bmatrix} \begin{Bmatrix} 0 \\ 0 \\ 0 \\ mu_2 \\ mv_2 \\ mw_2 \end{Bmatrix}$$

Figure 6.5: Step 4.1

Then, fig. 6.6 shows how the measured properties are introduced. See that the fifth column of the mass matrix corresponds to the variables mv_2, which are both known. Therefore, the complete column is moved outside of the mass matrix and corresponds to the so-called independent term.

$$\begin{bmatrix} 0 & 0 & 0 & -\frac{E}{L} & 0 & 0 \\ 0 & 0 & 0 & 0 & -\frac{12Ev_2}{L^3} & \frac{6E}{L^2} \\ 0 & 0 & 0 & 0 & -\frac{6Ev_2}{L^2} & -\frac{2E}{L} \\ 0 & 0 & 0 & \frac{E}{L} & 0 & 0 \\ 0 & 0 & 0 & 0 & \frac{12Ev_2}{L^3} & -\frac{6E}{L^2} \\ 0 & 0 & 0 & 0 & -\frac{6Ev_2}{L^2} & \frac{4E}{L} \end{bmatrix} \begin{Bmatrix} 0 \\ 0 \\ 0 \\ Au_2 \\ I \\ Iw_2 \end{Bmatrix} = \lambda_1 \begin{bmatrix} 0 & 0 & 0 & \frac{Lm}{6} & 0 \\ 0 & 0 & 0 & 0 & -\frac{13mL^2}{420} \\ 0 & 0 & 0 & 0 & -\frac{L^3m}{140} \\ 0 & 0 & 0 & \frac{Lm}{3} & 0 \\ 0 & 0 & 0 & 0 & -\frac{11L^2m}{210} \\ 0 & 0 & 0 & 0 & \frac{L^3m}{105} \end{bmatrix} \begin{Bmatrix} 0 \\ 0 \\ 0 \\ u_2 \\ w_2 \end{Bmatrix} + \begin{Bmatrix} 0 \\ \frac{9\lambda_1 mv_2L}{70} \\ \frac{13\lambda_1 mv_2L^2}{420} \\ 0 \\ \frac{13\lambda_1 mv_2L}{35} \\ -\frac{11\lambda_1 mv_2L^2}{210} \end{Bmatrix}$$

Figure 6.6: Step 4.2

Step 5. Eliminating duplicated variables and removing null columns

In this step of the algorithm, the duplicated variables are identified and put together into the same column. However, as it can be seen, no duplicated variables exist in the displacements vectors $\{\Phi_K^*\}$ and $\{\Phi_M^*\}$. This will be seen in further examples.

Also, when some displacements - measured ones or coming from boundary conditions - are null, they generate a null column that can be removed from the modified stiffness and mass matrices, together with their associated variable in the displacement vector.

$$\begin{bmatrix} -\frac{E}{L} & 0 & 0 \\ 0 & -\frac{12Ev_2}{L^3} & \frac{6E}{L^2} \\ 0 & -\frac{6Ev_2}{L^2} & -\frac{2E}{L} \\ \frac{E}{L} & 0 & 0 \\ 0 & \frac{12Ev_2}{L^3} & -\frac{6E}{L^2} \\ 0 & -\frac{6Ev_2}{L^2} & \frac{4E}{L} \end{bmatrix} \begin{Bmatrix} Au_2 \\ I \\ Iw_2 \end{Bmatrix} = \lambda_1 \begin{bmatrix} \frac{Lm}{6} & 0 \\ 0 & -\frac{13mL^2}{420} \\ 0 & -\frac{L^3m}{140} \\ \frac{Lm}{3} & 0 \\ 0 & -\frac{11L^2m}{210} \\ 0 & \frac{L^3m}{105} \end{bmatrix} \begin{Bmatrix} u_2 \\ w_2 \end{Bmatrix} + \begin{Bmatrix} 0 \\ \frac{9\lambda_1 mv_2L}{70} \\ \frac{13\lambda_1 mv_2L^2}{420} \\ 0 \\ \frac{13\lambda_1 mv_2L}{35} \\ -\frac{11\lambda_1 mv_2L^2}{210} \end{Bmatrix}$$

Figure 6.7: Step 5

Step 6. Building B matrix

In this step matrix $[B]$ and vectors $\{z\}$ and $\{D\}$ are built as it has been presented previously.

Matrix $[B]$ is assembled using both matrices $[K^*]$ and $[M^*]$ and the vector of unknowns $\{z\}$ is formed by setting together vectors $\{\Phi_K^*\}$ and $\{\Phi_M^*\}$. Then, the vector of completely known terms $\{D\}$ is set on the right-hand side of the equation. Note that it corresponds to the independent term that was previously defined.

$$\begin{bmatrix} -\frac{E}{L} & 0 & 0 & \frac{-\lambda_1 Lm}{6} & 0 \\ 0 & -\frac{12Ev_2}{L^3} & \frac{6E}{L^2} & 0 & \frac{\lambda_1 13mL^2}{420} \\ 0 & -\frac{6Ev_2}{L^2} & -\frac{2E}{L} & 0 & \frac{\lambda_1 L^3 m}{140} \\ \frac{E}{L} & 0 & 0 & \frac{-\lambda_1 Lm}{3} & 0 \\ 0 & \frac{12Ev_2}{L^3} & -\frac{6E}{L^2} & 0 & \frac{\lambda_1 11L^2 m}{210} \\ 0 & -\frac{6Ev_2}{L^2} & \frac{4E}{L} & 0 & \frac{-\lambda_1 L^3 m}{105} \end{bmatrix} \begin{Bmatrix} Au_2 \\ I \\ Iw_2 \\ u_2 \\ w_2 \end{Bmatrix} = \begin{Bmatrix} 0 \\ \frac{9\lambda_1 mv_2L}{70} \\ \frac{13\lambda_1 mv_2L^2}{420} \\ 0 \\ \frac{13\lambda_1 mv_2L}{35} \\ -\frac{11\lambda_1 mv_2L^2}{210} \end{Bmatrix}$$

Figure 6.8: Step 6

Step 7. Obtaining null space of matrix B

The last step of each recursive loop is to determine the null space of the matrix $[B]$, assembled in step 6, with the goal of identifying the observable variables.

Also, the parametric equations are derived in this step. It is to note that the null space of matrix $[B]$ is computed with the *null* command of Matlab. Studying the null rows of the null space of matrix $[B]$ allows to identify which of the variables in vector $\{z\}$ have a unique solution, meaning that they are observable.

In this case, the null space of the problem is:

$$NullSpace = \begin{pmatrix} 0 \\ 0 \\ 0 \\ 0 \\ 0 \end{pmatrix} \tag{6.1}$$

Step 8. Identifying the observable variables

From the previous step in which the null space was found, it can be deduced that the observable and unobservable variables are:

$$Observable = \begin{pmatrix} Au_2 \\ I \\ Iw_2 \\ u_2 \\ w_2 \end{pmatrix} ; \quad Unobservable = \varnothing \tag{6.2}$$

It might be seen that both coupled and uncoupled variables have been observed. One of the interesting points of the observability method is that it is possible to define a particular parametric solution of the system.

This means that an equation might be obtained that relates the observed variables with other known variables. In order to obtain these parametric equations it is necessary to calculate the inverse matrix of matrix $[B]$, $[B]^{-1}$, as shown in eq. (6.3)

$$\{z\} = \begin{Bmatrix} Au_2 \\ I \\ Iw_2 \\ u_2 \\ w_2 \end{Bmatrix} = [B]^{-1}\{D\} \tag{6.3}$$

Sometimes matrix $[B]$ is not a square matrix and therefore this operation is performed by using the pseudo-inverse matrix instead of the inverse one.

For the first time in the literature, a set of parametric equations might be obtained by the method of observability over dynamic SSI. All the relationships are quotient ones and problems may arise when the values on the denominators tend to zero. The behaviour of the solution might be studied in order to check which of the observed variables are more sensitive to certain small perturbations or in which case the observed variables would present non-reliable results.

If working with these equations it can be seen, first of all, that a system of equations including the variables Au_2 and u_2 can be obtained. This system is shown in eq. (6.4).

$$\begin{cases} -\frac{E}{L}Au_2 - \frac{\lambda_1 Lm}{6}u_2 = 0 \\ \frac{E}{L}Au_2 - \frac{\lambda_1 Lm}{3}u_2 = 0 \end{cases} \tag{6.4}$$

If the system is solved as a simple two equations system with two unknowns (Au_2 and u_2) it is obtained that:

$$\frac{3E}{L}\left(Au_2\right) = 0 \tag{6.5}$$

This is so because the horizontal motion at node 2 is 0, and therefore the product $A \cdot u_2$ is zero too. Hence, although the product Au_2 can be said to be observable, the variable A is not observable in this case, although the program would give a result for the area such as $A = 0$.

This problem arises in this example because the vibration natural deflections constrain the horizontal motion, making u_i always zero, for any node or mode of vibration.

Step 9. Recursive process

If there were any observed variables, they would be used here to repeat the process from step 6 in order to try to observe more new variables.

The algorithm introduces the observed variables from previous recursive steps into step 6, directly into matrix $[B]$. Then, structural parameters such as E_j, A_j, I_j and m_j are considered and treated in the same way as known modal displacements. Then, the iterations are performed until no unknown variable can be observed or until all variables have been observed (fact that depends on the complexity of the problem and initial set of inputs).

6.1.2 Example 2: cantilever (multiple vibration modes)

In the previous example, a cantilever was studied using the observability method with only one mode. Now, in order to illustrate how the dynamic method works when more than one mode are available, the same structure from section 4.3.3 is used, but now two modes, f_1 and f_2 are studied.

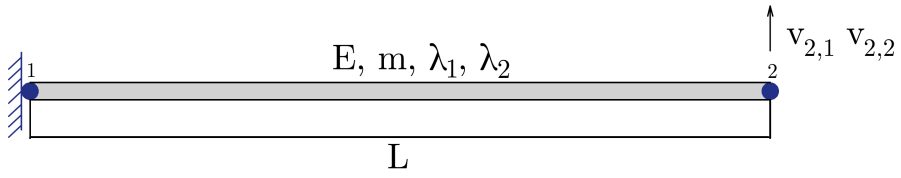

Figure 6.9: Illustration of the cantilever beam used in the example for the two modes symbolic application and the known parameters

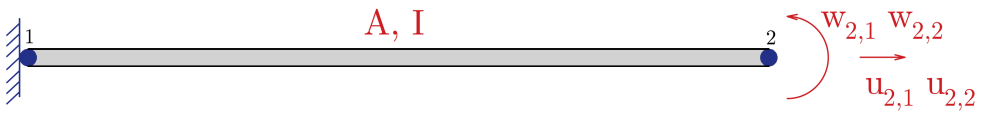

Figure 6.10: Illustration of the cantilever beam used in the two modes example for the symbolic application and the unknown parameters

Step 1. Building stiffness and mass matrices

Firstly, the assemblage of the stiffness and mass matrices, $[K]$ and $[M]$ is carried out based on the topology of the structure. The difference when working with different modes of vibration is that the matrices increase its size because the matrices regarding each mode have to be put in the diagonals of $[K]$ and $[M]$ and the displacements for each mode have to be put into the vectors as shown in eq. (6.6).

$$\begin{bmatrix} K_1 & 0 \\ 0 & K_2 \end{bmatrix} \begin{Bmatrix} u_{K,1} \\ u_{K,2} \end{Bmatrix} = \{\lambda\} \begin{bmatrix} M_1 & 0 \\ 0 & M_2 \end{bmatrix} \begin{Bmatrix} u_{M,1} \\ u_{M,2} \end{Bmatrix} \tag{6.6}$$

The resulting system of matrices is therefore the one in fig. 6.11.

$$\begin{bmatrix}
\frac{EA}{L} & 0 & 0 & -\frac{EA}{L} & 0 & 0 & 0 & 0 & 0 & 0 & 0 & 0 \\
0 & \frac{12EI}{L^3} & \frac{6EI}{L^2} & 0 & -\frac{12EI}{L^3} & \frac{6EI}{L^2} & 0 & 0 & 0 & 0 & 0 & 0 \\
0 & \frac{6EI}{L^2} & \frac{4EI}{L} & 0 & -\frac{6EI}{L^2} & -\frac{2EI}{L} & 0 & 0 & 0 & 0 & 0 & 0 \\
-\frac{EA}{L} & 0 & 0 & \frac{EA}{L} & 0 & 0 & 0 & 0 & 0 & 0 & 0 & 0 \\
0 & -\frac{12EI}{L^3} & -\frac{6EI}{L^2} & 0 & \frac{12EI}{L^3} & -\frac{6EI}{L^2} & 0 & 0 & 0 & 0 & 0 & 0 \\
0 & \frac{6EI}{L^2} & 0 & 0 & -\frac{6EI}{L^2} & \frac{4EI}{L} & 0 & 0 & 0 & 0 & 0 & 0 \\
0 & 0 & 0 & 0 & 0 & 0 & \frac{EA}{L} & 0 & 0 & -\frac{EA}{L} & 0 & 0 \\
0 & 0 & 0 & 0 & 0 & 0 & 0 & \frac{12EI}{L^3} & \frac{6EI}{L^2} & 0 & -\frac{12EI}{L^3} & \frac{6EI}{L^2} \\
0 & 0 & 0 & 0 & 0 & 0 & 0 & \frac{6EI}{L^2} & \frac{4EI}{L} & 0 & -\frac{6EI}{L^2} & -\frac{2EI}{L} \\
0 & 0 & 0 & 0 & 0 & 0 & -\frac{EA}{L} & 0 & 0 & \frac{EA}{L} & 0 & 0 \\
0 & 0 & 0 & 0 & 0 & 0 & 0 & -\frac{12EI}{L^3} & -\frac{6EI}{L^2} & 0 & \frac{12EI}{L^3} & -\frac{6EI}{L^2} \\
0 & 0 & 0 & 0 & 0 & 0 & 0 & \frac{6EI}{L^2} & 0 & 0 & -\frac{6EI}{L^2} & \frac{4EI}{L}
\end{bmatrix}
\begin{Bmatrix}
u_{1,1} \\ v_{1,1} \\ w_{1,1} \\ u_{2,1} \\ v_{2,1} \\ w_{2,1} \\ u_{1,2} \\ v_{1,2} \\ w_{1,2} \\ u_{2,2} \\ v_{2,2} \\ w_{2,2}
\end{Bmatrix} =$$

$$[\lambda_0]
\begin{bmatrix}
\frac{mL}{3} & 0 & 0 & \frac{mL}{6} & 0 & 0 & 0 & 0 & 0 & 0 & 0 & 0 \\
0 & \frac{13mL}{35} & \frac{11mL^2}{210} & 0 & \frac{9mL}{70} & -\frac{13mL^2}{420} & 0 & 0 & 0 & 0 & 0 & 0 \\
0 & \frac{11mL^2}{210} & \frac{mL^3}{105} & 0 & \frac{13mL^2}{420} & -\frac{mL^3}{140} & 0 & 0 & 0 & 0 & 0 & 0 \\
\frac{mL}{6} & 0 & 0 & \frac{mL}{3} & 0 & 0 & 0 & 0 & 0 & 0 & 0 & 0 \\
0 & \frac{9mL}{70} & \frac{13mL^2}{420} & 0 & \frac{13mL}{35} & -\frac{11mL^2}{210} & 0 & 0 & 0 & 0 & 0 & 0 \\
0 & -\frac{13mL^2}{420} & -\frac{mL^3}{140} & 0 & -\frac{11mL^2}{210} & \frac{mL^3}{105} & 0 & 0 & 0 & 0 & 0 & 0 \\
0 & 0 & 0 & 0 & 0 & 0 & \frac{mL}{3} & 0 & 0 & \frac{mL}{6} & 0 & 0 \\
0 & 0 & 0 & 0 & 0 & 0 & 0 & \frac{13mL}{35} & \frac{11mL^2}{210} & 0 & \frac{9mL}{70} & -\frac{13mL^2}{420} \\
0 & 0 & 0 & 0 & 0 & 0 & 0 & \frac{11mL^2}{210} & \frac{mL^3}{105} & 0 & \frac{13mL^2}{420} & -\frac{mL^3}{140} \\
0 & 0 & 0 & 0 & 0 & 0 & \frac{mL}{6} & 0 & 0 & \frac{mL}{3} & 0 & 0 \\
0 & 0 & 0 & 0 & 0 & 0 & 0 & \frac{9mL}{70} & \frac{13mL^2}{420} & 0 & \frac{13mL}{35} & -\frac{11mL^2}{210} \\
0 & 0 & 0 & 0 & 0 & 0 & 0 & -\frac{13mL^2}{420} & -\frac{mL^3}{140} & 0 & -\frac{11mL^2}{210} & \frac{mL^3}{105}
\end{bmatrix}
\begin{Bmatrix}
u_{1,1} \\ v_{1,1} \\ w_{1,1} \\ u_{2,1} \\ v_{2,1} \\ w_{2,1} \\ u_{1,2} \\ v_{1,2} \\ w_{1,2} \\ u_{2,2} \\ v_{2,2} \\ w_{2,2}
\end{Bmatrix}$$

Figure 6.11: Step 1

Where $[\lambda_0]$ equals the following expression:

$$\begin{bmatrix}
\lambda_{0,1} & 0 & 0 & 0 & 0 & 0 & 0 & 0 & 0 & 0 & 0 & 0 \\
0 & \lambda_{0,1} & 0 & 0 & 0 & 0 & 0 & 0 & 0 & 0 & 0 & 0 \\
0 & 0 & \lambda_{0,1} & 0 & 0 & 0 & 0 & 0 & 0 & 0 & 0 & 0 \\
0 & 0 & 0 & \lambda_{0,1} & 0 & 0 & 0 & 0 & 0 & 0 & 0 & 0 \\
0 & 0 & 0 & 0 & \lambda_{0,1} & 0 & 0 & 0 & 0 & 0 & 0 & 0 \\
0 & 0 & 0 & 0 & 0 & \lambda_{0,1} & 0 & 0 & 0 & 0 & 0 & 0 \\
0 & 0 & 0 & 0 & 0 & 0 & \lambda_{0,2} & 0 & 0 & 0 & 0 & 0 \\
0 & 0 & 0 & 0 & 0 & 0 & 0 & \lambda_{0,2} & 0 & 0 & 0 & 0 \\
0 & 0 & 0 & 0 & 0 & 0 & 0 & 0 & \lambda_{0,2} & 0 & 0 & 0 \\
0 & 0 & 0 & 0 & 0 & 0 & 0 & 0 & 0 & \lambda_{0,2} & 0 & 0 \\
0 & 0 & 0 & 0 & 0 & 0 & 0 & 0 & 0 & 0 & \lambda_{0,2} & 0 \\
0 & 0 & 0 & 0 & 0 & 0 & 0 & 0 & 0 & 0 & 0 & \lambda_{0,2}
\end{bmatrix} \tag{6.7}$$

Steps 2 and 3. Generating modified stiffness and mass matrices

In order to obtain the modified stiffness and mass matrices, the terms made up of summands must be separated. However, as it happened before, this does not apply to this case since there are not compound terms. This would be step 2.

As for the third step, the list of product variables is now to be generated. The set of all product

variables is identified and they are moved to their respective column vector of displacement.

After these steps, it can be seen how the modified matrices $[K^*]$ and $[M^*]$ and vectors $\{\Phi_K^*\}$ and $\{\Phi_M^*\}$ have been obtained.

$$\begin{bmatrix}
\frac{1}{L} & 0 & 0 & -\frac{1}{L} & 0 & 0 & 0 & 0 & 0 & 0 & 0 & 0 \\
0 & \frac{12}{L^3} & \frac{6}{L^2} & 0 & -\frac{12}{L^3} & \frac{6}{L^2} & 0 & 0 & 0 & 0 & 0 & 0 \\
0 & \frac{6}{L^2} & \frac{4}{L} & 0 & -\frac{6}{L^2} & & 0 & 0 & 0 & 0 & 0 & 0 \\
-\frac{1}{L} & 0 & 0 & \frac{1}{L} & 0 & 0 & 0 & 0 & 0 & 0 & 0 & 0 \\
0 & -\frac{12}{L^3} & -\frac{6}{L^2} & 0 & \frac{12}{L^3} & -\frac{6}{L^2} & 0 & 0 & 0 & 0 & 0 & 0 \\
0 & \frac{6}{L^2} & -\frac{2EI}{L} & 0 & -\frac{6}{L^2} & \frac{4}{L} & 0 & 0 & 0 & 0 & 0 & 0 \\
0 & 0 & 0 & 0 & 0 & 0 & \frac{1}{L} & 0 & 0 & -\frac{1}{L} & 0 & 0 \\
0 & 0 & 0 & 0 & 0 & 0 & 0 & \frac{12}{L^3} & \frac{6}{L^2} & 0 & -\frac{12}{L^3} & \frac{6}{L^2} \\
0 & 0 & 0 & 0 & 0 & 0 & 0 & \frac{6}{L^2} & \frac{4}{L} & 0 & -\frac{6}{L^2} & \\
0 & 0 & 0 & 0 & 0 & 0 & -\frac{1}{L} & 0 & 0 & \frac{1}{L} & 0 & 0 \\
0 & 0 & 0 & 0 & 0 & 0 & 0 & -\frac{12}{L^3} & -\frac{6}{L^2} & 0 & \frac{12}{L^3} & -\frac{6}{L^2} \\
0 & 0 & 0 & 0 & 0 & 0 & 0 & \frac{6}{L^2} & -\frac{2EI}{L} & 0 & -\frac{6}{L^2} & \frac{4}{L}
\end{bmatrix}
\begin{Bmatrix}
EAu_{1,1} \\ EIv_{1,1} \\ EIw_{1,1} \\ EAu_{2,1} \\ EIv_{2,1} \\ EIw_{2,1} \\ EAu_{1,2} \\ EIv_{1,2} \\ EIw_{1,2} \\ EAu_{2,2} \\ EIv_{2,2} \\ EIw_{2,2}
\end{Bmatrix} =$$

$$[\lambda_0]
\begin{bmatrix}
\frac{L}{3} & 0 & 0 & \frac{L}{6} & 0 & 0 & 0 & 0 & 0 & 0 & 0 & 0 \\
0 & \frac{13L}{35} & \frac{11L^2}{210} & 0 & \frac{9L}{70} & -\frac{13L^2}{420} & 0 & 0 & 0 & 0 & 0 & 0 \\
0 & \frac{11L^2}{210} & \frac{L^3}{105} & 0 & \frac{13L^2}{420} & -\frac{L^3}{140} & 0 & 0 & 0 & 0 & 0 & 0 \\
\frac{L}{6} & 0 & 0 & \frac{L}{3} & 0 & 0 & 0 & 0 & 0 & 0 & 0 & 0 \\
0 & \frac{9L}{70} & \frac{13L^2}{420} & 0 & \frac{13L}{35} & -\frac{11L^2}{210} & 0 & 0 & 0 & 0 & 0 & 0 \\
0 & -\frac{13L^2}{420} & -\frac{L^3}{140} & 0 & -\frac{11L^2}{210} & \frac{L^3}{105} & 0 & 0 & 0 & 0 & 0 & 0 \\
0 & 0 & 0 & 0 & 0 & 0 & \frac{L}{3} & 0 & 0 & \frac{L}{6} & 0 & 0 \\
0 & 0 & 0 & 0 & 0 & 0 & 0 & \frac{13L}{35} & \frac{11L^2}{210} & 0 & \frac{9L}{70} & -\frac{13L^2}{420} \\
0 & 0 & 0 & 0 & 0 & 0 & 0 & \frac{11L^2}{210} & \frac{L^3}{105} & 0 & \frac{13L^2}{420} & -\frac{L^3}{140} \\
0 & 0 & 0 & 0 & 0 & 0 & \frac{L}{6} & 0 & 0 & \frac{L}{3} & 0 & 0 \\
0 & 0 & 0 & 0 & 0 & 0 & 0 & \frac{9L}{70} & \frac{13L^2}{420} & 0 & \frac{13L}{35} & -\frac{11L^2}{210} \\
0 & 0 & 0 & 0 & 0 & 0 & 0 & -\frac{13L^2}{420} & -\frac{L^3}{140} & 0 & -\frac{11L^2}{210} & \frac{L^3}{105}
\end{bmatrix}
\begin{Bmatrix}
mu_{1,1} \\ mv_{1,1} \\ mw_{1,1} \\ mu_{2,1} \\ mv_{2,1} \\ mw_{2,1} \\ mu_{1,2} \\ mv_{1,2} \\ mw_{1,2} \\ mu_{2,2} \\ mv_{2,2} \\ mw_{2,2}
\end{Bmatrix}$$

Figure 6.12: Steps 2 and 3

Step 4. Imposing boundary conditions, removing measured variables and updating matrices

Now the boundary conditions are applied. In this case, the displacements at node 1 are zero, and therefore the columns corresponding to the degrees of freedom of node 1 become 0. Note that since there are two vibration modes, this applies to both of them and therefore there are six columns in the matrices that change, as well as six rows in the vectors that do so.

As well, the measured variables are moved from the vectors of displacements to the matrices (these are E, m and v_2). Also, the frequencies are known, and therefore $[\lambda_0]$ converts to $[\lambda_1]$

$$
\begin{bmatrix}
0 & 0 & 0 & -\frac{E}{L} & 0 & 0 & 0 & 0 & 0 & 0 & 0 & 0 \\
0 & 0 & 0 & 0 & -\frac{12Ev_2}{L^3} & \frac{6E}{L^2} & 0 & 0 & 0 & 0 & 0 & 0 \\
0 & 0 & 0 & 0 & -\frac{6Ev_2}{L^2} & & 0 & 0 & 0 & 0 & 0 & 0 \\
0 & 0 & 0 & \frac{E}{L} & 0 & 0 & 0 & 0 & 0 & 0 & 0 & 0 \\
0 & 0 & 0 & 0 & \frac{12Ev_2}{L^3} & -\frac{6E}{L^2} & 0 & 0 & 0 & 0 & 0 & 0 \\
0 & 0 & 0 & 0 & -\frac{6Ev_2}{L^2} & \frac{4E}{L} & 0 & 0 & 0 & 0 & 0 & 0 \\
0 & 0 & 0 & 0 & 0 & 0 & 0 & 0 & 0 & -\frac{E}{L} & 0 & 0 \\
0 & 0 & 0 & 0 & 0 & 0 & 0 & 0 & 0 & 0 & -\frac{12Ev_2}{L^3} & \frac{6E}{L^2} \\
0 & 0 & 0 & 0 & 0 & 0 & 0 & 0 & 0 & 0 & -\frac{6Ev_2}{L^2} & \\
0 & 0 & 0 & 0 & 0 & 0 & 0 & 0 & 0 & \frac{E}{L} & 0 & 0 \\
0 & 0 & 0 & 0 & 0 & 0 & 0 & 0 & 0 & 0 & \frac{12Ev_2}{L^3} & -\frac{6E}{L^2} \\
0 & 0 & 0 & 0 & 0 & 0 & 0 & 0 & 0 & 0 & -\frac{6Ev_2}{L^2} & \frac{4E}{L}
\end{bmatrix}
\begin{Bmatrix}
0 \\ 0 \\ 0 \\ Au_{2,1} \\ Iv_{2,1} \\ Iw_{2,1} \\ 0 \\ 0 \\ 0 \\ Au_{2,2} \\ Iv_{2,2} \\ Iw_{2,2}
\end{Bmatrix} =
$$

$$
[\lambda_1]
\begin{bmatrix}
0 & 0 & 0 & \frac{Lm}{6} & 0 & 0 & 0 & 0 & 0 & 0 & 0 & 0 \\
0 & 0 & 0 & 0 & -\frac{13mL^2}{420} & -\frac{13mL^2}{420} & 0 & 0 & 0 & 0 & 0 & 0 \\
0 & 0 & 0 & 0 & -\frac{L^3m}{140} & -\frac{mL^3}{140} & 0 & 0 & 0 & 0 & 0 & 0 \\
0 & 0 & 0 & \frac{Lm}{3} & 0 & 0 & 0 & 0 & 0 & 0 & 0 & 0 \\
0 & 0 & 0 & 0 & -\frac{11L^2m}{210} & -\frac{11mL^2}{210} & 0 & 0 & 0 & 0 & 0 & 0 \\
0 & 0 & 0 & 0 & \frac{L^3m}{105} & \frac{mL^3}{105} & 0 & 0 & 0 & 0 & 0 & 0 \\
0 & 0 & 0 & 0 & 0 & 0 & 0 & 0 & 0 & \frac{Lm}{6} & 0 & 0 \\
0 & 0 & 0 & 0 & 0 & 0 & 0 & 0 & 0 & 0 & \frac{9mL}{70} & -\frac{13mL^2}{420} \\
0 & 0 & 0 & 0 & 0 & 0 & 0 & 0 & 0 & 0 & \frac{13mL^2}{420} & -\frac{L^3m}{140} \\
0 & 0 & 0 & 0 & 0 & 0 & 0 & 0 & 0 & \frac{Lm}{3} & 0 & 0 \\
0 & 0 & 0 & 0 & 0 & 0 & 0 & 0 & 0 & 0 & \frac{13mL}{35} & -\frac{11L^2m}{210} \\
0 & 0 & 0 & 0 & 0 & 0 & 0 & 0 & 0 & 0 & -\frac{11mL^2}{210} & \frac{L^3m}{105}
\end{bmatrix}
\begin{Bmatrix}
0 \\ 0 \\ 0 \\ u_{2,1} \\ v_{2,1} \\ w_{2,1} \\ 0 \\ 0 \\ 0 \\ u_{2,2} \\ v_{2,2} \\ w_{2,2}
\end{Bmatrix}
$$

Figure 6.13: Step 4

Step 5. Eliminating duplicated variables and removing null columns

At this step the duplicated variables would be identified and put together into the same column.

Also, when some displacements - measured ones or coming from boundary conditions - are null, they generate a null column that can be removed from the modified stiffness and mass matrices, together with their associated variable in the displacement vector. In this case, columns 1, 2, 3, 7, 8 and 9.

First of all, no duplicated variables seem to appear, but after introducing the known parameters (fig. 6.15), it can be seen how I appears in two positions. Therefore, its corresponding columns can be put together. Figure 6.15 shows how these columns and its corresponding variables are grouped together.

Also, known $[\lambda_1]$ separates into $[\lambda_{10}]$ and $[\lambda_{11}]$; the first one corresponds to the squared frequencies that are multiplying unknown terms, while the second one corresponds to those squared frequencies that multiply known terms.

$$\begin{bmatrix} -\frac{E}{L} & 0 & 0 & 0 & 0 & 0 \\ 0 & -\frac{12Ev_{2,1}}{L^3} & \frac{6E}{L^2} & 0 & 0 & 0 \\ 0 & -\frac{6Ev_{2,1}}{L^2} & -\frac{2E}{L} & 0 & 0 & 0 \\ \frac{E}{L} & 0 & 0 & 0 & 0 & 0 \\ 0 & \frac{12Ev_{2,1}}{L^3} & -\frac{6E}{L^2} & 0 & 0 & 0 \\ 0 & -\frac{6Ev_{2,1}}{L^2} & \frac{4E}{L} & 0 & 0 & 0 \\ 0 & 0 & 0 & -\frac{E}{L} & 0 & 0 \\ 0 & 0 & 0 & 0 & -\frac{12Ev_{2,2}}{L^3} & \frac{6E}{L^2} \\ 0 & 0 & 0 & 0 & -\frac{6Ev_{2,2}}{L^2} & -\frac{2E}{L} \\ 0 & 0 & 0 & \frac{E}{L} & 0 & 0 \\ 0 & 0 & 0 & 0 & \frac{12Ev_{2,2}}{L^3} & -\frac{6E}{L^2} \\ 0 & 0 & 0 & 0 & -\frac{6Ev_{2,2}}{L^2} & \frac{4E}{L} \end{bmatrix} \begin{Bmatrix} Au_{2,1} \\ I \\ Iw_{2,1} \\ Au_{2,2} \\ I \\ Iw_{2,2} \end{Bmatrix} =$$

$$\lambda_1 \begin{bmatrix} \frac{Lm}{6} & 0 & 0 & 0 \\ 0 & -\frac{13mL^2}{420} & 0 & 0 \\ 0 & -\frac{L^3m}{140} & 0 & 0 \\ \frac{Lm}{3} & 0 & 0 & 0 \\ 0 & -\frac{11L^2m}{210} & 0 & 0 \\ 0 & \frac{L^3m}{105} & 0 & 0 \\ 0 & 0 & \frac{Lm}{6} & 0 \\ 0 & 0 & 0 & -\frac{13mL^2}{420} \\ 0 & 0 & 0 & -\frac{L^3m}{140} \\ 0 & 0 & \frac{Lm}{3} & 0 \\ 0 & 0 & 0 & -\frac{11L^2m}{210} \\ 0 & 0 & 0 & \frac{L^3m}{105} \end{bmatrix} \begin{Bmatrix} u_{2,1} \\ w_{2,1} \\ u_{2,2} \\ w_{2,2} \end{Bmatrix} + \lambda_1 \begin{Bmatrix} 0 \\ -\frac{13mv_{2,1}L^2}{420} \\ -\frac{L^3mv_{2,1}}{140} \\ 0 \\ -\frac{11v_{2,1}L^2m}{210} \\ \frac{L^3mv_{2,1}}{105} \\ 0 \\ \frac{9mv_{2,2}L}{70} \\ \frac{13mv_{2,2}L^2}{420} \\ 0 \\ \frac{13mv_{2,2}L}{35} \\ -\frac{11mv_{2,2}L^2}{210} \end{Bmatrix}$$

Figure 6.14: Step 5.1

$$\begin{bmatrix} -\frac{E}{L} & 0 & 0 & 0 & 0 \\ 0 & -\frac{12Ev_{2,1}}{L^3} & \frac{6E}{L^2} & 0 & 0 \\ 0 & -\frac{6Ev_{2,1}}{L^2} & -\frac{2E}{L} & 0 & 0 \\ \frac{E}{L} & 0 & 0 & 0 & 0 \\ 0 & \frac{12Ev_{2,1}}{L^3} & -\frac{6E}{L^2} & 0 & 0 \\ 0 & -\frac{6Ev_{2,1}}{L^2} & \frac{4E}{L} & 0 & 0 \\ 0 & 0 & 0 & -\frac{E}{L} & 0 \\ 0 & -\frac{12Ev_{2,2}}{L^3} & 0 & 0 & \frac{6E}{L^2} \\ 0 & -\frac{6Ev_{2,2}}{L^2} & 0 & 0 & -\frac{2E}{L} \\ 0 & 0 & 0 & \frac{E}{L} & 0 \\ 0 & \frac{12Ev_{2,2}}{L^3} & 0 & 0 & -\frac{6E}{L^2} \\ 0 & -\frac{6Ev_{2,2}}{L^2} & 0 & 0 & \frac{4E}{L} \end{bmatrix} \begin{Bmatrix} Au_{2,1} \\ I \\ Iw_{2,1} \\ Au_{2,2} \\ Iw_{2,2} \end{Bmatrix} =$$

$$\lambda_1 \begin{bmatrix} \frac{Lm}{6} & 0 & 0 & 0 \\ 0 & -\frac{13mL^2}{420} & 0 & 0 \\ 0 & -\frac{L^3m}{140} & 0 & 0 \\ \frac{Lm}{3} & 0 & 0 & 0 \\ 0 & -\frac{11L^2m}{210} & 0 & 0 \\ 0 & \frac{L^3m}{105} & 0 & 0 \\ 0 & 0 & \frac{Lm}{6} & 0 \\ 0 & 0 & 0 & -\frac{13mL^2}{420} \\ 0 & 0 & 0 & -\frac{L^3m}{140} \\ 0 & 0 & \frac{Lm}{3} & 0 \\ 0 & 0 & 0 & -\frac{11L^2m}{210} \\ 0 & 0 & 0 & \frac{L^3m}{105} \end{bmatrix} \begin{Bmatrix} u_{2,1} \\ w_{2,1} \\ u_{2,2} \\ w_{2,2} \end{Bmatrix} + \lambda_1 \begin{Bmatrix} 0 \\ -\frac{13mv_{2,1}L^2}{420} \\ -\frac{L^3mv_{2,1}}{140} \\ 0 \\ -\frac{11v_{2,1}L^2m}{210} \\ \frac{L^3mv_{2,1}}{105} \\ 0 \\ \frac{9mv_{2,2}L}{70} \\ \frac{13mv_{2,2}L^2}{420} \\ 0 \\ \frac{13mv_{2,2}L}{35} \\ -\frac{11mv_{2,2}L^2}{210} \end{Bmatrix}$$

Figure 6.15: Step 5.2

Step 6. Building B matrix

Now matrix $[B]$ and vectors $\{z\}$ and $\{D\}$ are built. To do so, matrices $[K^*]$ and $[M^*]$ are put together to form matrix $[B]$ and the vector of unknowns $\{z\}$ is formed by putting together vectors $\{\Phi_K^*\}$ and $\{\Phi_M^*\}$.

Finally, the vector of completely known terms $\{D\}$ is set on the right-hand side of the equation. Note that it corresponds to the independent term that was previously defined.

$$\begin{bmatrix} -\frac{E}{L} & 0 & 0 & 0 & 0 & \frac{Lm}{6} & 0 & 0 & 0 \\ 0 & -\frac{12Ev_{2,1}}{L^3} & \frac{6E}{L^2} & 0 & 0 & 0 & -\frac{13mL^2}{420} & 0 & 0 \\ 0 & -\frac{6Ev_{2,1}}{L^2} & -\frac{2E}{L} & 0 & 0 & 0 & -\frac{L^3m}{140} & 0 & 0 \\ \frac{E}{L} & 0 & 0 & 0 & 0 & \frac{Lm}{3} & 0 & 0 & 0 \\ 0 & \frac{12Ev_{2,1}}{L^3} & -\frac{6E}{L^2} & 0 & 0 & 0 & -\frac{11L^2m}{210} & 0 & 0 \\ 0 & -\frac{6Ev_{2,1}}{L^2} & \frac{4E}{L} & 0 & 0 & 0 & \frac{L^3m}{105} & 0 & 0 \\ 0 & 0 & 0 & -\frac{E}{L} & 0 & 0 & 0 & \frac{Lm}{6} & 0 \\ 0 & -\frac{12Ev_{2,2}}{L^3} & 0 & 0 & \frac{6E}{L^2} & 0 & 0 & 0 & -\frac{13mL^2}{420} \\ 0 & -\frac{6Ev_{2,2}}{L^2} & 0 & 0 & -\frac{2E}{L} & 0 & 0 & 0 & -\frac{L^3m}{140} \\ 0 & 0 & 0 & \frac{E}{L} & 0 & 0 & 0 & \frac{Lm}{3} & 0 \\ 0 & \frac{12Ev_{2,2}}{L^3} & 0 & 0 & -\frac{6E}{L^2} & 0 & 0 & 0 & -\frac{11L^2m}{210} \\ 0 & -\frac{6Ev_{2,2}}{L^2} & 0 & 0 & \frac{4E}{L} & 0 & 0 & 0 & \frac{L^3m}{105} \end{bmatrix} \begin{Bmatrix} Au_{2,1} \\ I \\ Iw_{2,1} \\ Au_{2,2} \\ Iw_{2,2} \\ u_{2,1} \\ w_{2,1} \\ u_{2,2} \\ w_{2,2} \end{Bmatrix} =$$

$$\lambda_1 \begin{Bmatrix} 0 \\ -\frac{13mv_{2,1}L^2}{420} \\ -\frac{L^3mv_{2,1}}{140} \\ 0 \\ -\frac{11v_{2,1}L^2m}{210} \\ \frac{L^3mv_{2,1}}{105} \\ 0 \\ \frac{9mv_{2,2}L}{70} \\ \frac{13mv_{2,2}L^2}{420} \\ 0 \\ \frac{13mv_{2,2}L}{35} \\ -\frac{11mv_{2,2}L^2}{210} \end{Bmatrix}$$

Figure 6.16: Step 6

Step 7. Obtaining null space of matrix B

The last step of each recursive loop is to determine the null space of the matrix $[B]$, assembled in step 6, with the goal of identifying the observable variables.

Also, the parametric equations are derived in this step. It is to note that the null space of matrix $[B]$ is computed with the *null* command of Matlab. Studying the null rows of the null space of matrix $[B]$ allows to identify which of the variables in vector $\{z\}$ have a unique solution, meaning that they are observable.

In this case, the null space of the problem is:

$$NullSpace = \begin{pmatrix} 0 \\ 0 \\ 0 \\ 0 \\ 0 \\ 0 \\ 0 \\ 0 \\ 0 \\ 0 \\ 0 \end{pmatrix} \tag{6.8}$$

Step 8. Identifying the observable variables

From the previous step in which the null space was found, it can be deduced that the observable and unobservable variables are:

$$Observable = \begin{pmatrix} Au_{2,1} \\ I \\ Iw_{2,1} \\ Au_{2,2} \\ Iw_{2,2} \\ u_{2,1} \\ w_{2,1} \\ u_{2,2} \\ w_{2,2} \end{pmatrix}; \quad Unobservable = \varnothing \tag{6.9}$$

It can be seen how all the variables that were in $\{z\}$ are observed, leaving the set of unobservable variables empty.

Step 9. Recursive process

In this case, the program would run a second iteration in order to calculate the area A separately, since it was coupled in the previous calculation.

6.1.3 Example 3: frame

Finally, in the last example a simple frame is considered. Its vertical and horizontal displacements are constrained in nodes 1 and 3.

Each element, 1 and 2, is defined by its own mechanical properties: Young's modulus E_1 and E_2, intertia I_1 and I_2, area A_1 and A_2, length L_1 and L_2, and mass m_1 and m_2.

Figure 6.17 shows the structure. The assumed known properties are shown in green, while the unknown ones are shown in red. It is assumed that the horizontal displacement of node 2 and its rotation are measured.

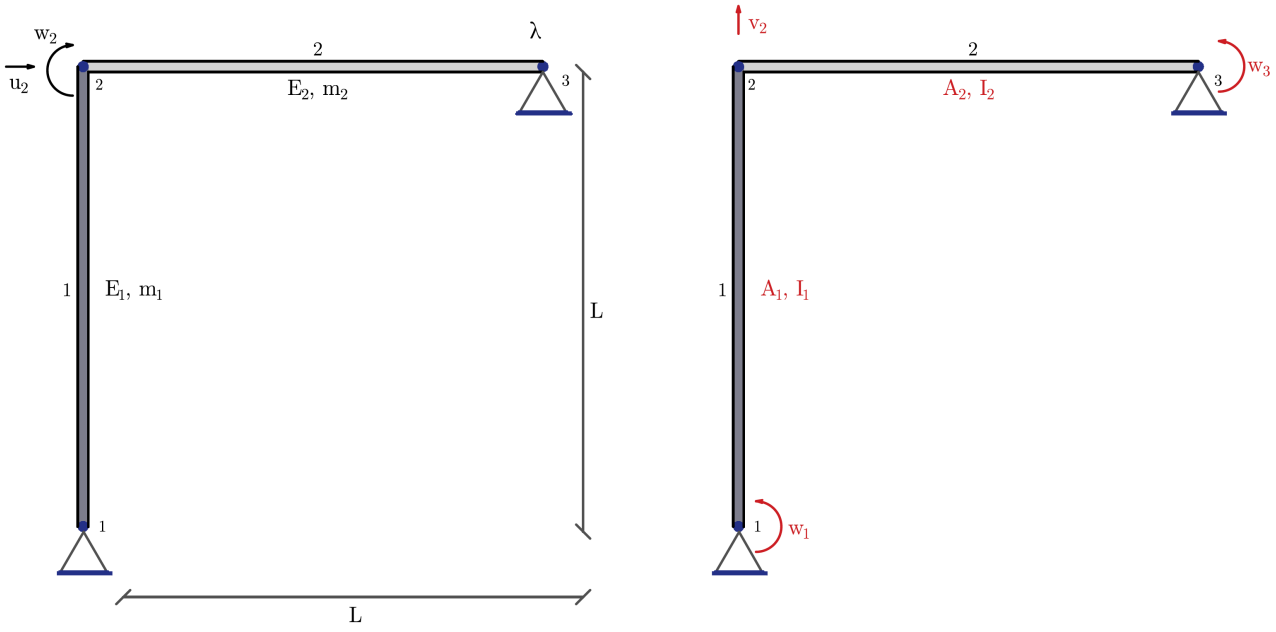

Figure 6.17: Illustration of the frame used in the example for the symbolic application

Step 1. Building stiffness and mass matrices

In the first place the stiffness and mass matrices are assembled according to the topology of the structure and following the structural bar theory. In this case, a consistent mass matrix has been chosen.

This first step is shown in fig. 6.18.

Steps 2 and 3. Generating modified stiffness and mass matrices

Secondly, the modified stiffness and mass matrices are built. Since beam element 1 and beam element 2 are connected through node 2, the matrix columns associated to modal displacements of this node

$$
\begin{bmatrix}
\frac{12E_1I_1}{L_1^3} & 0 & \frac{6E_1I_1}{L_1^2} & -\frac{12E_1I_1}{L_1^3} & 0 & \frac{6E_1I_1}{L_1^2} & 0 & 0 & 0 \\
0 & \frac{E_1A_1}{L_1} & 0 & 0 & -\frac{E_1A_1}{L_1} & 0 & 0 & 0 & 0 \\
\frac{6E_1I_1}{L_1^2} & 0 & \frac{4E_1I_1}{L_1} & -\frac{6E_1I_1}{L_1^2} & 0 & \frac{2E_1I_1}{L_1} & 0 & 0 & 0 \\
-\frac{12E_1I_1}{L_1^3} & 0 & -\frac{6E_1I_1}{L_1^2} & -\frac{12E_1I_1}{L_1^3}+\frac{E_2A_2}{L_2} & 0 & -\frac{6E_1I_1}{L_1^2} & -\frac{E_2A_2}{L_2} & 0 & 0 \\
0 & -\frac{E_1A_1}{L_1} & 0 & 0 & \frac{E_1A_1}{L_1}+\frac{12E_2I_2}{L_2^3} & \frac{6E_2I_2}{L_2^2} & 0 & -\frac{12E_2I_2}{L_2^3} & \frac{6E_2I_2}{L_2^2} \\
\frac{6E_1I_1}{L_1^2} & 0 & \frac{2E_1I_1}{L_1} & -\frac{6E_1I_1}{L_1^2} & \frac{6E_2I_2}{L_2^2} & \frac{4E_1I_1}{L_1}+\frac{4E_2I_2}{L_2} & 0 & -\frac{6E_2I_2}{L_2^2} & \frac{2E_2I_2}{L_2} \\
0 & 0 & 0 & -\frac{E_2A_2}{L_2} & 0 & 0 & \frac{E_2A_2}{L_2} & 0 & 0 \\
0 & 0 & 0 & 0 & -\frac{12E_2I_2}{L_2^3} & -\frac{6E_2I_2}{L_2^2} & 0 & \frac{12E_2I_2}{L_2^3} & -\frac{6E_2I_2}{L_2^2} \\
0 & 0 & 0 & 0 & \frac{6E_2I_2}{L_2^2} & \frac{2E_2I_2}{L_2} & 0 & -\frac{6E_2I_2}{L_2^2} & \frac{4E_2I_2}{L_2}
\end{bmatrix}
\begin{Bmatrix} u_1 \\ v_1 \\ w_1 \\ u_2 \\ v_2 \\ w_2 \\ u_3 \\ v_3 \\ w_3 \end{Bmatrix} =
$$

$$
\lambda_0
\begin{bmatrix}
\frac{13m_1L_1}{35} & 0 & \frac{-11m_1L_1^2}{210} & \frac{9m_1L_1}{70} & 0 & \frac{13m_1L_1^2}{420} & 0 & 0 & 0 \\
0 & \frac{m_1L_1}{3} & 0 & 0 & \frac{m_1L_1}{6} & 0 & 0 & 0 & 0 \\
\frac{-11m_1L_1^2}{210} & 0 & \frac{m_1L^3}{105} & \frac{-13m_1L_1^2}{420} & 0 & \frac{-m_1L_1^2}{140} & 0 & 0 & 0 \\
\frac{9m_1L_1}{70} & 0 & \frac{-13m_1L_1^2}{420} & \frac{13m_1}{35L_1}+\frac{m_2L_2}{3} & 0 & \frac{11m_1L_1^2}{210} & \frac{m_2L_2}{6} & 0 & 0 \\
0 & \frac{m_1L_1}{6} & 0 & 0 & \frac{m_1L_1}{3}+\frac{13m_2L_2}{35} & \frac{11m_2L_2^2}{210} & 0 & \frac{9m_2L_2}{70} & \frac{-13m_2L_2^2}{420} \\
\frac{13m_1L_1^2}{420} & 0 & \frac{-m_1L_1^2}{140} & \frac{11m_1L_1^2}{210} & \frac{11m_2L_2^2}{210} & \frac{m_1L_1^3}{105}+\frac{m_2L_2^3}{105} & 0 & \frac{13m_2L_2^2}{420} & \frac{-m_2L_2^2}{140} \\
0 & 0 & 0 & \frac{m_2L_2}{6} & 0 & 0 & \frac{m_2L_2}{3} & 0 & 0 \\
0 & 0 & 0 & 0 & \frac{9m_2L_2}{70} & \frac{13m_2L_2^2}{420} & 0 & \frac{13m_2L_2}{35} & \frac{-11m_2L_2^2}{210} \\
0 & 0 & 0 & 0 & \frac{-13m_2L_2^2}{420} & \frac{-m_2L_2^2}{140} & 0 & \frac{-11m_2L_2^2}{210} & \frac{m_2L_2^3}{105}
\end{bmatrix}
\begin{Bmatrix} u_1 \\ v_1 \\ w_1 \\ u_2 \\ v_2 \\ w_2 \\ u_3 \\ v_3 \\ w_3 \end{Bmatrix}
$$

Figure 6.18: Step 1

have summands that include parameters of both beam elements.

Hence, some the beam parameters of both members (E_1, A_1, I_1, L_1 and E_2, A_2, I_2, L_2) are coupled in some of the columns of matrix K.

It happens the same with some of the columns in the mass matrix M since the variables for the mass, m_1 and m_2 are coupled in some of the matrix elements.

This is why in this step these coupled elements are split up. To do so, the columns are separated so that the summands related to each element can be treated independently. Note that this independence is a necessary condition for the application of the observability method. In the third step all the variables are taken out from the stiffness and mass matrices K and M. They are moved to their corresponding row of the vectors of displacements. Doing so, the matrices become constant (no variables inside).

$$\begin{bmatrix}
\frac{12E_1I_1}{L_1^3} & 0 & \frac{6E_1I_1}{L_1^2} & -\frac{12E_1I_1}{L_1^3} & 0 & 0 & 0 & \frac{6E_1I_1}{L_1^2} & 0 & 0 & 0 & 0 \\
0 & \frac{E_1A_1}{L_1} & 0 & 0 & 0 & -\frac{E_1A_1}{L_1} & 0 & 0 & 0 & 0 & 0 & 0 \\
\frac{6E_1I_1}{L_1^2} & 0 & \frac{4E_1I_1}{L_1} & -\frac{6E_1I_1}{L_1^2} & 0 & 0 & 0 & \frac{2E_1I_1}{L_1} & 0 & 0 & 0 & 0 \\
-\frac{12E_1I_1}{L_1^3} & 0 & -\frac{6E_1I_1}{L_1^2} & -\frac{12E_1I_1}{L_1^3} & \frac{E_2A_2}{L_2} & 0 & 0 & -\frac{6E_1I_1}{L_1^2} & 0 & -\frac{E_2A_2}{L_2} & 0 & 0 \\
0 & -\frac{E_1A_1}{L_1} & 0 & 0 & 0 & \frac{E_1A_1}{L_1} & \frac{12E_2I_2}{L_2^3} & 0 & \frac{6E_2I_2}{L_2^2} & 0 & -\frac{12E_2I_2}{L_2^3} & \frac{6E_2I_2}{L_2^2} \\
\frac{6E_1I_1}{L_1^2} & 0 & \frac{2E_1I_1}{L_1} & -\frac{6E_1I_1}{L_1^2} & 0 & 0 & \frac{6E_2I_2}{L_2^2} & \frac{4E_1I_1}{L_1} & \frac{4E_2I_2}{L_2} & 0 & -\frac{6E_2I_2}{L_2^2} & \frac{2E_2I_2}{L_2} \\
0 & 0 & 0 & 0 & -\frac{E_2A_2}{L_2} & 0 & 0 & 0 & 0 & \frac{E_2A_2}{L_2} & 0 & 0 \\
0 & 0 & 0 & 0 & 0 & 0 & -\frac{12E_2I_2}{L_2^3} & 0 & -\frac{6E_2I_2}{L_2^2} & 0 & \frac{12E_2I_2}{L_2^3} & -\frac{6E_2I_2}{L_2^2} \\
0 & 0 & 0 & 0 & 0 & 0 & \frac{6E_2I_2}{L_2^2} & 0 & \frac{2E_2I_2}{L_2} & 0 & -\frac{6E_2I_2}{L_2^2} & \frac{4E_2I_2}{L_2}
\end{bmatrix}
\begin{Bmatrix} u_1 \\ v_1 \\ w_1 \\ u_2 \\ u_2 \\ v_2 \\ v_2 \\ w_2 \\ w_2 \\ u_3 \\ v_3 \\ w_3 \end{Bmatrix} =$$

$$\lambda_0 \begin{bmatrix}
\frac{13m_1L_1}{35} & 0 & \frac{-11m_1L_1^2}{210} & \frac{9m_1L_1}{70} & 0 & 0 & 0 & \frac{13m_1L_1^2}{420} & 0 & 0 & 0 & 0 \\
0 & \frac{m_1L_1}{3} & 0 & 0 & 0 & \frac{m_1L_1}{6} & 0 & 0 & 0 & 0 & 0 & 0 \\
\frac{-11m_1L_1^2}{210} & 0 & \frac{m_1L^3}{105} & \frac{-13m_1L_1^2}{420} & 0 & 0 & 0 & \frac{-m_1L_1^2}{140} & 0 & 0 & 0 & 0 \\
\frac{9m_1L_1}{70} & 0 & \frac{-13m_1L_1^2}{420} & \frac{13m_1}{35L_1} & \frac{m_2L_2}{3} & 0 & 0 & \frac{11m_1L_1^2}{210} & 0 & \frac{m_2L_2}{6} & 0 & 0 \\
0 & \frac{m_1L_1}{6} & 0 & 0 & 0 & \frac{m_1L_1}{3} & \frac{13m_2L_2}{35} & 0 & \frac{11m_2L_2^2}{210} & 0 & \frac{9m_2L_2}{70} & \frac{-13m_2L_2^2}{420} \\
\frac{13m_1L_1^2}{420} & 0 & \frac{-m_1L_1^2}{140} & \frac{11m_1L_1^2}{210} & 0 & 0 & \frac{11m_2L_2^2}{210} & \frac{m_1L_1^3}{105} & \frac{m_2L_2^3}{105} & 0 & \frac{13m_2L_2^2}{420} & \frac{-m_2L_2^2}{140} \\
0 & 0 & 0 & 0 & \frac{m_2L_2}{6} & 0 & 0 & 0 & \frac{13m_2L_2^2}{420} & \frac{m_2L_2}{3} & 0 & 0 \\
0 & 0 & 0 & 0 & 0 & 0 & \frac{9m_2L_2}{70} & 0 & \frac{-m_2L_2^2}{140} & 0 & \frac{13m_2L_2}{35} & \frac{-11m_2L_2^2}{210} \\
0 & 0 & 0 & 0 & 0 & 0 & \frac{-13m_2L_2^2}{420} & 0 & 0 & 0 & \frac{-11m_2L_2^2}{210} & \frac{m_2L_2^3}{105}
\end{bmatrix}
\begin{Bmatrix} u_1 \\ v_1 \\ w_1 \\ u_2 \\ u_2 \\ v_2 \\ v_2 \\ w_2 \\ w_2 \\ u_3 \\ v_3 \\ w_3 \end{Bmatrix}$$

Figure 6.19: Step 2

$$\begin{bmatrix}
\frac{12}{L_1^3} & 0 & \frac{6}{L_1^2} & -\frac{12}{L_1^3} & 0 & 0 & 0 & \frac{6}{L_1^2} & 0 & 0 & 0 & 0 \\
0 & \frac{1}{L_1} & 0 & 0 & 0 & -\frac{1}{L_1} & 0 & 0 & 0 & 0 & 0 & 0 \\
\frac{6}{L_1^2} & 0 & \frac{4}{L_1} & -\frac{6}{L_1^2} & 0 & 0 & 0 & \frac{2}{L_1} & 0 & 0 & 0 & 0 \\
-\frac{12}{L_1^3} & 0 & -\frac{6}{L_1^2} & -\frac{12}{L_1^3} & \frac{1}{L_2} & 0 & 0 & -\frac{6}{L_1^2} & 0 & -\frac{1}{L_2} & 0 & 0 \\
0 & -\frac{1}{L_1} & 0 & 0 & 0 & \frac{1}{L_1} & \frac{12}{L_2^3} & 0 & \frac{6}{L_2^2} & 0 & -\frac{12}{L_2^3} & \frac{6}{L_2^2} \\
\frac{6}{L_1^2} & 0 & \frac{2}{L_1} & -\frac{6}{L_1^2} & 0 & 0 & \frac{6}{L_2^2} & \frac{4}{L_1} & \frac{4}{L_2} & 0 & -\frac{6}{L_2^2} & \frac{2}{L_2} \\
0 & 0 & 0 & 0 & -\frac{1}{L_2} & 0 & 0 & 0 & 0 & \frac{1}{L_2} & 0 & 0 \\
0 & 0 & 0 & 0 & 0 & 0 & -\frac{12}{L_2^3} & 0 & -\frac{6}{L_2^2} & 0 & \frac{12}{L_2^3} & -\frac{6}{L_2^2} \\
0 & 0 & 0 & 0 & 0 & 0 & \frac{6}{L_2^2} & 0 & \frac{2}{L_2} & 0 & -\frac{6}{L_2^2} & \frac{4}{L_2}
\end{bmatrix}
\begin{Bmatrix} E_1I_1u_1 \\ E_1A_1v_1 \\ E_1I_1w_1 \\ E_1I_1u_2 \\ E_2A_2u_2 \\ E_1A_1v_2 \\ E_2I_2v_2 \\ E_1I_1w_2 \\ E_2I_2w_2 \\ E_2A_2u_3 \\ E_2I_2v_3 \\ E_2I_2w_3 \end{Bmatrix} =$$

$$\lambda_0 \begin{bmatrix}
\frac{13L_1}{35} & 0 & \frac{-11L_1^2}{210} & \frac{9L_1}{70} & 0 & 0 & 0 & \frac{13L_1^2}{420} & 0 & 0 & 0 & 0 \\
0 & \frac{L_1}{3} & 0 & 0 & 0 & \frac{L_1}{6} & 0 & 0 & 0 & 0 & 0 & 0 \\
\frac{-11L_1^2}{210} & 0 & \frac{L^3}{105} & \frac{-13L_1^2}{420} & 0 & 0 & 0 & \frac{-L_1^2}{140} & 0 & 0 & 0 & 0 \\
\frac{9L_1}{70} & 0 & \frac{-13L_1^2}{420} & \frac{13}{35L_1} & \frac{L_2}{3} & 0 & 0 & \frac{11L_1^2}{210} & 0 & \frac{L_2}{6} & 0 & 0 \\
0 & \frac{L_1}{6} & 0 & 0 & 0 & \frac{L_1}{3} & \frac{13L_2}{35} & 0 & \frac{11L_2^2}{210} & 0 & \frac{9L_2}{70} & \frac{-13L_2^2}{420} \\
\frac{13L_1^2}{420} & 0 & \frac{-L_1^2}{140} & \frac{11L_1^2}{210} & 0 & 0 & \frac{11L_2^2}{210} & \frac{L_1^3}{105} & \frac{L_2^3}{105} & 0 & \frac{13L_2^2}{420} & \frac{-L_2^2}{140} \\
0 & 0 & 0 & 0 & \frac{L_2}{6} & 0 & 0 & 0 & \frac{13L_2^2}{420} & \frac{L_2}{3} & 0 & 0 \\
0 & 0 & 0 & 0 & 0 & 0 & \frac{9L_2}{70} & 0 & \frac{-L_2^2}{140} & 0 & \frac{13L_2}{35} & \frac{-11L_2^2}{210} \\
0 & 0 & 0 & 0 & 0 & 0 & \frac{-13L_2^2}{420} & 0 & 0 & 0 & \frac{-11L_2^2}{210} & \frac{L_2^3}{105}
\end{bmatrix}
\begin{Bmatrix} m_1u_1 \\ m_1v_1 \\ m_1w_1 \\ m_1u_2 \\ m_2u_2 \\ m_1v_2 \\ m_2v_2 \\ m_1w_2 \\ m_2w_2 \\ m_2u_3 \\ m_2v_3 \\ m_2w_3 \end{Bmatrix}$$

Figure 6.20: Step 3

Step 4. Imposing boundary conditions, removing measured variables and updating matrices

In the fourth step the boundary conditions are introduced into the matrices. In this case, $u_1 = 0$, $v_1 = 0$, $u_3 = 0$ and $v_3 = 0$. Therefore, the corresponding rows of δ_K^* and δ_M^* and columns of K^* and M^* become zero.

Also, the known parameters are introduced into the matrices. These known variables are E_1, E_2, m_1 and m_2.

$$\begin{bmatrix} 0 & 0 & \frac{6E_1}{L_1^2} & -\frac{12E_1u_2}{L_1^3} & 0 & 0 & 0 & \frac{6E_2w_2}{L_1^2} & 0 & 0 & 0 \\ 0 & 0 & 0 & 0 & 0 & -\frac{E_1}{L_1} & 0 & 0 & 0 & 0 & 0 \\ 0 & 0 & \frac{4E_1}{L_1} & -\frac{6E_1u_2}{L_1^2} & 0 & 0 & 0 & \frac{2E_2w_2}{L_1} & 0 & 0 & 0 \\ 0 & 0 & -\frac{6E_1}{L_1^2} & -\frac{12E_1u_2}{L_1^3} & \frac{E_2u_2}{L_2} & 0 & 0 & -\frac{6E_2w_2}{L_1^2} & 0 & 0 & 0 \\ 0 & 0 & 0 & 0 & 0 & \frac{E_1}{L_1} & \frac{12E_2}{L_2^3} & 0 & \frac{6E_2w_2}{L_2^2} & 0 & 0 & \frac{6E_2}{L_2^2} \\ 0 & 0 & \frac{2E_1}{L_1} & -\frac{6E_1u_2}{L_1^2} & 0 & 0 & \frac{6E_2}{L_2^2} & \frac{4E_2w_2}{L_1} & \frac{4E_2^2w_2}{L_2} & 0 & 0 & \frac{2E_2}{L_2} \\ 0 & 0 & 0 & 0 & -\frac{E_2u_2}{L_2} & 0 & 0 & 0 & 0 & 0 & 0 \\ 0 & 0 & 0 & 0 & 0 & 0 & -\frac{12E_2}{L_2^3} & 0 & -\frac{6E_2w_2}{L_2^2} & 0 & 0 & -\frac{6E_2}{L_2^2} \\ 0 & 0 & 0 & 0 & 0 & 0 & \frac{6E_2}{L_2^2} & 0 & \frac{2E_2w_2}{L_2} & 0 & 0 & \frac{4E_2}{L_2} \end{bmatrix} \begin{Bmatrix} 0 \\ 0 \\ I_1w_1 \\ I_1 \\ A_2 \\ A_1v_2 \\ I_2v_2 \\ I_1 \\ I_2 \\ 0 \\ 0 \\ I_2w_3 \end{Bmatrix} =$$

$$\lambda_1 \begin{bmatrix} 0 & 0 & \frac{-11m_1L_1^2}{210} & 0 & 0 & 0 & 0 \\ 0 & 0 & 0 & \frac{m_1L_1}{6} & 0 & 0 & 0 \\ 0 & 0 & \frac{m_1L^3}{105} & 0 & 0 & 0 & 0 \\ 0 & 0 & \frac{-13m_1L_1^2}{420} & 0 & 0 & 0 & 0 \\ 0 & 0 & 0 & \frac{m_1L_1}{3} & \frac{13m_2L_2}{35} & 0 & \frac{-13m_2L_2^2}{420} \\ 0 & 0 & \frac{-m_1L_1^2}{140} & 0 & \frac{11m_2L_2^2}{210} & 0 & \frac{-m_2L_2^2}{140} \\ 0 & 0 & 0 & 0 & 0 & 0 & 0 \\ 0 & 0 & 0 & 0 & \frac{9m_2L_2}{70} & 0 & \frac{-11m_2L_2^2}{210} \\ 0 & 0 & 0 & 0 & \frac{-13m_2L_2^2}{420} & 0 & \frac{m_2L_2^3}{105} \end{bmatrix} \begin{Bmatrix} 0 \\ 0 \\ w_1 \\ v_2 \\ v_2 \\ 0 \\ 0 \\ w_3 \end{Bmatrix} + \lambda_1 \begin{Bmatrix} \frac{9u_2m_1L_1}{70} + \frac{13w_2m_1L_1^2}{420} \\ 0 \\ \frac{-13u_2m_1L_1^2}{420} - \frac{w_2m_1L_1^2}{140} \\ \frac{13u_2m_1}{35L_1} + \frac{u_2m_2L_2}{3} + \frac{11w_2m_1L_1^2}{210} \\ \frac{11w_2m_2L_2^2}{210} \\ \frac{11u_2m_1L_1^2}{210} + \frac{w_2m_1L_1^3}{105} + \frac{w_2m_2L_2^3}{105} \\ \frac{u_2m_2L_2}{6} + \frac{13w_2m_2L_2^2}{420} \\ \frac{-w_2m_2L_2^2}{140} \\ 0 \end{Bmatrix}$$

Figure 6.21: Step 4

Step 5. Eliminating duplicated variables and removing null columns

At this point it is necessary to check whether there are duplicated variables inside of the modified vectors of displacement δ_K^* and δ_M^*.

It can be seen that in vector Φ_K^* the variable I_1 is duplicated and therefore, the corresponding columns of the two variables are put together. The same happens in vector Φ_M^*, where the variable v_2 appears twice.

$$\begin{bmatrix} \frac{6E_1}{L_1^2} & -\frac{12E_1u_2}{L_1^3}+\frac{6E_2w_2}{L_1^2} & 0 & 0 & 0 & 0 & 0 \\ 0 & 0 & 0 & -\frac{E_1}{L_1} & 0 & 0 & 0 \\ \frac{4E_1}{L_1} & -\frac{6E_1u_2}{L_1^2}+\frac{2E_2w_2}{L_1} & 0 & 0 & 0 & 0 & 0 \\ -\frac{6E_1}{L_1^2} & -\frac{12E_1u_2}{L_1^3}-\frac{6E_2w_2}{L_1^2} & \frac{E_2u_2}{L_2} & 0 & 0 & 0 & 0 \\ 0 & 0 & 0 & \frac{E_1}{L_1} & \frac{12E_2}{L_2^3} & \frac{6E_2w_2}{L_2^2} & \frac{6E_2}{L_2^2} \\ \frac{2E_1}{L_1} & -\frac{6E_1u_2}{L_1^2}+\frac{4E_2w_2}{L_1} & 0 & 0 & \frac{6E_2}{L_2^2} & \frac{4E_2w_2}{L_2} & \frac{2E_2}{L_2} \\ 0 & 0 & -\frac{E_2u_2}{L_2} & 0 & 0 & 0 & 0 \\ 0 & 0 & 0 & 0 & -\frac{12E_2}{L_2^3} & -\frac{6E_2w_2}{L_2^2} & -\frac{6E_2}{L_2^2} \\ 0 & 0 & 0 & 0 & \frac{6E_2}{L_2^2} & \frac{2E_2w_2}{L_2} & \frac{4E_2}{L_2} \end{bmatrix} \begin{Bmatrix} I_1w_1 \\ I_1 \\ A_2u_2 \\ A_1v_2 \\ I_2v_2 \\ I_2 \\ I_2w_3 \end{Bmatrix} =$$

$$\lambda_1 \begin{bmatrix} \frac{-11m_1L_1^2}{210} & 0 & 0 \\ 0 & \frac{m_1L_1}{6} & 0 \\ \frac{m_1L^3}{105} & 0 & 0 \\ \frac{-13m_1L_1^2}{420} & 0 & 0 \\ 0 & \frac{m_1L_1}{3}+\frac{13m_2L_2}{35} & \frac{-13m_2L_2^2}{420} \\ \frac{-m_1L_1^2}{140} & \frac{11m_2L_2^2}{210} & \frac{-m_2L_2^2}{140} \\ 0 & 0 & 0 \\ 0 & \frac{9m_2L_2}{70} & \frac{-11m_2L_2^2}{210} \\ 0 & \frac{-13m_2L_2^2}{420} & \frac{m_2L_2^3}{105} \end{bmatrix} \begin{Bmatrix} w_1 \\ v_2 \\ w_3 \end{Bmatrix} + \lambda_1 \begin{Bmatrix} \frac{9u_2m_1L_1}{70}+\frac{13w_2m_1L_1^2}{420} \\ 0 \\ \frac{-13u_2m_1L_1^2}{420}-\frac{w_2m_1L_1^2}{140} \\ \frac{13u_2m_1}{35L_1}+\frac{u_2m_2L_2}{3}+\frac{11w_2m_1L_1^2}{210} \\ \frac{11w_2m_2L_2^2}{210} \\ \frac{11u_2m_1L_1^2}{210}+\frac{w_2m_1L_1^3}{105}+\frac{w_2m_2L_2^3}{105} \\ \frac{u_2m_2L_2}{6}+\frac{13w_2m_2L_2^2}{420} \\ \frac{-w_2m_2L_2^2}{140} \\ 0 \end{Bmatrix}$$

Figure 6.22: Step 5

Step 6. Building B matrix

At this point, matrix B is built by taking the mass matrix to the left-hand side of the equation (hence, changing its sign). Then, in the right-hand side of the expression stay only the known variables.

$$\begin{bmatrix} \frac{6E_1}{L_1^2} & -\frac{12E_1u_2}{L_1^3}+\frac{6E_2w_2}{L_1^2} & 0 & 0 & 0 & 0 & 0 & \frac{11\lambda_1m_1L_1^2}{210} & 0 & 0 \\ 0 & 0 & 0 & -\frac{E_1}{L_1} & 0 & 0 & 0 & 0 & \frac{-\lambda_1m_1L_1}{6} & 0 \\ \frac{4E_1}{L_1} & -\frac{6E_1u_2}{L_1^2}+\frac{2E_2w_2}{L_1} & 0 & 0 & 0 & 0 & 0 & \frac{-\lambda_1m_1L^3}{105} & 0 & 0 \\ -\frac{6E_1}{L_1^2} & -\frac{12E_1u_2}{L_1^3}-\frac{6E_2w_2}{L_1^2} & \frac{E_2u_2}{L_2} & 0 & 0 & 0 & 0 & \frac{13\lambda_1m_1L_1^2}{420} & 0 & 0 \\ 0 & 0 & 0 & \frac{E_1}{L_1} & \frac{12E_2}{L_2^3} & \frac{6E_2w_2}{L_2^2} & \frac{6E_2}{L_2^2} & 0 & \frac{-\lambda_1m_1L_1}{3}-\frac{13\lambda_1m_2L_2}{35} & \frac{13\lambda_1m_2L_2^2}{420} \\ \frac{2E_1}{L_1} & -\frac{6E_1u_2}{L_1^2}+\frac{4E_2w_2}{L_1} & 0 & 0 & \frac{6E_2}{L_2^2} & \frac{4E_2w_2}{L_2} & \frac{2E_2}{L_2} & \frac{\lambda_1m_1L_1^2}{140} & \frac{-11\lambda_1m_2L_2^2}{210} & \frac{\lambda_1m_2L_2^2}{140} \\ 0 & 0 & -\frac{E_2u_2}{L_2} & 0 & 0 & 0 & 0 & 0 & 0 & 0 \\ 0 & 0 & 0 & 0 & -\frac{12E_2}{L_2^3} & -\frac{6E_2w_2}{L_2^2} & -\frac{6E_2}{L_2^2} & 0 & \frac{-9\lambda_1m_2L_2}{70} & \frac{11\lambda_1m_2L_2^2}{210} \\ 0 & 0 & 0 & 0 & \frac{6E_2}{L_2^2} & \frac{2E_2w_2}{L_2} & \frac{4E_2}{L_2} & 0 & \frac{13\lambda_1m_2L_2^2}{420} & \frac{-\lambda_1m_2L_2^3}{105} \end{bmatrix} \begin{Bmatrix} I_1w_1 \\ I_1 \\ A_2u_2 \\ A_1v_2 \\ I_2v_2 \\ I_2 \\ I_2w_3 \\ w_1 \\ v_2 \\ w_3 \end{Bmatrix} =$$

$$\lambda_1 \begin{bmatrix} \frac{9u_2m_1L_1}{70}+\frac{13w_2m_1L_1^2}{420} \\ 0 \\ \frac{-13u_2m_1L_1^2}{420}-\frac{w_2m_1L_1^2}{140} \\ \frac{13u_2m_1}{35L_1}+\frac{u_2m_2L_2}{3}+\frac{11w_2m_1L_1^2}{210} \\ \frac{11w_2m_2L_2^2}{210} \\ \frac{11u_2m_1L_1^2}{210}+\frac{w_2m_1L_1^3}{105}+\frac{w_2m_2L_2^3}{105} \\ \frac{u_2m_2L_2}{6}+\frac{13w_2m_2L_2^2}{420} \\ \frac{-w_2m_2L_2^2}{140} \\ 0 \end{bmatrix}$$

Figure 6.23: Step 6

Step 7. Obtaining null space of matrix B

Finally, the last step of the recursive loop is to determine the null space of the matrix $[B]$, assembled in step 6, with the goal of identifying the observable variables.

In this case, the null space of the problem is:

$$NullSpace = \begin{pmatrix} 0 \\ 0 \\ 0 \\ 0 \\ \frac{1}{w_2} \\ -L \\ 1 \\ 0 \\ 0 \\ 0 \end{pmatrix} \tag{6.10}$$

Step 8. Identifying the observable variables

From the previous step in which the null space was found, it can be deduced that the observable and unobservable variables are:

$$Observable = \begin{pmatrix} I_1 w_1 \\ I_1 \\ A_2 u_2 \\ A_1 v_2 \\ w_1 \\ v_2 \\ w_3 \end{pmatrix}; \quad Unobservable = \begin{pmatrix} I_2 v_2 \\ I_2 \\ I_2 w_3 \end{pmatrix} \tag{6.11}$$

Step 9. Recursive process

If the following recursive step was performed, it would be found that the null space is:

$$NullSpace = \begin{pmatrix} 0 \\ 0 \\ 0 \\ 0 \\ 0 \\ 0 \\ 0 \\ 0 \\ 0 \\ 0 \end{pmatrix} \tag{6.12}$$

and that, therefore, all the variables can be observed within two iterations.

One of the advantages of the method is that it makes it possible to obtain the symbolic equations to obtain the unknown variables. In this case, these equations are the following ones:

$$\begin{cases} I_1 w_1 = \frac{L^2\lambda_1\left(28m_1u_2^2+42m_2u_2^2+L^2m_1w_2^2-11Lm_1u_2w_2-10Lm_2u_2w_2\right)}{420E(u_2-Lw_2)} \\ I_1 = \frac{L^2\lambda_1\left(41Lm_1u_2-5L^2m_1w_2+64Lm_2u_2\right)}{840E(u_2-Lw_2)} \\ A_2 = -\frac{L\lambda_1 m_2}{6E} \\ A_1 v_2 = -\frac{L\lambda_1\left(9m_1^2u_2+18m_1m_2u_2-Lm_1^2w_2-Lm_1m_2w_2\right)}{54E(2m_1+m_2)} \\ w_1 = -\frac{6m_1u_2+6m_2u_2-Lm_1w_2}{Lm_1} \\ v_2 = \frac{9m_1u_2+18m_2u_2-Lm_1w_2-Lm_2w_2}{9(2m_1+m_2)} \\ w_3 = \frac{18m_1^2u_2+36m_2^2u_2+54m_1m_2u_2-2Lm_1^2w_2+Lm_2^2w_2+2Lm_1m_2w_2}{3m_2(2Lm_1+Lm_2)} \end{cases} \tag{6.13}$$

6.2 Numerical verification of the equations

In order to verify that the afore-mentioned solution of the problem of dynamic observability is correct, in the following subsections the equations are verified.

In order to do so, the modal deflections and natural frequency of the cantilever are obtained through

the direct method and afterwards, this very same data is used in the inverse SSI in order to check the feasibility of the technique. Namely, this data is used within the equations in order to check whether both sides of the equations yield into the same results.

This is done for a cantilever beam and a simple frame. For the first case the equations are checked step-by-step. In the second one, only the first one and the last one are checked.

6.2.1 Cantilever beam

Discretisation into 1 element

In this section the same structure as in section 4.3.3 is studied.

First of all, the study is carried out with the cantilever discretised only in 1 element. The obtained modal shapes are shown in table 6.1.

Node 1		Node 2	
u_1	0,000	u_2	0,000
v_1	0,000	v_2	-2,282
w_1	0,000	w_2	-3,144

Table 6.1: Numerical dynamic deflections of the cantilever

Step 1 is checked. Its expanded matrix expression can be found in fig. 6.3. Simplified, it is reminded that it corresponds to:

$$[K]\{\phi\} = \lambda[M]\{\phi\} \tag{6.14}$$

Following is the equation expression of it (eq. (6.15)):

$$\begin{cases} -\frac{EA}{L}u_1 - \frac{EA}{L}u_2 = \lambda_0\frac{mL}{3}u_1 + \lambda_0\frac{mL}{6}u_2 \\ \frac{12EI}{L^3}v_1 + \frac{6EI}{L^2}w_1 - \frac{6EI}{L^2}v_2 - \frac{2EI}{L}w_2 = \lambda_0\frac{13mL}{35}v_1 + \lambda_0\frac{11mL^2}{210}w_1 + \lambda_0\frac{9mL}{70}v_2 - \lambda_0\frac{13mL^2}{420}w_2 \\ \frac{6EI}{L^2}v_1 + \frac{4EI}{L}w_1 - \frac{6EI}{L^2}v_2 - \frac{2EI}{L}w_2 = \lambda_0\frac{11mL^2}{210}v_1 + \lambda_0\frac{mL^3}{105}w_1 + \lambda_0\frac{13mL^2}{420}v_2 - \lambda_0\frac{mL^3}{140}w_2 \\ -\frac{EA}{L}u_1 + \frac{EA}{L}u_2 = \lambda_0\frac{mL}{6}u_1 + \lambda_0\frac{mL}{3}u_2 \\ -\frac{12EI}{L^3}v_1 - \frac{6EI}{L^2}w_1 + \frac{6EI}{L^2}v_2 - \frac{6EI}{L}w_2 = \lambda_0\frac{9mL}{70}v_1 + \lambda_0\frac{13mL^2}{420}w_1 + \lambda_0\frac{13mL}{35}v_2 - \lambda_0\frac{11mL^2}{210}w_2 \\ \frac{6EI}{L^2}v_1 - \frac{2EI}{L}w_1 - \frac{6EI}{L^2}v_2 + \frac{4EI}{L}w_2 = -\lambda_0\frac{13mL^2}{420}v_1 - \lambda_0\frac{mL^3}{140}w_1 - \lambda_0\frac{11mL^2}{210}v_2 + \lambda_0\frac{mL^3}{105}w_2 \end{cases} \tag{6.15}$$

Considering that the calculations to be performed on the left hand-side of the equation are the ones in eq. (6.16) (they correspond to the stiffness matrix side):

$$LHS_1 = \begin{bmatrix} 2,07E+07 & 0,000 & 0,000 & -2,07E+07 & 0,000 & 0,000 \\ 0,000 & 2,07E+03 & 1,03E+03 & 0,000 & -2,07E+03 & 1,03E+03 \\ 0,000 & 1,03E+03 & 6,89E+02 & 0,000 & -1,03E+03 & 3,45E+02 \\ -2,07E+07 & 0,000 & 0,000 & 2,07E+07 & 0,000 & 0,000 \\ 0,000 & -2,07E+03 & -1,03E+03 & 0,000 & 2,07E+03 & -1,03E+03 \\ 0,000 & 1,03E+03 & 3,45E+02 & 0,000 & -1,03E+03 & 6,89E+02 \end{bmatrix} \begin{Bmatrix} 0 \\ 0 \\ 0 \\ 0 \\ -2,282 \\ -3,144 \end{Bmatrix} \tag{6.16}$$

and the ones on the right hand side are (corresponding to the mass matrix side):

$$RHS_1 = 2746 \cdot \begin{bmatrix} 2,61E-01 & 0,000 & 0,000 & 1,31E-01 & 0,000 & 0,000 \\ 0,000 & 2,91E-01 & 4,10E-02 & 0,000 & 1,01E-01 & -2,42E-02 \\ 0,000 & 4,10E-02 & 7,46E-03 & 0,000 & 2,42E-02 & -5,59E-03 \\ 1,31E-01 & 0,000 & 0,000 & 2,61E-01 & 0,000 & 0,000 \\ 0,000 & 1,01E-01 & 2,42E-02 & 0,000 & 2,91E-01 & -4,10E-02 \\ 0,000 & -2,42E-02 & -5,59E-03 & 0,000 & -4,10E-02 & 7,46E-03 \end{bmatrix} \begin{Bmatrix} 0 \\ 0 \\ 0 \\ 0 \\ -2,282 \\ -3,144 \end{Bmatrix} \tag{6.17}$$

When the operations of eq. (6.14) are performed, the left-hand side and right-hand side of the equation yield the vectors:

$$LHS_1 = \begin{Bmatrix} -1,54E-15 \\ 1,47E+03 \\ 1,28E+03 \\ \mathbf{5,34E-20} \\ \mathbf{-1,47E+03} \\ \mathbf{1,93E+02} \end{Bmatrix} \longleftrightarrow \begin{Bmatrix} 2,67E-20 \\ -4,22E+02 \\ -1,04E+02 \\ \mathbf{5,34E-20} \\ \mathbf{-1,47E+03} \\ \mathbf{1,93E+02} \end{Bmatrix} = RHS_1 \tag{6.18}$$

It can be immediately seen that they are not exactly the same. The first three terms are not the same, but the last three terms are. This is so because when the frequencies are computed through the eigenvalue method, the terms corresponding to the boundary conditions are taken out (this is, the first three columns and rows of matrices [K] and [M]).

Next, as for **steps 2 and 3**, the equation expression is shown in eq. (6.19).

$$\begin{cases} \frac{1}{L}EAu_1 - \frac{1}{L}EAu_2 = \lambda_0\frac{L}{3}mu_1 + \lambda_0\frac{L}{6}mu_2 \\ \frac{12}{L^3}EIv_1 + \frac{6}{L^2}EIw_1 - \frac{12}{L^3}EIv_2 + \frac{6}{L^2}EIw_2 = \lambda_0\frac{13L}{35}mv_1 + \lambda_0\frac{11L^2}{210}mw_1 + \lambda_0\frac{9L}{70}mv_2 - \lambda_0\frac{13L^2}{420}mw_2 \\ \frac{6}{L^2}EIv_1 + \frac{4}{L}EIw_1 - \frac{6}{L^2}EIv_2 - \frac{2}{L}EIw_2 = \lambda_0\frac{11L^2}{210}mv_1 + \lambda_0\frac{L^3}{105}mw_1 + \lambda_0\frac{13L^3}{140}mv_2 - \lambda_0\frac{L^3}{140}mw_2 \\ -\frac{1}{L}EAu_1 + \frac{1}{L}EAu_2 = \lambda_0\frac{L}{6}mu_1 + \lambda_0\frac{L}{3}mu_2 \\ -\frac{12}{L^3}EIv_1 - \frac{6}{L^2}EIw_1 + \frac{12}{L^3}EIv_2 - \frac{6}{L^2}EIw_2 = \lambda_0\frac{9L}{70}mv_1 + \lambda_0\frac{13L^2}{420}mw_1 + \lambda_0\frac{13L}{35}mv_2 - \lambda_0\frac{11L^2}{210}mw_2 \\ \frac{6}{L^2}EIv_1 - \frac{2}{L}EIw_1 - \frac{6}{L^2}EIv_2 + \frac{4}{L}EIw_2 = -\lambda_0\frac{13L^2}{420}mv_1 - \lambda_0\frac{L^3}{140}mw_1 - \lambda_0\frac{11L^2}{210}mv_2 + \lambda_0\frac{L^3}{105}mw_2 \end{cases} \tag{6.19}$$

In this case, the values to be introduced into the system are the ones in eqs. (6.20) and (6.21).

$$LHS_{2,3} = \begin{bmatrix} 1,000 & 0,000 & 0,000 & -1,000 & 0,000 & 0,000 \\ 0,000 & 12,000 & 6,000 & 0,000 & -12,000 & 6,000 \\ 0,000 & 6,000 & 4,000 & 0,000 & -6,000 & -2,000 \\ -1,000 & 0,000 & 0,000 & 1,000 & 0,000 & 0,000 \\ 0,000 & -12,000 & -6,000 & 0,000 & 12,000 & -6,000 \\ 0,000 & 6,000 & -2,000 & 0,000 & -6,000 & 4,000 \end{bmatrix} \begin{Bmatrix} 3,86E-13 \\ 1,47E+03 \\ 3,44E+03 \\ -3,86E-13 \\ -1,47E+03 \\ 1,93E+02 \end{Bmatrix} \tag{6.20}$$

$$RHS_{2,3} = 2746\cdot \begin{bmatrix} 3,33E-01 & 0,000 & 0,000 & 1,67E-01 & 0,000 & 0,000 \\ 0,000 & 3,71E-01 & 5,24E-02 & 0,000 & 1,29E-01 & -3,10E-02 \\ 0,000 & 5,24E-02 & 9,52E-03 & 0,000 & 3,10E-02 & -7,14E-03 \\ 1,67E-01 & 0,000 & 0,000 & 3,33E-01 & 0,000 & 0,000 \\ 0,000 & 1,29E-01 & 3,10E-02 & 0,000 & 3,71E-01 & -5,24E-02 \\ 0,000 & -3,10E-02 & -7,14E-03 & 0,000 & -5,24E-02 & 9,52E-03 \end{bmatrix} \begin{Bmatrix} -6,68E-18 \\ -4,22E+02 \\ -1,04E+02 \\ -1,34E-17 \\ -1,47E+03 \\ 1,93E+02 \end{Bmatrix} \tag{6.21}$$

Now, if the operations corresponding to eq. (6.19) are performed, the left-hand side and right-hand side of the equations yield the vectors in eq. (6.22):

$$LHS_{2,3} = \begin{Bmatrix} 3,86E-13 \\ 1,47E+03 \\ 3,44E+03 \\ \mathbf{-3,86E-13} \\ \mathbf{-1,47E+03} \\ \mathbf{1,93E+02} \end{Bmatrix} \longleftrightarrow \begin{Bmatrix} -6,68E-18 \\ -4,22E+02 \\ -1,04E+02 \\ \mathbf{-3,86E-13} \\ \mathbf{-1,47E+03} \\ \mathbf{1,93E+02} \end{Bmatrix} = RHS_{2,3} \tag{6.22}$$

The next step to be checked is **step 4**. Its equation expression is shown in eq. (6.23).

$$\begin{cases} -\frac{1}{L}EAu_2 = \lambda_1 \frac{L}{6} mu_2 \\ -\frac{12v_2}{L^3}EIv_2 + \frac{6}{L^2}EIw_2 = \lambda_1 \frac{9v_2 L}{70} mv_2 - \lambda_1 \frac{13L^2}{420} mw_2 \\ -\frac{6v_2}{L^2}EIv_2 - \frac{2}{L}EIw_2 = \lambda_1 \frac{13v_2 L^2}{420} mv_2 - \lambda_1 \frac{L^3}{140} mw_2 \\ \frac{1}{L}EAu_2 = \lambda_1 \frac{L}{3} mu_2 \\ \frac{12v_2}{L^3}EIv_2 - \frac{6}{L^2}EIw_2 = \lambda_1 \frac{13v_2 L}{35} mv_2 - \lambda_1 \frac{11L^2}{210} mw_2 \\ -\frac{6}{L^2}EIv_2 + \frac{4}{L}EIw_2 = -\lambda_1 \frac{11v_2 L^2}{210} mv_2 + \lambda_1 \frac{L^3}{105} mw_2 \end{cases} \tag{6.23}$$

Then, the numerical expression of eq. (6.23) can be seen in eqs. (6.24) and (6.25).

$$\begin{bmatrix} 0,000 & 0,000 & 0,000 & -2,07E+11 & 0,000 & 0,000 \\ 0,000 & 0,000 & 0,000 & 0,000 & 5,66E+12 & 1,24E+12 \\ 0,000 & 0,000 & 0,000 & 0,000 & 2,83E+12 & -4,14E+11 \\ 0,000 & 0,000 & 0,000 & 2,07E+11 & 0,000 & 0,000 \\ 0,000 & 0,000 & 0,000 & 0,000 & -5,66E+12 & -1,24E+12 \\ 0,000 & 0,000 & 0,000 & 0,000 & 2,83E+12 & 8,27E+11 \end{bmatrix} \begin{Bmatrix} 3,86E-13 \\ 1,47E+03 \\ 3,44E+03 \\ -3,86E-13 \\ -1,47E+03 \\ 1,93E+02 \end{Bmatrix} \tag{6.24}$$

$$2746 \cdot \begin{bmatrix} 0,000 & 0,000 & 0,000 & 1,31E-01 & 0,000 \\ 0,000 & 0,000 & 0,000 & 0,000 & -2,42E-02 \\ 0,000 & 0,000 & 0,000 & 0,000 & -5,59E-03 \\ 0,000 & 0,000 & 0,000 & 2,61E-01 & 0,000 \\ 0,000 & 0,000 & 0,000 & 0,000 & -4,10E-02 \\ 0,000 & 0,000 & 0,000 & 0,000 & 7,46E-03 \end{bmatrix} \begin{Bmatrix} -6,68E-18 \\ -4,22E+02 \\ -1,04E+02 \\ -1,34E-17 \\ -1,47E+03 \\ 1,93E+02 \end{Bmatrix} + 2746 \cdot \begin{Bmatrix} 0,000 \\ -2,30E-01 \\ -5,53E-02 \\ 0,000 \\ -6,64E-01 \\ 9,36E-02 \end{Bmatrix} \tag{6.25}$$

After carrying out the operations in eqs. (6.24) and (6.25), the results for the left-hand side and right-hand side are (see eq. (6.26)):

$$LHS_4 = \begin{Bmatrix} 3,86E-13 \\ 1,47E+03 \\ 3,44E+03 \\ \mathbf{-3,86E-13} \\ \mathbf{-1,47E+03} \\ \mathbf{1,93E+02} \end{Bmatrix} \longleftrightarrow \begin{Bmatrix} -6,68E-18 \\ -4,22E+02 \\ -1,04E+02 \\ \mathbf{-3,86E-13} \\ \mathbf{-1,47E+03} \\ \mathbf{1,93E+02} \end{Bmatrix} = RHS_4 \tag{6.26}$$

As for **step 5**, again the equation expression is the one in eq. (6.27) and its numerical realisation can be found in both eqs. (6.28) and (6.29).

$$\begin{cases} -\frac{E}{L}Au_2 = \lambda_1 \frac{Lm}{6}u_2 \\ -\frac{12Ev_2}{L^3}I + \frac{6E}{L^2}Iw_2 = -\lambda_1 \frac{13mL^2}{420}w_2 + \frac{9\lambda_1 mv_2 L}{70} \\ -\frac{6Ev_2}{L^2}I - \frac{2E}{L}Iw_2 = -\lambda_1 \frac{L^3 m}{140} + \frac{13\lambda_1 mv_2 L^2}{420} \\ \frac{E}{L}Au_2 = \lambda_1 \frac{Lm}{3}u_2 \\ \frac{12Ev_2}{L^3}I - \frac{6E}{L^2}Iw_2 = -\lambda_1 \frac{11L^2 m}{210}w_2 + \frac{13\lambda_1 mv_2 L}{35} \\ -\frac{6Ev_2}{L^2}I + \frac{4E}{L}Iw_2 = \lambda_1 \frac{L^3 m}{105}w_2 - \frac{11\lambda_1 mv_2 L^2}{210} \end{cases} \tag{6.27}$$

$$LHS_5 = \begin{bmatrix} -2,07E+11 & 0,000 & 0,000 \\ 0,000 & 5,66E+12 & 1,24E+12 \\ 0,000 & 2,83E+12 & -4,14E+11 \\ 2,07E+11 & 0,000 & 0,000 \\ 0,000 & -5,66E+12 & -1,24E+12 \\ 0,000 & 2,83E+12 & 8,27E+11 \end{bmatrix} \begin{Bmatrix} 3,86E-13 \\ 1,47E+03 \\ 3,44E+03 \\ -3,86E-13 \\ -1,47E+03 \\ 1,93E+02 \end{Bmatrix} \tag{6.28}$$

$$RHS_5 = 2746 \cdot \begin{bmatrix} 1,31E-01 & 0,000 \\ 0,000 & -2,42E-02 \\ 0,000 & -5,59E-03 \\ 2,61E-01 & 0,000 \\ 0,000 & -4,10E-02 \\ 0,000 & 7,46E-03 \end{bmatrix} \begin{Bmatrix} -6,68E-18 \\ -4,22E+02 \\ -1,04E+02 \\ -1,34E-17 \\ -1,47E+03 \\ 1,93E+02 \end{Bmatrix} + 2746 \cdot \begin{Bmatrix} 0,000 \\ -2,30E-01 \\ -5,53E-02 \\ 0,000 \\ -6,64E-01 \\ 9,36E-02 \end{Bmatrix} \tag{6.29}$$

$$LHS_5 = \begin{Bmatrix} 3,86E-13 \\ 1,47E+03 \\ 3,44E+03 \\ \mathbf{-3,86E-13} \\ \mathbf{-1,47E+03} \\ \mathbf{1,93E+02} \end{Bmatrix} \longleftrightarrow \begin{Bmatrix} -6,68E-18 \\ -4,22E+02 \\ -1,04E+02 \\ \mathbf{-3,86E-13} \\ \mathbf{-1,47E+03} \\ \mathbf{1,93E+02} \end{Bmatrix} = RHS_5 \tag{6.30}$$

Finally, as for **step 6**, which is the step in which matrix $[B]$ and vectors $\{z\}$ and $\{D\}$ are built, the equation expression of it is the following one:

$$\begin{cases} -\frac{E}{L}Au_2 - \frac{\lambda_1 Lm}{6}u_2 = 0 \\ -\frac{12Ev_2}{L^3}I + \frac{6E}{L^2}Iw_2 + \frac{\lambda_1 13mL^2}{420}w_2 = \frac{9\lambda_1 mv_2 L}{70} \\ -\frac{6Ev_2}{L^2}I - \frac{2E}{L}Iw_2 + \frac{\lambda_1 L^3 m}{140}w_2 = \frac{13\lambda_1 mv_2 L^2}{420} \\ \frac{E}{L}Au_2 - \frac{\lambda_1 Lm}{3}u_2 = 0 \frac{12Ev_2}{L^3}I - \frac{6E}{L^2}Iw_2 + \frac{\lambda_1 11L^2 m}{210}w_2 = \frac{13\lambda_1 mv_2 L}{35} \\ -\frac{6Ev_2}{L^2}I + \frac{4E}{L}Iw_2 - \frac{\lambda_1 L^3 m}{105}w_2 = -\frac{11\lambda_1 mv_2 L^2}{210} \end{cases} \tag{6.31}$$

In matrix form, this yields into eq. (6.32) for the left hand side and into eq. (6.34) for the right hand side:

$$LHS_6 = \begin{bmatrix} -2,07E+11 & 0,000 & 0,000 & -3,58E+02 & 0,000 \\ 0,000 & 5,66E+12 & 1,24E+12 & 0,000 & 6,65E+01 \\ 0,000 & 2,83E+12 & -4,14E+11 & 0,000 & 1,54E+01 \\ 2,07E+11 & 0,000 & 0,000 & -7,17E+02 & 0,000 \\ 0,000 & -5,66E+12 & -1,24E+12 & 0,000 & 1,13E+02 \\ 0,000 & 2,83E+12 & 8,27E+11 & 0,000 & -2,05E+01 \end{bmatrix} \begin{Bmatrix} -1,87E-24 \\ 8,33E-10 \\ -2,62E-09 \\ -1,87E-20 \\ -3,14E+00 \end{Bmatrix} \tag{6.32}$$

$$RHS_6 = \begin{Bmatrix} 0,000 \\ -6,31E+02 \\ -1,52E+02 \\ 0,000 \\ -1,82E+03 \\ 2,57E+02 \end{Bmatrix} \tag{6.33}$$

If the operations are performed, the two vectors yield into:

$$LHS_6 = \begin{Bmatrix} 3,86E-13 \\ 1,26E+03 \\ 3,39E+03 \\ \mathbf{0,000} \\ \mathbf{-1,82E+03} \\ \mathbf{2,57E+02} \end{Bmatrix} \longleftrightarrow \begin{Bmatrix} 0,000 \\ -6,31E+02 \\ -1,52E+02 \\ \mathbf{0,000} \\ \mathbf{-1,82E+03} \\ \mathbf{2,57E+02} \end{Bmatrix} = RHS_6 \tag{6.34}$$

Discretisation into 2 elements

The previous steps show how the equations are verified for the degrees of freedom that do not correspond to boundary conditions (in this case, u_1, v_1 and w_1).

In order to check this hypothesis, the same cantilever beam is studied but instead of analysing it as a single element beam, it is divided into two elements as shown in fig. 6.24.

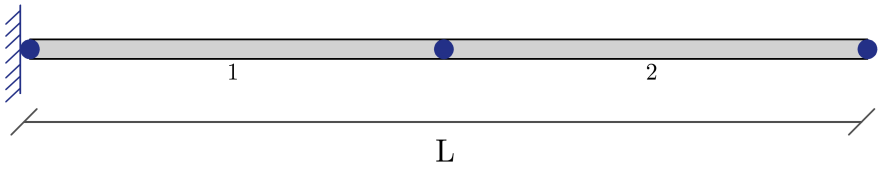

Figure 6.24: Illustration of the cantilever beam divided into 2 elements

Now only two steps will be checked since it is assumed that if the first and last steps are verified then the mid steps must also verify the equations.

First of all, the results for **Step 1** are shown.

$$LHS_1 = \left\{ \begin{array}{c} 7,69E-14 \\ 1,82E+03 \\ 1,36E+03 \\ \mathbf{-1,96E-18} \\ \mathbf{-8,67E+02} \\ \mathbf{-4,47E+01} \\ \mathbf{-1,61E-18} \\ \mathbf{-9,57E+02} \\ \mathbf{7,29E+01} \end{array} \right\} \longleftrightarrow \left\{ \begin{array}{c} -3,30E-19 \\ -6,19E+01 \\ -7,66E+00 \\ \mathbf{-1,96E-18} \\ \mathbf{-8,67E+02} \\ \mathbf{-4,47E+01} \\ \mathbf{-1,61E-18} \\ \mathbf{-9,57E+02} \\ \mathbf{7,29E+01} \end{array} \right\} = RHS_1 \tag{6.35}$$

It can be seen that the measurements verify the equations in both sides.

Next, as for **Step 6**, as it was observed previously, the equations are once again verified. However, it

has to be noted that a small error has been propagated. See eq. (6.36)

$$LHS_6 = \left\{ \begin{array}{c} 7,69E-14 \\ 1,87E+03 \\ 1,37E+03 \\ \mathbf{0,00E+00} \\ \mathbf{-9,16E+02} \\ \mathbf{-3,22E+01} \\ \mathbf{0,00E+00} \\ \mathbf{-9,96E+02} \\ \mathbf{7,50E+01} \end{array} \right\} \longleftrightarrow \left\{ \begin{array}{c} 0,00E+00 \\ -1,05E+02 \\ -1,27E+01 \\ \mathbf{0,00E+00} \\ \mathbf{-9,18E+02} \\ \mathbf{-3,73E+01} \\ \mathbf{0,00E+00} \\ \mathbf{-1,00E+03} \\ \mathbf{7,58E+01} \end{array} \right\} = RHS_6 \tag{6.36}$$

6.2.2 Simple frame

After having performed the verification for the cantilever beam, in this study case the equations are again checked step by step for the simple frame in fig. 6.17. The mechanical properties are the same ones as in section 6.1.3.

First, as for **Step 1**, when the calculations are performed, the results lead to the following vectors for each side of the equation:

$$LHS_1 = \left\{ \begin{array}{c} 1,32E-01 \\ 7,54E+03 \\ \mathbf{1,51E+03} \\ \mathbf{-7,54E+03} \\ \mathbf{-7,54E+03} \\ \mathbf{-3,02E+03} \\ 7,54E+03 \\ 1,32E-01 \\ \mathbf{1,51E+03} \end{array} \right\} \longleftrightarrow \left\{ \begin{array}{c} -7,54E+03 \\ -1,26E+00 \\ \mathbf{1,51E+03} \\ \mathbf{-7,54E+03} \\ \mathbf{-7,54E+03} \\ \mathbf{-3,02E+03} \\ -1,26E+00 \\ -7,54E+03 \\ \mathbf{1,51E+03} \end{array} \right\} = RHS_1 \tag{6.37}$$

And next, as for the last step, **Step 6**, the results obtained are:

$$LHS_6 = \left\{ \begin{array}{c} -4,52E+04 \\ 1,26E+02 \\ \mathbf{-1,51E+04} \\ \mathbf{4,60E+04} \\ \mathbf{-9,48E+04} \\ \mathbf{-7,69E+04} \\ -7,54E+02 \\ 9,50E+04 \\ \mathbf{-4,83E+04} \end{array} \right\} \longleftrightarrow \left\{ \begin{array}{c} -3,10E-02 \\ -7,14E-03 \\ \mathbf{-1,52E+04} \\ \mathbf{4,69E+04} \\ \mathbf{-9,47E+04} \\ \mathbf{-7,69E+04} \\ -5,24E-02 \\ 9,52E-03 \\ \mathbf{-4,83E+04} \end{array} \right\} = RHS_6 \tag{6.38}$$

This shows that the equations that were presented in the previous chapters are satisfied and that therefore, the method is applicable.

6.3 Numerical application

Up to this point the dynamic observability method has been presented and developed, and its equations verified. Also, symbolic examples with simple structures have been shown. However, in order to validate the method a numerical example needs to be completed and successfully solved.

In this section, two numerical analysis are performed over two of the structures that have already been presented in the preceding sections. On the one hand, a cantilever beam will be taken into study. On the other hand, a simple frame will also be analysed.

In each of the analysis, different sets of variables are assumed as known as well as both studies with a single mode of vibration and multiple modes are carried out.

6.3.1 Cantilever beam

Firstly, a cantilever beam is taken into study. Since it was seen that the natural frequencies and modal shapes obtained were more accurate if the level of discretisation was higher, in this example the cantilever is divided in 10 elements as shown in fig. 6.25. Its properties are the ones in table 6.2.

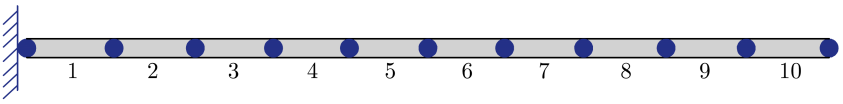

Figure 6.25: Cantilever beam studied in the numerical application

$\mathbf{L_i}$	$0,1\ m$	$\mathbf{A}$	$0,0001\ m^2$
$\mathbf{E}$	$2,068E+9\ N/m^2$	$\boldsymbol{\rho}$	$7830\ kg/m^3$
$\mathbf{I}$	$8,33E-5\ m^4$	$\boldsymbol{\nu}$	$0,33$

Table 6.2: Properties of the cantilever beam used in the numerical application

The different considered subsets are the following ones:

1. All displacements u_{1-11}, v_{1-11}, w_{1-11}
2. All vertical displacements v_{1-11}
3. All horizontal displacements u_{1-11}
4. All rotations w_{1-11}
5. One vertical displacement v_k
6. One horizontal displacement u_k
7. One rotation w_k
8. One vertical and one horizontal displacement v_k, u_k
9. One rotation and one horizontal displacement w_k, u_k

The analysis has been carried out for the nine different subsets of known variables Subsets *5*, *6*, *7*, *8* and *9* have been analysed using the displacement in one node, but the results that are shown in table 6.3 can be generalised to each of the nodes from 2 to 11, since the results obtained with the program were the same for each node.

In table 6.3 the results for the 8 subsets and using only the first mode of vibration are shown. As it can be seen, the study has focused on two variables: the inertia and the area. The results for these variables and its associated errors are shown.

Then, table 6.4 shows the results for subsets *1* to *9* for the same structure but using two modes of vibration. Note that the subsets that were defined refer to one mode of vibration. In the two modes

case, the same displacements have been measured for the two different modes. For example, for subset *5* the vertical displacement has been measured at the same node but in the first and the second mode. The same happens for subsets *6* and *7*; then, in *8* and *9* foursmeasurements are assumed as known in the same nodes: one vertical/rotation and one horizontal displacement of the first mode and one vertical/rotation and one horizontal displacement for the second one.

Subset	**Observed inertia *I***	**Error (%)**	**Observed area *A***	**Error (%)**
1 (u_{1-11}, v_{1-11}, w_{1-11})	—	—	—	—
2 (v_{1-11})	—	—	—	—
3 (u_{1-11})	—	—	—	—
4 (w_{1-11})	—	—	—	—
5 (v_k)	8,33E-05	0,04	—	—
6 (u_k)	—	—	—	—
7 (w_k)	8,33E-05	0,00	—	
8 (v_k, u_k)	8,33E-05	0,04	—	—
9 (w_k, u_k)	8,33E-05	0,00	—	—

Table 6.3: Observed inertias and areas and its corresponding errors in the analysis of the cantilever beam using one single mode

Subset	**Observed inertia *I***	**Error (%)**	**Observed area *A***	**Error (%)**
1 ($u_{1-11,1-2}$, $v_{1-11,1-2}$, $w_{1-11,1-2}$)	—	—	—	—
2 ($v_{1-11,1-2}$)	—	—	—	—
3 ($u_{1-11,1-2}$)	—	—	—	—
4 ($w_{1-11,1-2}$)	—	—	—	—
5 ($v_{k,1-2}$)	8,33E-05	0,00	—	—
6 ($u_{k,1-2}$)	—	—	1,00E-04	0,00
7 ($w_{k,1-2}$)	8,33E-05	0,00	—	—
8 ($v_{k,1-2}$, $u_{k,1-2}$)	8,33E-05	0,00	1,00E-04	0,00
9 ($w_{k,1-2}$, $u_{k,1-2}$)	8,33E-05	0,00	1,00E-04	0,00

Table 6.4: Observed inertias and areas and its corresponding errors in the analysis of the cantilever beam using two modes of vibration

As for the single mode of vibration, it can be seen, first of all, that when taking the whole set of displacements as measured, the errors obtained are extremely high. This is due to the fact that the inputs are redundant and this leads to errors. Also, since there is no horizontal modal displacement, but the results obtained show values that are of very low magnitudes (but not zero) for the horizontal

motion, this yields in more propagated error.

Secondly, it is noted that some of the variables (inertia or area) are not observed in some cases. The reason of this lies on the matrix formulation of the equations. On the one hand, the term EI of the bending stiffness is always coupled with the vertical displacements v_i or the rotations w_i; on the other hand, the term EA is always coupled with the horizontal displacements u_i. Therefore, *subset 1* is able to observe all the parameters since it includes all the displacements, *subsets 2* and *4* only observe inertia since they assumed vertical displacements or rotations as known; then, *subset 3* observes area only because it uses information of horizontal displacements.

Thirdly, *subsets 5*, *7*, *8* and *9* are able to observe the inertias with very low errors, some of them with an error equal to zero (*subset 7* and *9*). However, the areas are still observed with high errors. This is because in the first mode the horizontal displacements of the modal shape are almost zero and therefore this adds very high errors in the results.

Next, as for the study of two modes of vibration, again the first fours subsets yield into very high errors. This makes its results invalid. However, *subsets 5*, *7*, *8* and *9* are able to observe the inertias, but this time all of them with errors of a 0,00%. Also, it is important to remark that now *subsets 6*, *8* and *9* are able to observe the area with an error of 0,00%.

After performing the studies with different combinations of known and unknown variables some conclusions can be made.

The results of combining the knowledge or not of all the variables (which are the frequency λ, the mass m, the horizontal displacement u, the vertical displacement v and the rotation w) are shown in tables 6.5 and 6.6. In these tables, the different combinations of variables are presented, as well as whether they activate or not the objective variables (Young's modulus E, area A and inertia I).

First of all, it can be seen that in both cases (single mode and two-mode) if the mass and all the frequencies are unknown it is not possible to observe any of the variables. The reason for this is that these variables are multiplying the mass matrix and, when the formulation of matrix $[B]$ and vectors $\{z\}$ and $\{D\}$ is done, the $\{D\}$ results into an empty vector, and when the system has to be solved the solution obtained is also an empty vector.

Secondly, in the single mode cases, it can be seen that when both the mass and the frequency are known (variables m and λ), it is possible to observe all the unknown characteristics when horizontal

displacement plus vertical displacement and/or rotation are known. This results was already presented in the numerical application a few paragraphs before.

As for the multiple modes cases, the results are similar than those of the single mode cases. However, in order to observe all the variables it is only necessary that one mass and one frequency are known, apart from one horizontal displacement plus vertical displacement and/or rotation.

The reason for this is that some of the terms in vector $\{D\}$ might be built up by combinations of one λ (corresponding to the first or the second mode) and the mass, which leads to a non-empty vector.

Known variables		**Young's modulus *E***	**Area *A***	**Inertia *I***
	m	✗	✗	✗
u	**λ**	✗	✗	✗
	m & **λ**	✓	✓	✗
	m	✗	✗	✗
v	**λ**	✗	✗	✗
	m & **λ**	✓	✗	✓
	m	✗	✗	✗
w	**λ**	✗	✗	✗
	m & **λ**	✓	✗	✓
	m	✗	✗	✗
u & v	**λ**	✗	✗	✗
	m & **λ**	✓	✓	✓
	m	✗	✗	✗
u & w	**λ**	✗	✗	✗
	m & **λ**	✓	✓	✓

Table 6.5: Dependance on the measurements for the variables to be observable and non-observable in the single mode study of a cantilever

Known variables		Young's modulus E	Area A	Inertia I
u	**m**	✗	✗	✗
	$\boldsymbol{\lambda_1}$ & $\boldsymbol{\lambda_2}$	✗	✗	✗
	m & $\boldsymbol{\lambda_1}$	✓	✓	✗
	m & $\boldsymbol{\lambda_2}$	✓	✓	✗
v	**m**	✗	✗	✗
	$\boldsymbol{\lambda_1}$ & $\boldsymbol{\lambda_2}$	✗	✗	✗
	m & $\boldsymbol{\lambda_1}$	✓	✗	✓
	m & $\boldsymbol{\lambda_2}$	✓	✗	✓
w	**m**	✗	✗	✗
	$\boldsymbol{\lambda_1}$ & $\boldsymbol{\lambda_2}$	✗	✗	✗
	m & $\boldsymbol{\lambda_1}$	✓	✗	✓
	m & $\boldsymbol{\lambda_2}$	✓	✗	✓
u & v	**m**	✗	✗	✗
	$\boldsymbol{\lambda_1}$ & $\boldsymbol{\lambda_2}$	✗	✗	✗
	m & $\boldsymbol{\lambda_1}$	✓	✓	✓
	m & $\boldsymbol{\lambda_2}$	✓	✓	✓
u & w	**m**	✗	✗	✗
	$\boldsymbol{\lambda_1}$ & $\boldsymbol{\lambda_2}$	✗	✗	✗
	m & $\boldsymbol{\lambda_1}$	✓	✓	✓
	m & $\boldsymbol{\lambda_2}$	✓	✓	✓

Table 6.6: Dependance on the measurements for the variables to be observable and non-observable in the two-mode study of a cantilever

6.3.2 Frame

The frame used in the study is the one shown in fig. 6.26. It can be seen that its two elements have been discretised into four parts in order to increase the accuracy of the results. Its properties are in table 6.7.

L	$0,25\ m$	**A**	$0,0001\ m^2$
E	$2,068E+9\ N/m^2$	$\boldsymbol{\rho}$	$7830\ kg/m^3$
I	$8,33E-5\ m^4$	$\boldsymbol{\nu}$	$0,33$

Table 6.7: Properties of the frame used in the numerical application

The measurements subsets that have been used are the same as the ones in the previous case of study. Again, a direct numerical analysis has been performed first using the programmed method in Matlab. These results have then been used for the inverse analysis.

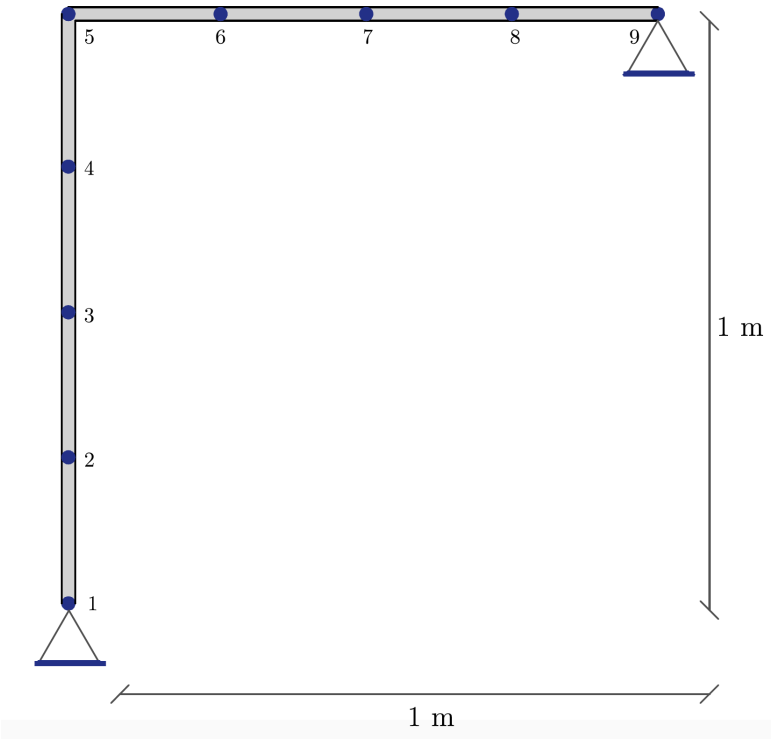

Figure 6.26: Frame studied in the numerical application

Table 6.8 shows the results for the observed variables when using only one mode of vibration. When working with *subsets 1* to *4*, the results are attained with high errors. As well as it happened previously, some of the cases are not able to observe the area because of the coupling in the matrices of some of the variables.

On the other hand, *subsets 5*, *7*, *8* to *9* are able to observe the inertia with rather low errors (0,07%).

Subset	**Observed inertia *I***	**Error (%)**	**Observed area *A***	**Error (%)**
1 (u_{1-11}, v_{1-11}, w_{1-11})	—	—	—	—
2 (v_{1-11})	—	—	—	—
3 (u_{1-11})	—	—	—	—
4 (w_{1-11})	—	—	2,11E-04	52,69
5 (v_k)	8,34E-05	0,07	—	—
6 (u_k)	—	—	—	—
7 (w_k)	8,34E-05	0,07	—	—
8 (v_k, u_k)	8,34E-05	0,07	—	—
9 (w_k, u_k)	8,34E-05	0,07	—	—

Table 6.8: Observed inertias and areas and its corresponding errors in the analysis of the frame using one single mode

Table 6.9 shows the same results but with a two modes analysis. Now, each of the measurements has been taken in the same node or nodes but in both modes of vibration.

In this case, also the study of *subsets 1* to *4* leads to bad results. However, now *subsets 5* and *7* can observe the inertia correctly (namely, with errors less than 0,1%), as *subset 6* can do it for the area (although, in this case, the resultant error is a bit higher).

It is important to emphasise that when taking measurements of one vertical and one horizontal displacements or one rotation and one horizontal displacement, the program is capable of observing both variables, inertia and area, with errors less than 0,1% for the inertia and less than 10% for the area.

Subset	**Observed inertia *I***	**Error (%)**	**Observed area *A***	**Error (%)**
1 ($u_{1-11,1-2}$, $v_{1-11,1-2}$, $w_{1-11,1-2}$)	—	—	—	—
2 ($v_{1-11,1-2}$)	—	—	—	—
3 ($u_{1-11,1-2}$)	—	—	—	—
4 ($w_{1-11,1-2}$)	—	—	—	—
5 ($v_{k,1-2}$)	8,33E-05	0,04	—	—
6 ($u_{k,1-2}$)	—	—	1,11E-04	9,91
7 ($w_{k,1-2}$)	8,33E-05	0,04	—	—
8 ($v_{k,1-2}$, $u_{k,1-2}$)	8,33E-05	0,04	1,07E-04	6,54
9 ($w_{k,1-2}$, $u_{k,1-2}$)	8,33E-05	0,04	1,07E-04	6,54

Table 6.9: Observed inertias and areas and its corresponding errors in the analysis of the frame using two modes of vibration

These analyses lead to conclude that the more modes of vibration are studied the more accuracy can be achieved. Also, it is important to choose smartly the measurements in order to be able to (1) observe all the variables, and (2) not fall into redundancies of measurements.

In the same way as it was done for the cantilever case, an analysis of possible combinations between known and unknown measurements has been carried out.

The results are shown in tables 6.10 and 6.11. As before, it is not possible to observe any variable when all the masses and/or all the frequencies are not known. However, when one of the masses (m_1 or m_2) are known together with one of the frequencies (λ_1 or λ_2) it is possible to observe some of the variables. As it was said, vertical displacements and rotations activate inertia and the Young's modulus, and horizontal displacements activate the area.

Known variables		Young's modulus E	Area A	Inertia I
u	m_1 & m_2	✗	✗	✗
	λ	✗	✗	✗
	m_1 & λ	✓	✓	✗
	m_2 & λ	✓	✓	✗
v	m_1 & m_2	✗	✗	✗
	λ	✗	✗	✗
	m_1 & λ	✓	✗	✓
	m_2 & λ	✓	✗	✓
w	m_1 & m_2	✗	✗	✗
	λ	✗	✗	✗
	m_1 & λ	✓	✗	✓
	m_2 & λ	✓	✗	✓
u & v	m_1 & m_2	✗	✗	✗
	λ	✗	✗	✗
	m_1 & λ	✓	✓	✓
	m_2 & λ	✓	✓	✓
u & w	m_1 & m_2	✗	✗	✗
	λ	✗	✗	✗
	m_1 & λ	✓	✓	✓
	m_2 & λ	✓	✓	✓

Table 6.10: Dependance on the measurements for the variables to be observable and non-observable in the single mode study of a frame

Known variables		Young's modulus E	Area A	Inertia I
u	m_1 & m_2	✗	✗	✗
	λ_1 & λ_2	✗	✗	✗
	m_1 & λ_1	✓	✓	✗
	m_2 & λ_2	✓	✓	✗
	m_1 & λ_2	✓	✓	✗
	m_2 & λ_1	✓	✓	✗
v	m_1 & m_2	✗	✗	✗
	λ_1 & λ_2	✗	✗	✗
	m_1 & λ_1	✓	✗	✓
	m_2 & λ_2	✓	✗	✓
	m_1 & λ_2	✓	✗	✓
	m_2 & λ_1	✓	✗	✓
w	m_1 & m_2	✗	✗	✗
	λ_1 & λ_2	✗	✗	✗
	m_1 & λ_1	✓	✗	✓
	m_2 & λ_2	✓	✗	✓
	m_1 & λ_2	✓	✗	✓
	m_2 & λ_1	✓	✗	✓
u & v	m_1 & m_2	✗	✗	✗
	λ_1 & λ_2	✗	✗	✗
	m_1 & λ_1	✓	✓	✓
	m_2 & λ_2	✓	✓	✓
	m_1 & λ_2	✓	✓	✓
	m_2 & λ_1	✓	✓	✓
u & w	m_1 & m_2	✗	✗	✗
	λ_1 & λ_2	✗	✗	✗
	m_1 & λ_1	✓	✓	✓
	m_2 & λ_2	✓	✓	✓
	m_1 & λ_2	✓	✓	✓
	m_2 & λ_1	✓	✓	✓

Table 6.11: Dependance on the measurements for the variables to be observable and non-observable in the two-mode study of a frame

6.4 Symbolic application to a large structure

In order to show to the reader the possible applications and potential of the proposed method, a more complex example is presented in this section.

6.4.1 13-story frame. Complete SSI

In this section, the SSI of a 13-story frame is presented. The structure is 32 m wide and 39 m high. Its modelling is done through 102 nodes and 149 bars as shown in fig. 6.27.

The structure is composed of a set of 8 different sections described in table 6.12. All sections are made of concrete with an specific weight of 25 kN/m^2 and a Young's modulus of 35000 MPa.

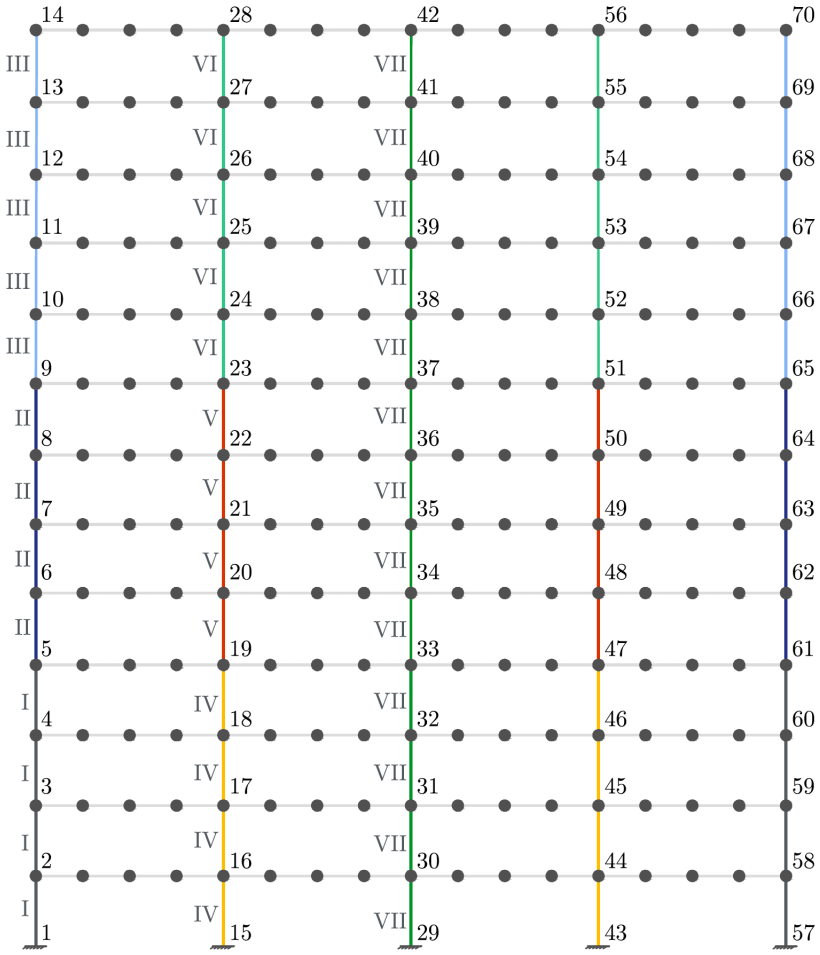

Figure 6.27: Illustration of the 13-floor frame used in the symbolic application

Section	Elements	**A** (m^2)	**I** (m^4)
I: Outer Bottom Columns	1 to 4 and 53 to 56	0,563	0,026
II: Outer Intermediate Columns	5 to 8 and 57 to 60	0,360	0,011
III: Outer Upper Columns	9 to 13 and 61 to 65	0,250	0,005
IV: Interior Bottom Columns	14 to 17 and 40 to 43	0,360	0,011
V: Interior Intermediate Columns	18 to 21 and 44 to 47	0,250	0,011
VI: Interior Upper Columns	22 to 26 and 48 to 52	0,160	0,002
VII: Central Core	27 to 39	1,800	5,400
VIII: Beams	66 to 273	0,180	0,005

Table 6.12: Properties of the studied 13-floor frame

After running the direct dynamic analysis the modal shapes and natural frequencies might be obtained. Just to show the magnitude of the vibration modes the frequencies obtained are shown in table 6.13.

Mode	**Frequency (Hz)**	
	Consistent mass matrix	*Lumped mass matrix*
1	0,139	0,139
2	0,678	0,670
3	0,954	0,933

Table 6.13: Numerical frequencies for the 13-story frame using a consistent or a lumped mass matrix

Several symbolic studies are carried out in order to check the effectiveness of the proposed method. For each analysis, the number of observed variables are checked — this is, the number of modal displacements, of bending stiffnesses and of axial stiffnesses. Moreover, the number of iterations (recursive steps) needed are also checked.

The four different studies carried out are shown in fig. 6.28: *study a* involves vertical and horizontal measurements at 15 nodes of the structure, study *study b* rotations at the same nodes, *study c* horizontal displacements and *study d* vertical ones.

The results show that when analysing *study a*, one iteration was needed to observe the stiffnesses of the eight types of beams; the other three studies needed two iterations each in order to observe the whole set o axial and bending stiffnesses. This information is summarised in table 6.14.

Note that it is coherent with one of the conclusions obtained from section 6.3.1, since when measuring horizontal and vertical displacements all the stiffnesses are observed in one step. Then, for example, as for the case when the measurements are only horizontal, this activates the axial stiffnesses of the beams, but as well the bending stiffnesses of the columns. Therefore, in the first step some axial

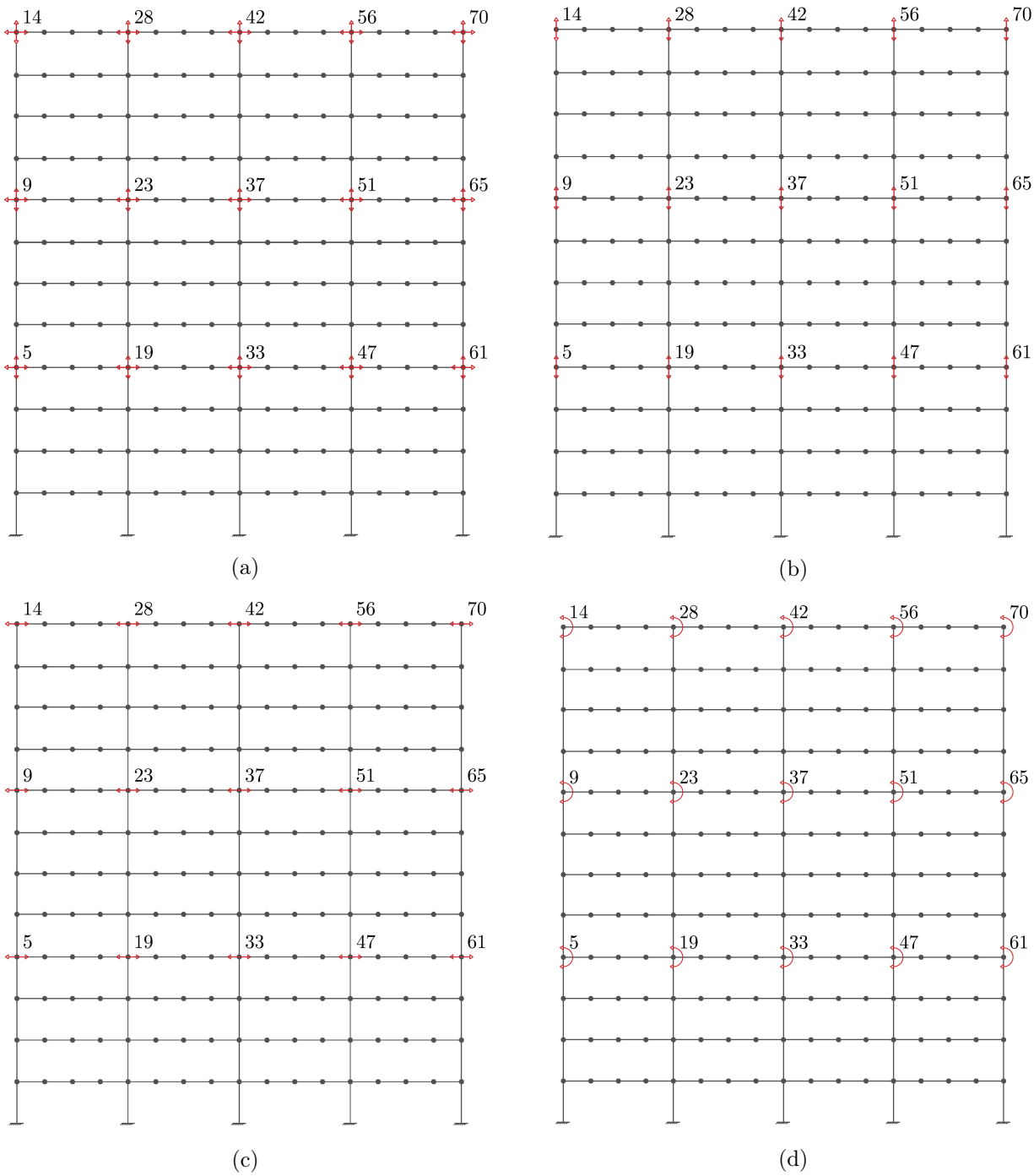

Figure 6.28: Symbolic studies performed on the 13-floor frame

and some bending stiffnesses can be observed. The very same happens when measuring rotations and vertical displacements.

It is important to remark the fact that the mathematical observability is not the same as the numerical one. This means that there might be occasions in which the numerical value of a variable can be obtained by means of the observability method, but leading to very high errors. This would be purely mathematical observability, since although the value for the variable was calculated, the achieved

results were not coherent.

In this case, the values for the variables would be able to be obtained, but an analysis of the errors should have to be carried out in order to check whether the results are accurate enough.

Therefore, in this type of structures (complex ones) it is of high importance to first carry a sensitivity analysis in order to obtain the minimum number of measurements that are needed for the structure to be observable.

Study case	**Recursive steps**	**Observed axial stiffnesses**	**Observed bending stiffnesses**
a	1	EA_{I-VIII}	EI_{I-VIII}
b	1	EA_{I-VII}	EI_{VIII}
	2	EA_{VIII}	EI_{I-VII}
c	1	EA_{VIII}	EI_{I-VII}
	2	EA_{I-VII}	EI_{VIII}
d	1	EA_{I-VII}	EI_{VIII}
	2	EA_{VIII}	EI_{I-VII}

Table 6.14: Observed parameters and needed recursive steps for each of the study cases of the 13-floor frame

6.4.2 13-story frame. Local SSI

There are occasions in which there is interest in obtaining only the properties of one or a few members of the structure to check, for example, if it is damaged.

The normal procedure is to measure some of the displacements around this element or elements in order to activate its matrix components.

An assumption is made that the axial and bending stiffnesses of the structure are unknown and that the mechanical properties of the floor slab of the 12th floor are different from the other ones.

Two sets of measurements are proposed. These are shown in fig. 6.29. After performing the analysis, all the properties can be observed.

It has to be emphasised that these bending and axial stiffnesses can be observed without knowing the surrounding ones, which shows the power of the method.

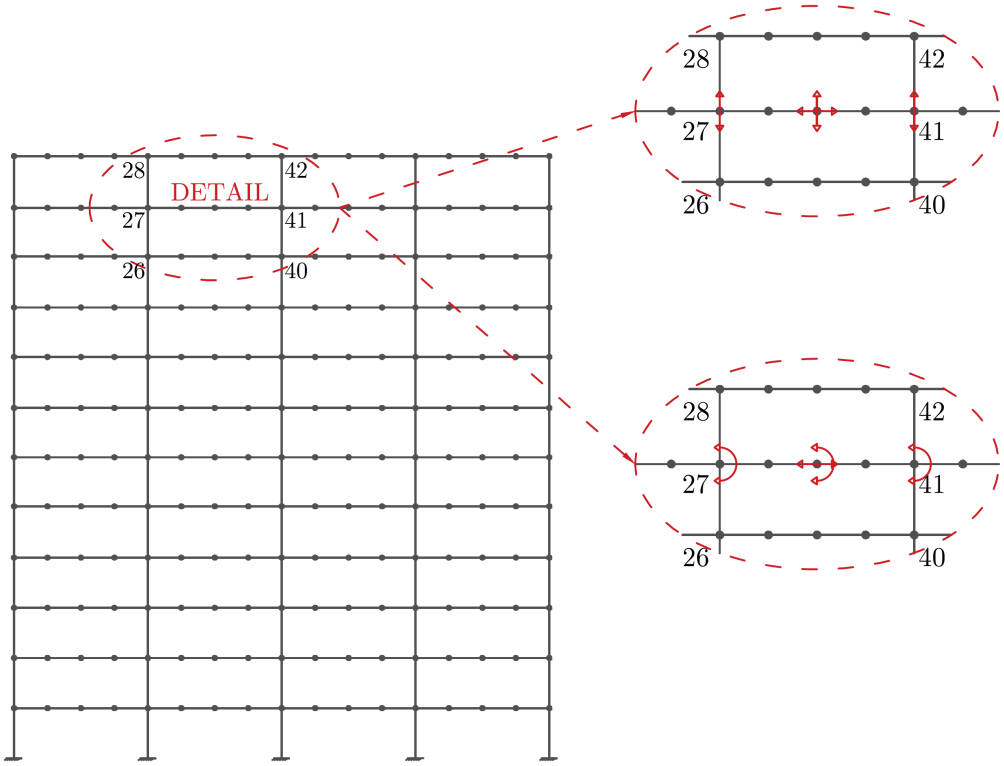

Figure 6.29: Detail of the two subsets of measurements used in the local SSI of a 13-story frame

Chapter 7

Conclusions

7.1 Introduction

This work presents a study of the Structural System Identification by observability techniques.

7.2 Conclusions

The conclusions of the work are divided into the following sections: (1) Conclusions about the *SSI*, (2) Conclusions about the direct dynamic *SSI* and (3) Conclusions about the inverse dynamic *SSI* based on observability techniques.

7.2.1 Conclusions about the *SSI*

This work shows that until the present a high number of methods that aim at identifying the parameters of the structure have been developed. These methods use some inputs (which usually come from experimental data) in order to describe the outputs, or response.

The many methods developed until the present can be separated into two main groups: those that are based on static data to do the calculations and those that are based on dynamic data. There are a few of the studies done that are rather interesting because of their usage of both static and dynamic data.

However, most of the techniques have a drawback: they adjust the outputs to inputs, creating a mathematical model to characterise the system. Doing so, the established relationship has no explicit

physical meaning (non-parametric models). This makes SSI by observability of interest, since it *does* establish a relationship with explicit physical meaning (based on equations of structures). Also, SSI by observability has the advantage that there might be variables that can be obtained without knowing the whole set of measurements.

7.2.2 Conclusions about the direct dynamic *SSI*

The first stage for the dynamic SSI by observability is to perform a direct analysis of the studied structure. This is so because the inputs needed to apply the method are the modal shapes of the structure and its natural frequency or frequencies. This data can be obtained by measuring either displacements, velocities or accelerations in all or some of the nodes of the structure in the three degrees of freedom (vertical, horizontal and rotation). When these experimental measurements have been obtained, then a modal analysis has to be carried out.

Modal analysis, as it was explained, has the main objective of getting the modal properties of a structure by taking the inputs and transforming them to modal shapes and frequencies. This process can be done in several ways and many methods have been developed until the present that deal with this problem. Examples of these methods are the Peak Picking method, known for its simplicity and ease of use, the Frequency Domain Decomposition method, which is an improvement of the previous method, and the Stochastic Subspace Identification, which is rather complex but achieves high accuracies.

Given the importance of obtaining the modal shapes and natural frequencies part of the study of this thesis focused on the development of a program to calculate them numerically. This program uses the mechanical properties of the structure and its boundary conditions and calculates the modal properties of the structure.

In order to check the feasibility of the program, patch tests were carried out. Firstly, the correct assemblage of the matrix was checked by performing analysis of the same structure (a cantilever beam) but changing the order of its nodes and elements. This proved that the matrices and its nodes connectivities had been well implemented in Matlab. Afterwards, the results for a cantilever beam, a simple frame and a two-floor frame were tested. For all of them, the frequencies were obtained up to 10 modes. Also, the number of elements in which each structure was discretised was changed, its value ranging from 1 single element to 120 elements. The last of the factors studied apart from the number of modes and level of discretisation was the influence of the mass matrix used in the calculations.

Commonly, the mass matrix might be assembled in two different ways: a consistent mass matrix or a lumped mass matrix. Each of the calculations was performed using Ansys, Midas and the developed program in Matlab in order to compare the results.

The results showed the following:

1. The higher the number of elements in which the structure is discretised, the lower the error is for the frequencies. This was shown by obtaining the theoretical frequencies of a cantilever beam and the numerical ones and comparing them. Also, as for the frames, the results obtained with the three softwares were compared and it was proved that all the frequencies converged to the same value for the highest number of elements.

2. Frequencies obtained using the consistent mass matrix formulation converge to their real value faster than the ones obtained using the lumped mass matrix. This was observed in the three analysed structures.

3. The more complex the structure is (considering, for example, a multiple floor frame more complex than a cantilever beam) the faster the frequencies converge and the closer the values are. Namely, when the frequencies were obtained for the frames, the values obtained by the three different methods were closer to each other than the ones of the cantilever beam were.

After all the analyses that were carried out, the program was proved to yield in very low errors.

7.2.3 Conclusions about the inverse dynamic *SSI* based on observability techniques

The interest of performing a SSI analysis based on observability techniques was demonstrated with the studies of the method applied on static measurements. However, it has to be taken into account that dynamic characteristics (which are the modal parameters) give information about the global response of structures and, therefore, they lack of sensitivity to local phenomena. On the other hand, static measurements (such as strains and displacements) do have more sensitivity to the response in their vicinity, which makes them more suitable for local defects determination.

Therefore, since the performance of the SSI by observability techniques and using static measurements was successful, a growing interest appeared on studying the very same method but using dynamic data. In the static SSI, the stiffness matrix method equations are used; in parallel to this, in the dynamic

SSI the equations used have been those of the dynamics of structures, which relate the stiffness and mass matrices using the modal shapes and the natural frequencies.

A program has been developed based on that one of the static SSI method. After applying the method both numerically and symbolically, some conclusions have been withdrawn:

1. The equations that were posed theoretically were checked; they were verified by obtaining the results of each of the sides of the equations in two different structures (cantilever beam and simple frame). It has been noted that the equations apply only for those degrees of freedom that do not correspond to boundary conditions.

2. When focusing the analysis on obtaining the inertia I and the area A the displacements that are measured have to be chosen accurately; because of the way that the matrices are assembled, horizontal displacements only activate axial stiffnesses ES, while bending stiffnesses EI are activate by vertical displacements or rotations. Therefore, if both the inertia and the area are to be estimated, it is recommended that the measurements include horizontal displacements and rotations and/or vertical displacements.

3. The method can be applied not only in simple structures such as beams or simple frames, but also in large structures such as the 13-story building that was taken into study.

4. The mechanical properties of a structure can be observed locally; this is, assuming all the properties of the structure as unknown, it is possible to estimate only some of the characteristics of some elements by taking measurements on that element or around it.

7.3 Major contributions

The major contributions of this work might be summarised as follows:

Chapter 2: the main objective of this chapter is to provide a comprehensive discussion on the concept of Structural System Identification in general. The most important issues concerning the identification techniques are reviewed on the basis of references. This chapter presents a detailed state of the art of the concept of SSI and of the development, until the present, of the techniques concerning it. Furthermore, it briefly presents the functioning of observability.

Chapter 3: in this chapter the static SSI by observability techniques is presented. Although this

thesis deals with dynamic SSI, a basis of the current knowledge of this technique is useful. The main objective, then, of the third chapter is to theoretically explain how the method works and what is the algorithm used for it and to make the concepts clear by going through an example of the identification of parameters of a simple frame.

Chapter 4: this chapter presents the first of the steps of the dynamic SSI – the direct dynamic analysis. The main issues concerning the theory of dynamics of structures is reviewed in order to lead the reader to a better understanding of the dynamic observability. Then, after analysing the theoretical modal analysis, the experimental modal analysis is reviewed. From all the existing methods for obtaining the modal parameters of a structure three are explained with more detail because of the differences in their performance and accuracy of results. Since the direct dynamic analysis is the first step of the developed Matlab program, patch tests are carried out in this chapter in order to verify the correct functioning of it. The factors that are analysed are the connectivities and assemblage of matrices and the results obtained from studying a cantilever beam, a simple frame and a two-floor frame. These tests prove the applicability of the developed method.

Chapter 5: this chapter presents an application of observability techniques to Structural System Identification – that with dynamic measurements. Until the present the main research on this area includes mainly static measurements.

Chapter 6: this chapter shows the potential of the proposed method of the dynamic SSI by observability techniques. First, the power of the method is presented by showing three symbolic applications (a cantilever beam using a single mode, using two modes and a simple frame). Secondly, the equations are numerically verified step-by-step. Then, the application of the method to two structures (a cantilever beam and a simple frame) is presented. Furthermore, a symbolic application of the method on a complex structure is done, both globally and locally.

7.4 Future research

The future research lines of this work are related mainly to the dynamic SSI by observability techniques and they might be summarised as follows.

1. Redundancy of measurements: it has been seen that when performing the system identification of structures, there might be occasions in which if too many measurements are taken, then the

equations are redundant and the final observed variables have high errors. One of the reasons for this is the existence of errors in the input variables. Therefore, in a future the method should be able to deal with these errors and the consequences of introducing too many measurements.

2. Optimising the developed program: the programmed algebraic subroutines in Matlab have been proved to solve correctly the equations. However, the code can still be improved by reducing operations and increasing its efficiency. Moreover, it has to be pointed out that although the use of the null space is a powerful and useful technique, it requires numerical methods which can lead to errors and/or problems. Also, this method is time consuming for large structures (as it was shown with the 13 floor frame analysis).

3. Optimising the measurement set for SSI: the parameters of the structure might be observed by using many different sets. In the static SSI by observability, a method was proposed to define a measurement set with a minimum number of measurements: the observability trees. This method has both advantages and disadvantages and it is useful in certain cases. Therefore, the definition of the measurement set could also be treated as an optimisation problem.

4. Measurement error analysis: the information obtained from monitoring the structure is inevitably coupled with errors, because of inaccuracies of the experimental equipment or because of interferences in the vibration of the structure. There is currently and study being carried out on error analysis for the static SSI; then, it would be advisable to also apply it to dynamic SSI.

5. Introducing damping and shear effects: the implementation of the observability technique to the dynamic eigenvalue equation may not provide enough accurate results when dealing with real structures, either because of the existence of damping or shear deformations, which have not been considered in this work. Therefore, the dynamic SSI could be applied to a more realistic equation in order to better reproduce the behaviour of real structures. To do so, the general dynamic equation should be used and its applicability studied.

6. SSI from actual monitoring information: the identification of the structures presented in this work is based on measurements obtained numerically with a Matlab program. However, to guarantee the application of the proposed method in real structures, dynamic measurements should be taken on site and introduced into the method.

Appendix A

Developed program

In this chapter the program that has been used and partially developed is presented in general terms. Many people has contributed to its development and since there is still research to be done, it might change in the next years. The writer of this thesis has contributed to it by developing the structural dynamics part.

A.1 Running the program

The first step to run the program is to open Matlab and call the function *Portal.m* by double-clicking it or by writing "Portal" in the command window. The screen shown in fig. A.1 should appear then on screen. In order to start the analysis the structure to be studied has to be chosen. To do so, it is

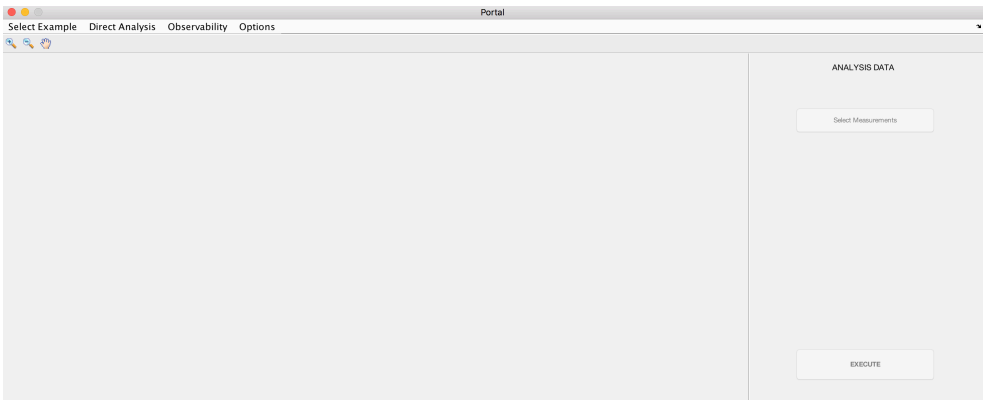

Figure A.1: Main screen of the Matlab program

necessary to click on *Select example*, and immediately a selection panel will show up. Now the data file that contains the information of the structure under study has to be chosen among all the files shown.

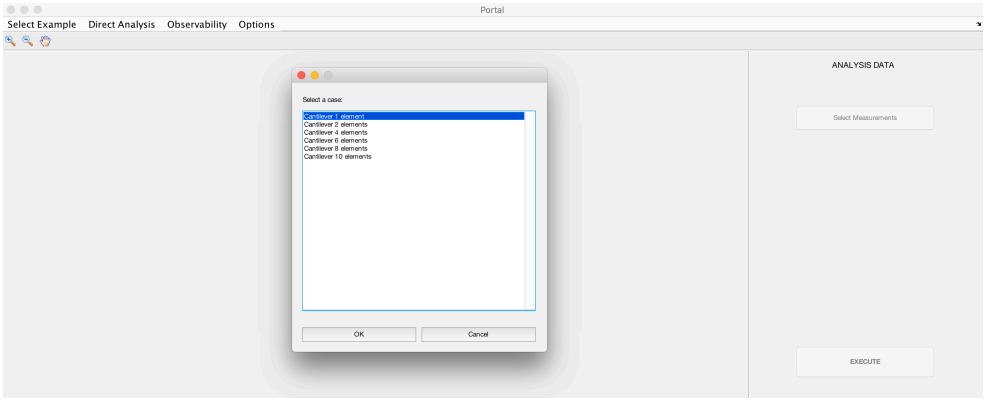

Figure A.2: Screen of the Matlab program when choosing the structure to be analysed

After selecting it the structure chosen will be drawn on the previous screen. Note that on the right-hand side of the panel, under "Analysis data", the type of analysis that is being done should appear in red. In this case, dynamic analysis. See fig. A.3.

After this, the direct analysis can be carried out by clicking on *Direct analysis* » *Perform analysis* (fig. A.4). After a few seconds the results of the direct analysis will appear on the command window.

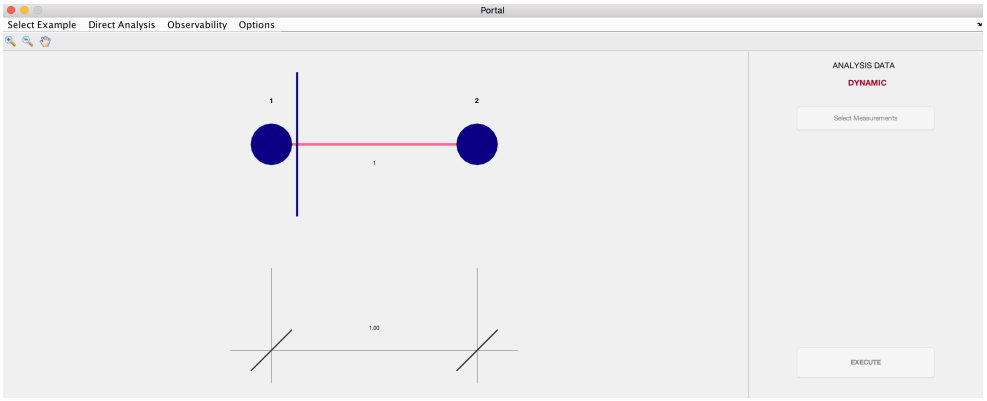

Figure A.3: Screen of the Matlab program when the structure to be analysed appears on the interface

In the case of the analysis being dynamic, the natural frequencies and modal shapes, and in the static case, the reactions and deflections.

After the direct analysis has been carried out a tab inside of *Observability* will be activated. If the analysis was dynamic, then the tabs inside of the *Dynamic observability* option will be switched on; if on the contrary it was static, it will be the tabs inside of the *Static observability* option that will switch on.

When clicking on *Observability* » *Dynamic observability* » *Modal shapes* / *Modal frequencies* the results will be displayed on screen in table format as in fig. A.6.

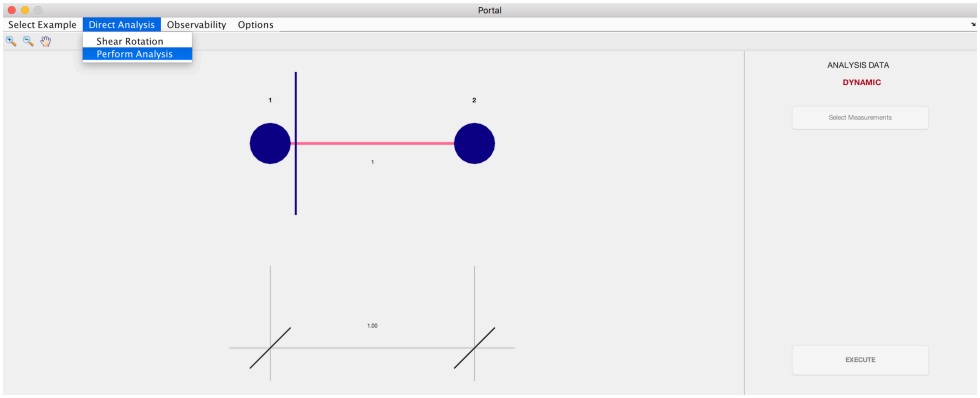

Figure A.4: Tab to be selected in order to run the direct analysis

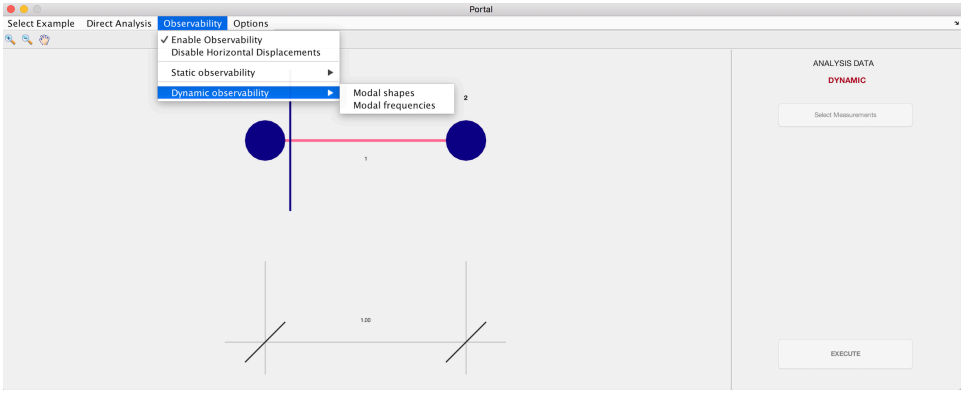

Figure A.5: Tabs to be selected in order to visualise the results of the direct analysis

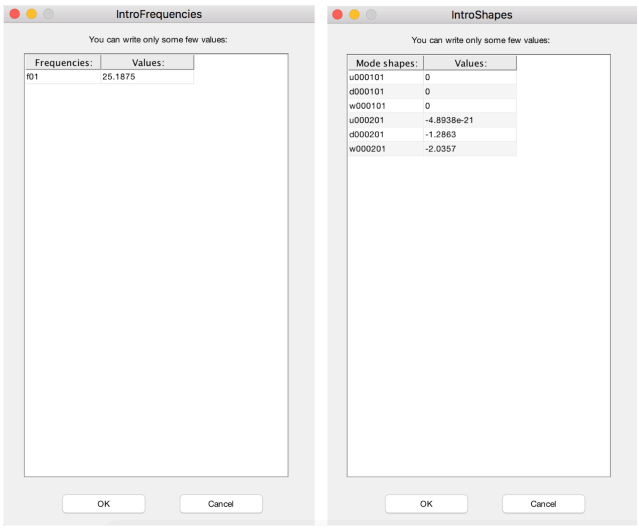

Figure A.6: Visualisation of the direct analysis results (natural frequencies and modal shapes)

After these results have been displayed, it will be possible to click on *Select measurements*, where something similar to fig. A.7 will appear on screen. This panel is used to choose those measurements that are assumed as known in the observability.

In this case, the frequency of the first mode (*f01*) and the vertical displacement of node 2 (*d000201*)

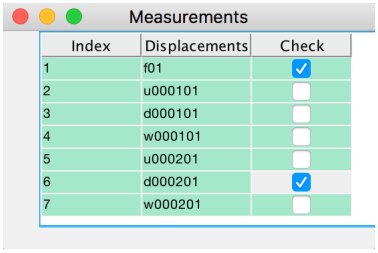

Figure A.7: Panel of selection of the known variables

have been selected.

When the measurements have been selected, the last step is just to select *Execute* and the observability analysis will be carried out.

A.2 Defining the characteristics of the analysis

Appendix A.1 showed how to run the program Portal. However, there are multiple functions behind the presented interface, and they are all programmed using Matlab. One of the most important points to emphasise is the way in which the structures to be analysed are defined.

This is done by directly modifying a Matlab file (usually named *ReadData.m* or similar). Figure A.8 shows an example of the file where the characteristics of the problem are changed.

`Analysistype`: it defines whether the analysis is a static one (`Analysistype=0`) or a dynamic one (`Analysistype=1`).

Under `INITIAL INFORMATION` the information regarding the topology and boundary conditions of the structure are defined:

`nodecoordinates` is used to define the coordinates of the elements of the structure (through x y positions).

In `beams` the connectivity of the different structural elements is defined.

In `knownuvw` the nodes whose boundary conditions are known are input. In this case, the horizontal (`[u]`) and vertical (`[v]`) displacements and rotation (`[w]`) are known in node `1`.

`valueuvw` is used to define the value of the boundary conditions that in `knownuvw` were defined as known. Since they are fixed for this example, the value is `0` for all of them.

```
case 'Cantilever 1 element'
  Analysistype=1;
  %--- INITIAL INFORMATION
  nodecoordinates=L*[ 0 0
                      1 0];
  beams=[ 1 2];
  %Boundary conditions
  knownuvw={[1]; [1]; [1]};  % [u] [v] [w]
  valueuvw={[0]; [0]; [0]};  % Only boundary conditions.

  %--- INVERSE ANALYSIS
  %--- FORCES, DISPLACEMENTS AND MECHANICAL PROPERTIES
  % Forces
  knownfxfym={[]; []; []};  % [Fx] [Fy] [M]
  valuefxfym={[]; []; []};   % Only external forces.
  % Masses
  knownm={[1]};  %added to indicate which discrete masses are known
  valuem={[1]};  %indicating the value of the known masses
  % Frequencies
  knownf={[]};  %added to indicate which squared vibration modes are known
  valuef={[]};  %indicating the value of the known vibration modes
  % Mechanical Properties
  knownEAIQI={[1]; [1]; []; [1]}; % [E] [A] [I] [QI] %
  valueEAIQI={[1e8]; [1]; []; [0]}; % Known parameters.

  %--- DIRECT ANALYSIS
  % Introduce the real values of the E, A, I & S parameters to calculate the stiffness method solution (DIRECT SOLUTION)
  knownEAISdirect={[1]; [1]; [1]; [1]}; % [E] [A] [I] [S] (S => Shear Area)
  valueEAISdirect={[1e8]; [1]; [5e-5]; [0]}; % Real values.
  % Introduce the real values of the m parameters to calculate the stiffness method solutio
  knownmdirect={[1]}; % [m] (m=> Mass)
  valuemdirect={[1]};

  % Indicate the list of beams
  knownEAEIEQI={[]; []; []};
  valueEAEIEQI={[]; []; []};
  % Diferents types of beams
  subbeamsEAIQI={[ones(1,1)];[ones(1,1)];[ones(1,1)];[ones(1,1)]};  % [E] [A] [I] [QI]
  subbeamsm={[ones(1,1)]}; % [m]

  knownvibrationmodes=1;

  massmatrix=1;
```

Figure A.8: Data reader file in which the properties of the analysis are modified

Under `INVERSE ANALYSIS` the variables that are assumed as known for the inverse analysis are defined.

Under `Forces` the external forces applied on the nodes of the structure are introduced. In `knownfxfym` the nodes on which there are forces acting have to be written. In `valuefxfym`, the values of these forces are put. If, for example, there was a vertical downwards force on node 2 of 100, it would be written as: `knownfxfym={[]; [2]; [] }`, `valuefxfym={[]; [-100]; [] }`.

Under `Masses` the value of the mass of each element that is known is introduced. If the structure had two elements and both masses were known and had a value of 25, for example, it would be written as: `knownm={[1 2]}`, `valuem={[25 25]}`. Again, see that the variable `knownm` is used to define which elements' characteristics are known and `valuem` to define the value of this characteristic.

Under `Frequencies` the natural frequencies of the modes of vibration that are known are defined. In `knownf` the modes of vibration that are known are written. See that in this case (it will be

seen in more detail later) there is only 1 mode of vibration studied, so the value of `knownf` can either be null `[]` or 1 `[1]` (first mode of vibration). Inside of `valuef` the value of the frequency (in Hz) would be input.

Under `Mechanical Properties` the known properties for the observability analysis are written. In this case, the Young's modulus E, area A and shear parameter Q are known for element `1`. See that the shear parameter is being defined equal to zero (`[0]`) because there is no shear considered in this example.

Under `DIRECT ANALYSIS` the parameters needed to perform the direct analysis are introduced. Note that this is necessary in order to obtain the reactions and displacements (static analysis) and frequencies and modal shapes (dynamic analysis) in the first step when running the program.

In `knownEAISdirect` and `valueEAISdirect` the Young's modulus, area, inertia and shear area are defined for each of the elements. Note that this structure is built up of only one element, but if it had, for example, four elements, it would be defined as: `knownEAISdirect={[1 2 3 4]; [1 2 3 4]; [1 2 3 4]; [1 2 3 4]}` and `knownEAISdirect={[1e8*ones(1,4)]; [ones(1,4)]; [5e-5 *ones(1,4)]; [0*ones(1,4)]}`.

In `knownmdirect` and `valuemdirect` the values of the known masses are introduced.

Under `Different types of beams`, as it itself expresses, if there are beams with different characteristics it has to be introduced here. If the structure had two elements and their characteristics were the same, it would look like:

`subbeamsEAIQI={[1 1]; [1 1]; [1 1]; [1 1]}; subbeamsm={[1 1]}`

However, if they were different:

`subbeamsEAIQI={[1 2]; [1 2]; [1 2]; [1 2]}; subbeamsm={[1 2]}`

On `knownvibrationmodes` the number of modes that will be studied and used in the analysis are introduced by simply writing a natural number corresponding to the amount of modes.

Finally, `massmatrix` is used to define which type of mass matrix will be assembled. Three types can be chosen: consistent mass matrix (`[0]`), lumped mass matrix with off-diagonal elements (`[1]`) and lumped mass matrix (`[2]`).

Appendix B

Further notes about future research

As it was said in section 7.4, two of the ways of improving the developed method are adding the effects of damping and the effects of shear deformation to the formulation of the dynamic SSI.

In this section this formulation is developed in more detail.

B.1 Observability over the general dynamics equation

In fig. 4.1 a general SDOF system was presented, its equation of motion being:

$$m\ddot{x} + c\dot{x} + kx = f(t) \tag{B.1}$$

Remember that in this equation m stands for the mass of the system, c is the damping coefficient and k is the stiffness constant. Then, x is the expression of the displacement as a function of time t and in the same way, $\dot{x}$ is the velocity and $\ddot{x}$ the acceleration of the system. Finally, $f(t)$ stands for an external force acting on the system.

If instead of considering a SDOF system a MDOF is considered, then the equation transforms into:

$$[M]\{\ddot{x}\} + [C]\{\dot{x}\} + [K]\{x\} = \{f\} \tag{B.2}$$

This equation can as well be written as:

$$[M]^{(3N_N \times 3N_N)}\{a\}^{(3N_N \times 1)} + [C]^{(3N_N \times 3N_N)}\{v\}^{(3N_N \times 1)} + [K]^{(3N_N \times 3N_N)}\{\delta\}^{(3N_N \times 1)} = \{f\}^{(3N_N \times 1)} \tag{B.3}$$

Where N_N is the number of nodes of the structure, $[M]$ is the mass matrix of the structure, $[C]$ is the matrix with the damping coefficients, $[K]$ is the stiffness matrix, $\{f\}$ is the vector of external forces, $\{a\}$ is the vector of accelerations, $\{v\}$ is the vector of velocities and finally $\{\delta\}$ is the vector of displacements.

Each of the matrices in eq. (B.3) includes a set of variables:

- $[M]$ and $[K]$ do not change with respect to the previously presented dynamic SSI method.
- $[C]$ is the Rayleigh damping matrix. It contains the contribution to the attenuation of oscillations of each structural element. Each bar element has an associated damping coefficient c_j. The calculation of these coefficients is complex and needs experimental assessment.
- $\{a\}$ includes the three acceleration components for each node: $\{a_x\}$, $\{a_y\}$ and $\{a_z\}$. The last one is only considered in 3D problems.
- $\{v\}$ includes the three velocity components: $\{v_x\}$, $\{v_y\}$ and $\{v_z\}$.
- $\{\delta\}$ includes the deflections of all N_N nodes.
- Finally, $\{f\}$ includes all the dynamic forces applied on the N_N nodes. It can be a force applied in the x-direction $\{f_x\}$, in the y-direction $\{f_y\}$ or an applied bending moment $\{f_m\}$.

Equation (B.3) might in turn be written as a partitioned matrices as follows:

$$\begin{bmatrix} M_{00} & M_{01} \\ M_{10} & M_{11} \end{bmatrix} \begin{Bmatrix} a_{M,0} \\ a_{M,1} \end{Bmatrix} + \begin{bmatrix} C_{00} & C_{01} \\ C_{10} & C_{11} \end{bmatrix} \begin{Bmatrix} v_{M,0} \\ v_{M,1} \end{Bmatrix} + \begin{bmatrix} K_{00} & K_{01} \\ K_{10} & K_{11} \end{bmatrix} \begin{Bmatrix} \delta_{K,0} \\ \delta_{K,1} \end{Bmatrix} = \begin{Bmatrix} f_0 \\ f_1 \end{Bmatrix} \tag{B.4}$$

In this new configuration of the system, subindices 0 and 1 refer to unknown and known parameters respectively. In the submatrices, the variables have a double subindex. The first subindex refers to the knowledge of the term in the matrix (mass, damping or stiffness), while the second one to the knowledge of the associated subset of acceleration, velocities or displacements. Hence, a double 0 means that the submatrix is made up of unknown terms that are multiplying a subset of unknown accelerations, velocities or displacements ($\{a_{M,0}\}$, $\{v_{C,0}\}$ or $\{\delta_{K,0}\}$). On the other hand, a double 1 on the subindex means that all the terms of the submatrix are known and are multiplying a subset of known accelerations, velocities or displacements ($\{a_{M,1}\}$, $\{v_{C,1}\}$ or $\{\delta_{K,1}\}$).

Unknown mechanical properties might be found in matrices $[M]$, $[C]$ and $[K]$. In order to analyse the observability of the unknown variables, the unknown products of variables of the mass, damping and

stiffness matrices are moved to their corresponding vectors of accelerations, velocities or displacements $\{a^*_M\}$, $\{v^*_C\}$ or $\{\delta^*_K\}$. Doing so, modified mass, damping and stiffness matrices $[M^*]$, $[C^*]$ and $[K^*]$ are matrices of known coefficients. The resulting system of equations is then written as:

$$\begin{bmatrix} M^*_{00} & M^*_{01} \\ M^*_{10} & M^*_{11} \end{bmatrix} \begin{Bmatrix} a^*_{M,0} \\ a^*_{M,1} \end{Bmatrix} + \begin{bmatrix} C^*_{00} & C^*_{01} \\ C^*_{10} & C^*_{11} \end{bmatrix} \begin{Bmatrix} v^*_{M,0} \\ v^*_{M,1} \end{Bmatrix} + \begin{bmatrix} K^*_{00} & K^*_{01} \\ K^*_{10} & K^*_{11} \end{bmatrix} \begin{Bmatrix} \delta^*_{K,0} \\ \delta^*_{K,1} \end{Bmatrix} = \begin{Bmatrix} f_0 \\ f_1 \end{Bmatrix} \tag{B.5}$$

If the length of the elements is assumed to be known the modified vectors of accelerations and velocities might include product variables of two terms (such as $m_j a_x$, $m_j a_y$ or $m_j w_{iz}$ and $c_j v_{ix}$, $c_j v_{iy}$ or $c_j v_{iz}$) or one single term (such as m_j, a_{ix}, a_{iy} or a_{iz} or c_j, v_{ix}, v_{iy} or v_{iz}). On the other hand, the modified vector of displacements might include product variables of three terms (such as $E_j A_j x_{ix}$, $E_j A_j x_{iy}$, $E_j I_j x_{iz}$), of two terms (such as $A_j x_{iy}$, $E_j x_{iy}$, $I_j x_{iy}$, $A_j x_{ix}$, $E_j x_{ix}$, $I_j x_{ix}$, $E_j x_{iz}$ or $I_j x_{iz}$) and a single term (such as A_j, I_j, E_j, x_{ix}, x_{iy} or x_{iz}).

With the purpose of applying observability over eq. (B.5), the unknown variables must be moved to a vector $\{z\}$; also, the known variables are joined into a vector $\{D\}$. This way, the previous equation might be rewritten as presented in the following equation:

$$[B]\{z\} = \begin{bmatrix} M^*_{00} & M^*_{10} \\ C^*_{00} & C^*_{10} \\ K^*_{00} & K^*_{10} \\ 0 & -I \end{bmatrix}^T \begin{Bmatrix} a^*_{M,0} \\ v^*_{M,0} \\ \delta^*_{K,0} \\ f_0 \end{Bmatrix} = \begin{Bmatrix} f_1 - M^*_{11} a^*_{M,1} - C^*_{11} v^*_{M,1} - K^*_{11} \delta^*_{K,1} \\ \\ -M^*_{01} a^*_{M,1} - C^*_{01} v^*_{M,1} - K^*_{01} \delta^*_{K,1} \end{Bmatrix} \tag{B.6}$$

expression in which $[B]$ is a matrix of constant known coefficients, $\{D\}$ is a known vector of coefficients and $\{z\}$ contains the full set of unknown variables.

Variables in $\{z\}$ might be single or coupled as a result of products of variables. Since vector $\{z\}$ contains the parameters to be observed, the study of the null space of $[B]$ allows to identify the set of observable variables as it has previously been done in the static measurements case.

Bibliography

[1] H. Adeli and X. Jiang. Dynamic fuzzy wavelet neural network model for structural system identification. *Journal of Structural Engineering*, 132(1):102–111, January 2006.

[2] H. Adeli and H. Kim. Wavelet-hybrid feedback-least mean square algorithm for robust control of structures. *Journal of Structural Engineering*, 130(1):128–137, 2004.

[3] H. Adeli and H. Park. Counterpropagation neural networks in structural engineering. *Journal of Structural Engineering*, 121(8):1205–1212, 1991.

[4] A. Altunisik, F. Okur, and V. Kahya. Modal parameter identification and vibration based damage detection of a multiple cracked cantilever beam. *Engineering Failure Analysis*, (79):154–170, 2017.

[5] A. Altunisik, F. Okur, and V. Kahya. Structural identification of a cantilever beam with multiple cracks: Modeling and validation. *International Journal of Mechanical Sciences*, (130):74–89, 2017.

[6] A. Benveniste and J. Fuchs. Single sample modal identication of a nonstationary stochastic process. *IEEE Transactions on Automatic Control*, 30(1):66–74, January 1985.

[7] E. Castillo, A. Conejo, R. Pruneda, and C. Solares. Observability in linear systems of equations and inequalities: Applications. *Computers and Operations Research*, 34:1708–1720, 2008.

[8] E. Castillo and A. Cornejo. The observability problem in traffic network models. *Computer-Aided Civil and Infrastructure Engineering*, (23):208–222, 2008.

[9] E. Castillo, F. Jubete, R. Pruneda, and C. Solares. Obtaining simultaneous solutions of linear subsystems of inequalities and duals. *Linear Algebra and its Applications*, 346:131–154, 2002.

[10] E. Castillo, J. M. Menendez, and P. Jimenez. Trip matrix and path flow reconstruction and estimation based on plate scanning and link observations. *Transportation Research*, 42:455–481, 2008.

[11] A. K. Chopra. *Dynamics of Structures Theory and Applications to Earthquake Engineering*. Prentice Hall, 1995.

[12] F. Cui, W. Yuan, and J. Shi. Damage detection of structures based on static response. *Journal of Tongji University*, 281:5–8, 2000 (in Chinese).

[13] A. Cunha and E. Caetano. Experimental modal analysis of civil engineering structures. Technical report, International Modal Analysis Conference, Copenhagen, Denmark, April 2005.

[14] J. Deng. Control problems of grey system. *Systems Control Lett*, 1:288–294, 1982 (in Chinese).

[15] A. Eraky, A. Anwar, A. Saad, and A. Abdo. Damage detection of flexural structural systems using damage index method – experimental approach. *Alexandria Engineering Journal*, (54):497–507, June 2015.

[16] D. Feng and M. Feng. Identification of structural stiffness and excitation forces in time domain using non contact vision-based displacement measurement. *Journal of Sound and Vibration*, (406):15–28, June 2017.

[17] G. Franco, R. Betti, and H. Lus. Identification of structural systems using an evolutionary strategy. *Journal of Engineering Engineering*, 130(10):1125–1139, 2004.

[18] P. Hajela and F. Soeiro. Structural damage detection based on static and modal analysis. *American Institute of Aeronautics and Astronautics Journal*, 28(9):1110–1115, 1990.

[19] P. Hajela and F. Soeiro. Structural damage detection based on static and modal analysis. *American Institute of Aeronautics and Astronautics Journal*, 28(6):1110–1115, 1990.

[20] K. Hejelmstad and S. Shin. Damage detection and assessment of structures from static response. *Journal of Engineering Mechanics*, 123:568–576, 1997.

[21] C. Huang, S. Hung, C. Lin, and W. Su. A wavelet-based approach to identifying structural modal parameters from seismic response and free vibration data. *Computer-Aided Civil and Infrastructure Engineering*, 20:408–423, 2005.

[22] S. Hung, C. Huang, and C. Wen. Using wavelet neural network for the identification of a building structure from experimental data. In *13th World Conference on Earthquake Engineering*, number 241, Canada, August 2004.

[23] R. Janeliukstis, S. Rucevskis, P. Akishin, and A. Chate. Wavelet transform based damage detection in a plate structure. *Procedia Engineering*, (161):127–132, 2016.

[24] G. S. Jr and H. Adeli. System identification in structural engineering. *Scientia Iranica*, 19(6):1355–1364, September 2012.

[25] J. Juang. *Applied system identication.* Prentice Hall, Englewood Cliffs, New Jersey, USA, 1994.

[26] J. Juang and M. Phan. Linear system identification via backward-time observer models. *Journal of Guidance, Control and Dynamics*, 17(3):505–512, 1994.

[27] A. Karim and H. Adeli. Comparison of fuzzy-wavelet radial basis function neural network freeway incident detection model with california algorithm comparison of fuzzy-wavelet radial basis function neural network freeway incident detection model with california algorithm. *Journal of Transportation Engineering*, 128(1):21–30, February 2002.

[28] A. Karim and H. Adeli. Radial basis function neural network for work zone capacity and queue estimation. *Journal of Transportation Engineering*, 129(5):494–503, September 2003.

[29] T. Kijewski and A. Kareem. Wavelet transforms for system identification: considerations for civil engineering applications. *Computer-Aided Civil and Infrastructure Engineering*, 18:339–355, 2003.

[30] M. Kummer. Eigenvalues of symmetric matrices over integral domains. *Journal of Algebra*, (466):195–203, May 2016.

[31] H. Li, Y. Huang, J. Ou, and Y. Bao. Fractal dimension-based damage detection method for beams with a uniform cross-section. *Computer-Aided Civil and Infrastructure Engineering*, 26:190–206, 2011.

[32] C. Ling, G. Wang, and H. He. A new levenberg–marquardt type algorithm for solving nonsmooth constrained equations. *Applied Mathematics and Computation*, (229):107–122, 2014.

[33] L. Liu, W. Hua, and Y. Lei. Measurement. *Real-time simultaneous identification of structural systems and unknown inputs without collocated acceleration measurements based on MEKF-UI*, July 2017.

[34] L. Ljung. *System identication: theory for the user.* Prentice Hall, Englewood Cliffs, New Jersey, USA, 1987.

[35] J. Lozano-Galant, M. Nogal, E. Castillo, and J. Turmo. Application of observability techniques to structural system identification. *Computer-Aided Civil and Infrastructure Engineering*, 28:434–450, 2013.

[36] J. Maroulas. Factorization of hessenberg matrices. *Linear Algebra and its Applications*, (506):226–243, May 2016.

[37] J. Noel and G. Kerschen. Nonlinear system identification in structural dynamics: 10 more years of progress. *Mechanical Systems and Signal Processing*, (83):2–35, August 2016.

[38] P. V. Overschee and B. D. Moor. *Subspace identication for linear systems: theory - implementation - applications*. Kluwer Academic Publishers, Dordrecht, Netherlands, 1996.

[39] S. Patel, A. Chourasria, S. Panigrahi, J. Parashar, N. Parvez, and M. Kumar. Damage identification of rc structures using wavelet transformation. *Procedia Engineering*, (144):336–342, 2016.

[40] B. Peeters and G. D. Roeck. Reference-based stochastic subspace identification for output-only modal analysis. *Mechanical Systems and Signal Processing*, 13(6):855–878, 1999.

[41] R. Perera, R. Marin, and A. Ruiz. Static–dynamic multi-scale structural damage identification in a multi-objective framework. *Journal of Sound and Vibration*, 332:1484–1500, 2013.

[42] P. Poozesh, A. Sarrafi, Z. Mao, and C. Niezrecki. Modal parameter estimation from optically-measured data using a hybrid output-only system identification method. *Measurement*, (110):134–145, June 2017.

[43] R. Pruneda, C. Solares, A. Cornejo, and E. Castillo. An efficient algebraic approach to observability analysis in state estimation. *Electric Power Systems Research*, 80:277–286, 2010.

[44] A. Raich and T. Liszkai. Improving the performance of structural damage detection methods using advanced genetic algorithms. *Journal of Structural Engineering*, 133(6):449–461, 2007.

[45] W. Rakowski. Wavelet approach to damage detection of mechanical systems and structures. *Procedia Engineering*, (182):594–601, 2017.

[46] M. Sanayei and R. Nelson. Identification of structural element stiffnesses from incomplete static test data. *Society of Automotive Engineers Technical Papers*, 1986.

[47] M. Sanayei and O. Onipede. Damage assessment of structures using static test data. *American Institute of Aeronautics and Astronautics Journal*, 29(7):1174–1179, 1991.

[48] M. Sanayei and M. Saletnik. Parameter estimation of structures from static strain measurements. i: Formulation. *Journal of Structural Engineering*, 122(5):555–562, May 1996.

[49] M. Sanayei and S. Scampoli. Structural damage detection based on static and modal analysis. *Journal of Engineering Mechanics*, 117(5):1021–1036, 1991.

[50] F. Schoefs, H. Yañez-Godoy, and F. Lanata. Polynomial chaos representation for identification of mechanical characteristics of instrumented structures. *Computer-Aided Civil and Infrastructure Engineering*, 26:173–189, April 2011.

[51] Z. Sheena, A. Unger, and A. Zalmanovich. Theoretical stiffness matrix correction by static test results. *Israel Journal of Technology*, (20):245–253, 1982.

[52] X. Shen, Q. Yang, Q. Li, and C. Li. Damage assessment for a awning beam by changes in the static displacement. In *9th International Conference on Fuzzy Systems and Knowledge Discovery*. Department of Civil Engineering (Shaoxing University, China), 2012.

[53] G. Suwala and L. Jankowski. Nonparametric identification of structural modifications in laplace domain. *Mechanical Systems and Signal Processing*, (85):867–878, September 2017.

[54] X. Wang, N. Hu, H. Fukunaga, and Z. Yao. Structural damage identification using static test data and changes in frequencies. *Engineering Structures*, 23:610–621, 2001.

[55] H. Yang and J. Zhou. Optimal traffic counting locations for origin-destination matrix estimation. *Transportation Research*, 32(2):109–126, 1998.

[56] G. Zhang, B. Tang, and G. Tang. An improved stochastic subspace identification for operational modal analysis. *Measurement*, 45:1246–1256, 2012.

[57] Z. Zhou and H. Adeli. Timefrequency signal analysis of earthquake records using mexican hat wavelets. *Computer-Aided Civil and Infrastructure Engineering*, 18(5):379–389, June 2003.